12-10-2012 12:00 AM

Production of Bio-coal and Activated Carbon from Biomass

Diana C. Cruz, *The University of Western Ontario*

Supervisor: Franco Berruti, *The University of Western Ontario*
Joint Supervisor: Cedric Briens, *The University of Western Ontario*
A thesis submitted in partial fulfillment of the requirements for the Master of Engineering Science degree in Chemical and Biochemical Engineering

PRODUCTION OF BIO-COAL AND ACTIVATED CARBON FROM BIOMASS

(Spine title: Production of Bio-Coal and Activated Carbon from Biomass)

(Thesis format: Integrated Article)

by

Diana C. Cruz Ceballos

Graduate Program in Engineering Science
Department of Chemical and Biochemical Engineering

A thesis submitted in partial fulfillment
of the requirements for the degree of
Master of Engineering Science

The School of Graduate and Postdoctoral Studies
The University of Western Ontario
London, Ontario, Canada

THE UNIVERSITY OF WESTERN ONTARIO
School of Graduate and Postdoctoral Studies

CERTIFICATE OF EXAMINATION

Joint-Supervisor

_____
Dr. Franco Berruti

Joint-Supervisor

_____
Dr. Cedric Briens

Examiners

_____
Dr. Paul A. Charpentier

_____
Dr. Charles Xu

_____
Dr. Hugh Henry

The thesis by

Diana Catalina Cruz-Ceballos

entitled:

Production of Bio-coal and Activated Carbon from Biomass

is accepted in partial fulfillment of the
requirements for the degree of
Master of Engineering Science

_____
Date

_____
Chair of the Thesis Examination Board

Abstract

The slow pyrolysis of different biomasses (maple wood, birch bark, switch grass, coffee pulp and corn stalk) was studied with the aim to produce a solid pyrolysis product (bio-coal) with promising properties and potential for use in traditional fossil-coal applications. Batch pyrolysis experiments were conducted in a Mechanically Fluidized Reactor (MFR) at temperatures ranging from 143 to 665 ^{o}C, which includes the torrefaction temperature range (200-300 ^{o}C). The effects of temperature and holding time on bio-coal mass yields were determined. The bio-coals were characterized in detail and a highly-controlled study on bio-coal hygroscopicity is presented. Optimal conditions for bio-coal production ranged from a top temperature of 238 °C for maple wood to 286 °C for birch bark. Converting these two feedstocks to bio-coal reduces hygroscopy by about 60 % and increases the heating value by 20 to 36 %, respectively. In both cases, 84 to 89 % of the energy of the original biomass is recovered in the bio-coal.

Surface area enhancement of the different biomasses was studied through pyrolysis (MFR) and CO_2 activation in a fixed bed reactor. Only birch bark and maple wood provided activated carbon with a high surface area of about 400 m^2/g. Interestingly, carbon dioxide activation greatly increases the surface areas of birch bark char but does not have a significant effect on maple wood char.

For birch bark, activation was performed either consecutively on the MFR, or as a second stage on a fixed bed reactor. Technologies provided activated carbons with similar surface areas and were compared according to their mass yield. The MFR provides a higher activated carbon yield, a more homogenous product and a more controllable process than the fixed bed reactor.

Keywords

Bio-coal, Bio-char, Torrefaction, Pyrolysis, Heat Treatment, Activated Carbon.

Co-Authorship Statement

Chapter 2

Article Title: Bio-coal Production from the Torrefaction of Maple Wood Biomass
Authors: Diana C. Cruz, Carole E. Baddour, Lorenzo Ferrante, Franco Berruti and Cedric Briens
Article Status: To be submitted
Contributions: Diana Cruz performed all experimental work, data analysis and writing, experimental method was developed by Diana Cruz, Lorenzo Ferrante, Cedric Briens, Franco Berruti, literature review was completed by Carole Baddour and Diana Cruz. Draft revision and guidance provided by Franco Berruti and Cedric Briens

Chapter 3

Article Title: Pyrolysis and Activation of Birch Bark Biomass by CO_2 Activation
Authors: Diana C. Cruz, Lorenzo Ferrante, Cedric Briens and Franco Berruti
Article Status: To be submitted
Contributions: Diana Cruz performed all experimental work, literature review, data analysis and writing, experimental method was developed by Diana Cruz, Lorenzo Ferrante, Cedric Briens, Franco Berruti. Draft revision and guidance provided by Franco Berruti and Cedric Briens

Chapter 4

Article Title: Analysis of the Production of Bio-coal and Activated Carbon for Different Biomasses
Authors: Diana C. Cruz, Lorenzo Ferrante, Franco Berruti and Cedric Briens
Article Status: To be submitted
Contributions: Diana Cruz performed all experimental work, literature review, data analysis and writing, experimental method was developed by Diana Cruz, Lorenzo Ferrante, Cedric Briens, Franco Berruti. Draft revision and guidance provided by Franco Berruti and Cedric Briens

Acknowledgments

I wish to acknowledge the guidance and support provided by Dr. Franco Berruti and Dr. Cedric Briens as my supervisors during my time at ICFAR. I would like to offer my special thanks to Dr. Lorenzo Ferrante who provided me with valuable background on the research exercise, and helped me throughout the planning and development of the project. I would like to acknowledge Dr. Carole Baddour for her assistance and advice with my work. I wish to acknowledge the valuable help provided by Rob Taylor with all experimental work; manufacture, set up modifications and experimental design. I would like to thank Ying Zhang and Caitlin Marshall for their help with the analytical work. I would also like to thank my colleagues at ICFAR for their kindest and friendship during the development of my project.

I would very much like to thank my parents and my brother; Luis Cruz, Edy Ceballos and Felipe Cruz, for all the support throughout my education journey

Table of Contents

CERTIFICATE OF EXAMINATION ii

Abstract iii

Co-Authorship Statement iv

Acknowledgments v

Table of Contents vi

List of Tables ix

List of Figures x

List of Appendices xv

1. Chapter 1: Introduction 1

    1.1 Present Thesis Work 1

    1.2 Pyrolysis and products 1

    1.3 Bio-char 2

    1.4 Pyrolysis for production of alternative energy 2

        1.4.1 Bio-char as a Product in Fast and Slow Pyrolysis 6

    1.5 Pyrolysis technologies 7

    1.6 Bio-char Applications 9

        1.6.1 Bio-char as Bio-coal 9

        1.6.2 Bio-carbon as Bio-char (soil amendment and fertilizer) 10

        1.6.3 Bio-char as a precursor of activated carbon 11

    1.7 References 22

2. Chapter 2: Bio-coal Production from the Torrefaction of Maple Wood Biomass 31

    2.1 Introduction 31

    2.1 Methods 36

        2.1.1 Biomass selection 36

2.1.2 Equipment description 36
2.1.3 Torrefaction experiments 40
2.1.4 Characterization 41
2.2 Results and Discussion 44
2.2.1 Yields 44
2.2.2 Effect of holding time on mass yields 46
2.2.3 Calorimetry Results 48
2.2.4 Ultimate Analysis and and Ash Content 50
2.2.5 FTIR 53
2.2.6 Hygroscopicity 54
2.2.7 pH 57
2.3 Conclusions 57
2.4 References 58
3. Chapter 3: Pyrolysis of Birch Bark Biomass and Production of Char by CO_2 Activation 63
3.1 Introduction 63
3.2 Method 64
3.2.1 Equipment set up 64
3.2.2 Characterization 66
3.3 Experiments 67
3.3.1 Bio-char Production 68
3.3.2 Process and Activation Technology Comparison Experiments 68
3.4 Results and Discussion 70
3.4.1 Bio-char Yields and Surface Areas 70
3.4.2 Activated Carbon Production using Different Technologies 72
3.4.3 Optimization of Activation in the Fixed Bed Reactor 75

3.4.4 pH of bio-chars and activated carbons 79
3.5 Conclusions 80
3.6 References 81
4. Chapter 4: Analysis of the Production of Bio-coal and Activated Carbon from Different Biomasses 85
4.1 Introduction 85
4.2 Methods 86
4.2.1 Equipment and Production Experiments 86
4.2.2 Characterization 88
4.3 Results and Discussion 89
4.3.1 Feedstock characterization 89
4.3.2 Pyrolysis Product Mass Yield 90
4.3.3 Calorimetry Results 93
4.3.4 Hygroscopicity 95
4.4 Activation Results 100
4.5 Conclusions 101
4.6 References 102
5. Chapter 5: Conclusions 106
5.1 Recommendations for Future Work 106
6. Appendix 108
Curriculum Vitae 111

List of Tables

Table 1-1. Slow Pyrolysis Technologies 7

Table 1-2. Fast Pyrolysis Technologies 8

Table 1-3. Application of activated carbon 11

Table 1-4. Comparison table between activation techniques 15

Table 1-5. Reviews on the production of activated carbon from agricultural material 21

Table 2-1. Overview: torrefaction in the literature 32

Table 2-2. Biomass Composition (dry basis) 50

Table 3-1. Feedstock elemental composition 67

Table 3-2. Surface Area and Mass Loss Values for Activation Experiments with CO_2 Injection at Different Temperatures, description of the experiment shown in Figure 3-13 ... 76

Table 4-1. Feedstocks Main Characteristics; Moisture Content, Elemental Composition, Ash Content, and High Heating Value 89

Table 4-2. Feedstock Main Components; Content of Cellulose, Hemi-cellulose and Lignin taken from Literature 90

Table 4-3. Bio-oil Water Content (From Bio-oil Production with a Maximum Pyrolysis temperature of 570°C) 92

Table 4-4. Main bio-coal characteristics of samples with lowest hygroscopy for each feedstock 99

List of Figures

Figure 1-1. Biomass Thermochemical Conversion Processes and Products (14) 3

Figure 1-2. Bio-char mass yield values gathered by C. Di Blasi (16) Bar grey sections represent typical ranges over which empirical data fall for the pyrolysis type and temperatures mentioned on the x-axis. 5

Figure 1-3. Non-condensable gas mass yield values gathered by C. Di Blasi (16) Bar grey sections represent typical ranges over which empirical data fall for the pyrolysis type and temperatures mention on the x-axis 5

Figure 2-1. (a) MFR Reactor; (b) Condenser..... 37

Figure 2-2. Detailed schematic of the MFR reactor 38

Figure 2-3. Relationship between the sample temperature and the thermocouple reading at the top of the reactor 39

Figure 2-4. Maple wood cumulative particle size distribution as feed in the reactor..... 41

Figure 2-5. Set up for hygroscopy measurement in a controlled saturated atmosphere..... 42

Figure 2-6. Humidity indicator graphs on hygroscopy set up; (a) Relative Humidity and (b) Temperature reaching Dew point..... 44

Figure 2-7. Yields at various reaction temperatures (a) bio-coal; (b) bio-oil; and (c) non-condensable (biomass load = 100 g; holding time = 30 min; heating rate = 12 ^{o}C/min; agitator velocity = 49.5 rpm) 45

Figure 2-8. Bio-coal products at the various temperatures studied 45

Figure 2-9. Yield variations at 30 min (square) and 50 min (circle) holding times at the maximum pyrolysis temperature for (a) bio-coal; (b) bio-oil; and (c) non-condensable gases (biomass load = 100 g; heating rate = 12 ^{o}C/min; agitator velocity = 49.5 rpm) 48

Figure 2-10. High heating values on a dry basis (biomass load = 100 g; holding time = 30 min; heating rate = 12 ^{o}C/min; agitator velocity = 49.5 rpm)..... 49

Figure 2-11. Percentage energy recovery in bio-coal (biomass load = 100 g; holding time = 30 min; heating rate = 12 ^{o}C/min; agitator velocity = 49.5 rpm)..... 49

Figure 2-12. Variation of (a) carbon; (b) hydrogen and (c) oxygen composition with maximum reaction temperature 51

Figure 2-13 Comparison between bomb calorimeter bio-coal's HHV values and bio-coal's HHV calculated from elemental composition..... 52

Figure 2-14. Van Krevelen diagram; variation on elemental composition..... 53

Figure 2-15. FTIR spectra for (a) feedstock biomass; and bio-coals produced at reaction temperatures of (b) 190 $^{\circ}$C, (c) 285 $^{\circ}$C, (d) 428 $^{\circ}$C and (e) 570 $^{\circ}$C..... 54

Figure 2-16. Hygroscopy of biomass, torrefied bio-coals and coke, reported in units of moisture at different tested times..... 55

Figure 2-17 Asymptotic hygroscopic values, reported in units of moisture when it has stabilized with time..... 56

Figure 2-18. pH of Bio-coal samples produced at different maximum temperature..... 57

Figure 3-1. MFR; General reactor diagram 65

Figure 3-2. Detail of the MFR flow feeding system..... 65

Figure 3-3. Fixed bed reactor diagram in a tubular furnace (1093 °C, 110 V, 8 Amp)..... 66

Figure 3-4. Feedstock; Birch bark biomass 67

Figure 3-5.Birch bark biomass cumulative particle size distribution as feed in the reactor... 68

Figure 3-6. Temperature history for the consecutive Pyrolysis – Activation Experiments at 665°C carried out in the MFR (holding times during activation of: 30min, 1h, 1h:30min, , CO_2 injection 0.59 L/min)..... 69

Figure 3-7. Process by stages for production of activated carbon: MFR pyrolysis experiment and activation in the fixed bed reactor (Figure 3-8). Activation done under equal conditions as MFR activation (Figure 3-6)..... 69

Figure 3-8. Temperature history for MFR bio-char production (with a maximum temperature of 665 °C) followed by fixed bed activation at 665 °C (holding times during activation of: 30min, 1h, 1h:30min, , CO_2 injection 0.59 L/min)..... 70

Figure 3-9. Bio-char Mass Yields at Different Maximum Process Temperatures in the MFR (Biomass load:100 g, Holding Time at a Maximum Temperature: 10 or 30 min, Agitator velocity: 49.5 rpm)..... 71

Figure 3-10. Bio-char Surface Areas at Different Maximum Pyrolysis Temperatures..... 71

Figure 3-11. (a) Activated Carbon Mass Yield from a Consecutive Pyrolysis - Activation in the MFR (Figure 3-6) and pyrolysis in the MFR with Activation in the Fixed Bed (Error! Reference source not found.) (Activation Temperature: 665 °C, CO_2 injection 0.59 L/min, holding times during activation of: 30min, 1h, 1h:30min) (b) Activated Carbon Mass Yield Presenting all data from Figure 3-11(a), Shifting Time on the x-axis for the Fixed Bed Activation..... 73

Figure 3-12. Activated Carbon Surface Areas with Consecutive Pyrolysis - Activation in the MFR (Figure 3-6) and Activation in the Fixed Bed (Figure 3-8) (Activation Temperature: 665 °C, CO_2 injection 0.59 L/min, holding times during activation of: 30min, 1h, 1h: 30min) 74

Figure 3-13. Activation Experiments Description; CO_2 Injection from a Low Temperature and CO_2 Injection only at a Maximum Process Temperature for Activation (Fixed Bed Reactor) (Maximum activation Temperature: 665 °C, CO_2 injection 0.59 L/min)..... 75

Figure 3-14. Overall Mass Loss during Pyrolysis and Activation with CO_2 Injection Points at different Temperatures (Figure 3-13)..... 77

Figure 3-15. Pyrolysis and Activation Experiments Description at Different Temperatures (Fixed Bed Reactor, activation holding time 1h, injection 0.59 L/min)..... 77

Figure 3-16. Activated carbons and bio-chars surface areas at different temperatures (Pyrolysis; maximum temperature holding time: 30 min, Activation; 1 h holding time at maximum temperature, 0.059 L/min CO_2, Figure 3-15) 78

Figure 3-17. Mass loss distribution on the fixed bed reactor; during pyrolysis and activation 79

Figure 3-18. Representative pH Values of high temperature bio-chars and activated carbon production at 665 °C (For different activation times: 30min, 1h, 1h 30min, 0.59 L/min CO_2) 80

Figure 4-1. MFR diagram 87

Figure 4-2. Fixed bed reactor in a tubular furnace (1093 °C, 110V, 8 Amp)..... 88

Figure 4-3 Bio-coal Mass Yields from Different Biomasses..... 90

Figure 4-4 Bio-oil Mass Yields from Different Biomasses 91

Figure 4-5. Non–condensable Gases Mass Yield from Different Biomasses..... 92

Figure 4-6 Biomass and Bio-coal High Heating Values for Different Biomasses 93

Figure 4-7 Percentage of Energy Recovery in Bio-coal from Different Biomasses..... 94

Figure 4-8. Maple wood biocoal – biomass hygroscopy, presented in moisture units reported at different tested times 95

Figure 4-9. Birch bark bio-coal – biomass hygroscopy, presented in moisture units reported at different tested times 96

Figure 4-10. Corn stalk bio-coal – biomass hygroscopy, presented in moisture units reported at different tested times 96

Figure 4-11. Switch grass bio-coal – biomass hygroscopy, presented in moisture units reported at different tested times..... 97

Figure 4-12. Coffee pulp bio-coal – biomass hygroscopy, presented in moisture units reported at different tested times..... 97

Figure 4-13. Microbial activity over bio-chars from coffee pulp, presented in moisture units reported at different tested times..... 98

Figure 4-14 Final hygroscopy values for biomass and bio-coal produced at different temperatures and from different feedstocks (units of final hygroscopy are given as equilibrium moisture percentage of samples exposed to saturated atmosphere)..... 99

Figure 4-15. Bio-char and activated carbon surface areas for different processed biomasses 100

Figure 4-16. Mass loss during activation for different feed biomasses 101

Figure 6-1. Gas Flow Diagram 108

Figure 6-2. Nitrogen flow calibration through pressure regulator..... 109

Figure 6-3 Carbon Dioxide Calibration through pressure regulator..... 109

Figure 6-4 Calibration Experimental set up..... 110

List of Appendices

Appendix 1 : Nozzle Calibration 108

1. Chapter 1: Introduction

1.1 Present Thesis Work

The aim of this thesis is to contribute with new knowledge to a better understanding of valorization of different biomass materials through slow pyrolysis for the production of bio-char and two possible commercial applications. Biomasses treated on this study are: a wood, a bark, a grass, and two agricultural residues. Applications studied are bio-coal production and bio-char production as a precursor of activated carbon. This study aims to understand better the operating conditions for the production and the product quality standards for both applications, to improve the characterization practices, and to select among the various types of biomass and process conditions those that are more suitable for bio-coal production or for further processing for activated carbon production.

This thesis is divided in three sections. The first section covers biomass torrefaction for bio-coal production utilizing woody biomass. The second deals with bio-char derived from birch bark biomass as precursor for activated carbon production. Finally, the third part discusses the suitability of different feedstocks for bio-coal and activated carbon production. This thesis is presented in an integrated article format.

The introduction chapter presents the background, motivation and needs for this research project by introducing pyrolysis processes and products, the bio-char definition, pyrolysis technologies for production of alternative energy, bio-char applications as a soil amendment, and production of activated carbon from a bio-char precursor.

1.2 Pyrolysis and products

Pyrolysis is defined as the thermal degradation of organic material in an oxygen-free atmosphere. This process is applied over a variety of feedstock, from agricultural and forestry biomass to municipal solid waste (1) and industry by-products. Thermal cracking of organic matter yields condensable vapors (typically referred to as “bio-oils”), gases (mainly carbon monoxide, carbon dioxide, and methane, with smaller amounts of hydrogen, ethane, and ethylene (2, 3)) and solid products (carbon-rich char and ashes).

Bio-oil is designated as a complex liquid mixture of depolymerisation products from cellulose, hemicelluloses and lignin, with hundreds of different organic compounds (3). It is typically produced as a dark, viscous liquid with a distinctive acidic and smoky smell, and it is considered as a valuable densified form of raw biomass material, precursor for the production of a variety of chemicals and fuels.

1.3 Bio-char

Bio-char is the solid product obtained through several thermal conversion processes (mostly torrefaction and pyrolysis and, to a minor extent, gasification and imperfect combustion). Bio-char's chemical and physical characteristics are prone to vary widely according to the processed feedstock and the production conditions. Bio-char is then defined by its production process rather than its chemical composition or structure (2).

1.4 Pyrolysis for production of alternative energy

Pyrolysis is a promising technology for production of alternative energy and chemical products. Its products are obtained through processing of renewable and abundant organic feedstocks and, particularly, inexpensive residual biomass derived from agricultural and forestry practices. Biomass is a renewable energy source defined as an organic material; it includes any plant material; agricultural and forestry, animal waste products, food residues, algae, etc (4). In addition to pyrolysis, other thermal conversion technologies for energy and chemicals production from biomass include torrefaction, gasification, hydro-thermal liquefaction and combustion processes (Figure 1-1). The main product of combustion is heat, which requires immediate use for heat and/or power generation. Gasification produces a fuel gas that can be used for combustion in turbines and engines for electrical power generation, or, better, as syngas, as a building block for many valuable chemicals. Drawbacks of this gas are high purity standards required for its applications, expensive storage and expensive upgrading processes.

Pyrolysis generates gas, liquids and solid products. The gas can be used to provide energy to power the pyrolysis process itself (5). The liquid Bio-oil can be a source of chemicals that could be extracted before further use or processing (6). The liquid Bio-oil can also be used as a low grade fuel oil and utilized for energy generation in specially designed

boilers or engines (7). Moreover, bio-oil can be upgraded to transportation fuels or co-processes with fossil fuels (8). Finally, bio-oil can also be gasified to produce clean ash-free tar-free syngas (9, 10). The solid bio-char product, on the other hand, once considered as a by-product to be minimized, is now being investigated as a potentially valuable co-product for numerous applications (11), such as Bio-coal as coal substitute (12), or Bio-char as a fertilizer and soil amendment, or as a Bio-adsorbent, especially when chemically or thermally activated.

An economical technology comparison was made by A. Evans (13) through a compilation of individual cost studies. The conclusions of this study highlight that combustion is still the cheapest technology due to the higher capital cost required by pyrolysis and gasification. In addition, this study reveals the reduction of gas emissions by the use of gasification and pyrolysis technologies, making evident the environmental benefits obtained by implementing pyrolysis and gasification processes (13).

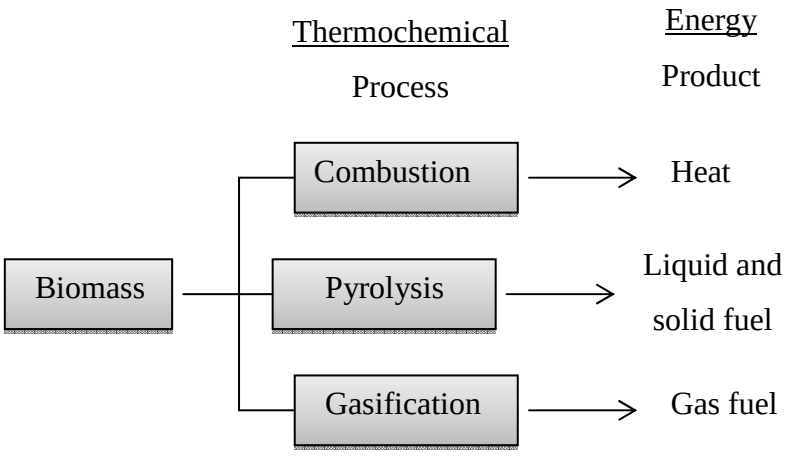

Figure 1-1. Biomass Thermochemical Conversion Processes and Products (14)

Pyrolysis processes are classified in two main groups, according to the characteristic process conditions: fast pyrolysis and slow pyrolysis. Such process conditions are: heating rate, final process temperature, and holding time at the maximum process temperature.

The typical characteristics of fast and slow pyrolysis are summarized as follows:

Fast pyrolysis processes are characterized by:

- High heating rates of the feedstock.
- Temperature ranging from 400 to 550 °C (2).
- Short vapor residence time around the order of 0.5 to 10 seconds (2)
- Low particle size of fed biomass (<3 mm); characteristic directly connected to high heating rates according to biomass low thermal conductivity.
- On the case of large biomass pieces; ablative techniques are used to expose the internal portions of the biomass (10).
- Rapid removal of char to avoid vapor catalytic cracking provoked by it (10).
- Rapid condensation of liquid products (10).

Slow pyrolysis processes are characterized by:

- Low heating rate of the feedstock.
- Long solid residence time: 30 min up to several hours (15)
- Final temperatures selected according to product requirements.

The yields of the pyrolysis products (bio-char, bio-oil and non-condensable gaseous products) depend highly on the process conditions and on the type of feedstock. A review by C. Di Blasi (10) discusses the main trends of the yields of Bio-char, Bio-oil and non - condensable gases achieved with fast and slow pyrolysis. The general trends discussed by C. Di Blasi can be summarized in relation to the various products as follows:

- Bio-oil production yield is favored by fast pyrolysis under optimal temperatures ranging between 470 to 550 °C. Yields achieved in this temperature range are typically between values of 65 wt% to 75 wt%. Bio-oil yields under and above this temperature range are lower. For slow pyrolysis Bio-oil yields are low at low pyrolysis temperatures, and range between 45 wt% to 55 wt % at the optimal pyrolysis temperatures of approximately 500°C.
- Bio-char yield trends under slow and fast pyrolysis progressively decrease with increasing the process temperature. Bio-char production is higher with slow pyrolysis compared to fast pyrolysis for a wide temperature range (Figure 1-2).

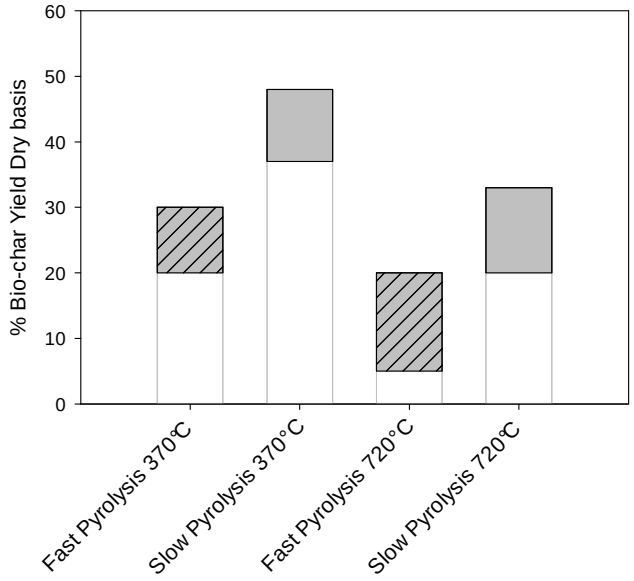

Figure 1-2. Bio-char mass yield values gathered by C. Di Blasi (16) Bar grey sections represent typical ranges over which empirical data fall for the pyrolysis type and temperatures mentioned on the x-axis.

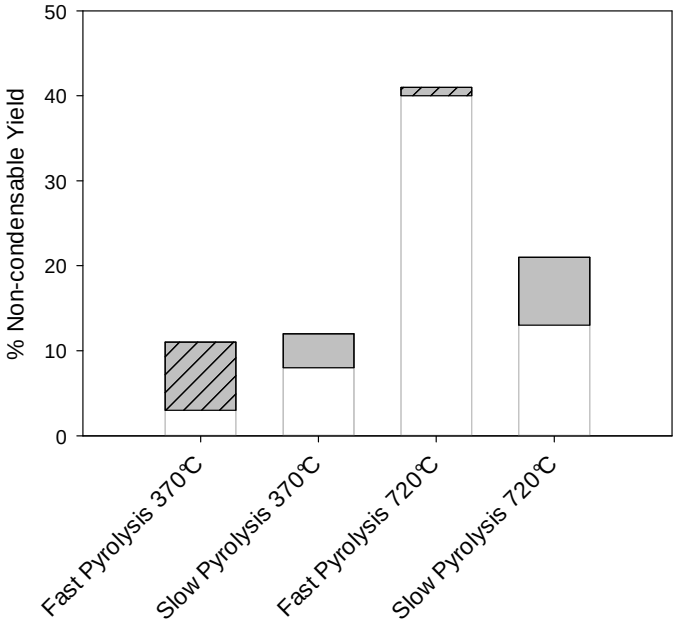

Figure 1-3. Non-condensable gas mass yield values gathered by C. Di Blasi (16) Bar grey sections represent typical ranges over which empirical data fall for the pyrolysis type and temperatures mention on the x-axis

Fast pyrolysis energetic studies are focused on Bio-oil production, foreseeing the benefits of using a liquid combustible for power generation (17). The main Bio-oil advantages are related to the high energy density, ease of handling liquids, low storage, and transportation costs (18). Uncertainties related to Bio-oil utilization for power generation are linked to instability, acids and alkali content (17), corrosiveness (3), fluctuation of bio-oil fuel quality, lack of available product specifications (18), costs and complexities of upgrading technologies. All of these are fields where research is still on-going. Bio-oil is produced under slow pyrolysis conditions with lower mass yields than under fast pyrolysis. However, the Bio-oil can still be used for both fuels as well as specialty chemicals; adhesives, resins, fertilizers, pesticides, food flavoring, and others (10).

1.4.1 Bio-char as a Product in Fast and Slow Pyrolysis

In the case of fast pyrolysis, Bio-char is typically considered a by-product that needs to be rapidly removed. Long residence times and high Bio-char hold ups are undesirable since Bio-char is known to act as a catalyst contributing to secondary vapor cracking, therefore decreasing Bio-oil yields. In addition, poor separation of Bio-char from condensed Bio-oil contributes to Bio-oil deterioration and instability. Separation of char in fluid bed pyrolyzers is usually carried out with one or more cyclones connected in series, and, sometimes, by hot filtration. Cyclones removal is not highly efficient while hot filtration has high efficiency but may lead to plugging problems. Bio-char removal for fast pyrolysis technologies is still an active area of research due to the difficulty of the downstream separation of Bio-char from Bio-oil (10). Some fast pyrolysis technologies utilize Bio-char to lower the energy input of the process. In this case, the produced Bio-char is transported to a combustion chamber as fuel to produce energy for the process.

Slow pyrolysis energetic studies are more directed to the use of Bio-char as Bio-coal, i.e. as a coal substitute. Slow pyrolysis produces higher Bio-char yields and high quality Bio-char. Advantages on using Bio-char for combustion are based on the expected lower net GHG emissions since the Bio-coal is produced from a renewable source (19).

1.5 Pyrolysis technologies

The accurate selection of the appropriate technology, including reactor design temperature control, inert gas flow, feeding system, is critically important in order to achieve the desired pyrolysis operating conditions of heating rate, temperature and holding time. Pyrolysis is known to be an unsteady process with difficult determination of kinetic constants, reason for which a great deal of empirical data is needed for technology optimization to achieve the desired product yields.

Nevertheless, there is abundant literature on kinetic studies, and plenty of new studies are still on-going within the scientific community for further optimization of technologies and product yields and quality (10). The major existing slow and fast pyrolysis technologies are listed and described in Table 1-1 and Table 1-2

Table 1-1. Slow Pyrolysis Technologies

Drum Pyrolyzer	Raw material is carried through a cylinder by paddles, the reactor is heated externally. Solid and vapour residence time is long, vapours experience high cracking producing high yield of non-condensable gases. Gases are usually sent to a firebox located below the drum to provide energy for the pyrolysis process (15).
Rotatory kilns	Inclined cylindrical reactor heated externally, biomass is moved by gravity through the kiln. Solid residence time is between 5 to 30 min (15).
Screw/Auger Pyrolyzers	Tubular reactor where biomass is moved through using an auger, it can be externally heated or heated by a heat carrier (sand, iron spheres). Operable at a small scale (15).
Flash Carbonizers	Ignition of flash fire in a packed bed under air flow and high pressure (15, 20).

Table 1-2. Fast Pyrolysis Technologies

Bubbling Fluidized Beds	High heating rates. Homogeneous temperature in the system providing good temperature control. Fluidizing gas flow and superficial velocity control the char and vapors residence times in the reactor. Technology highly researched; pilot plants have been implemented in Spain, Canada and UK. Char collection occurs by entrainment from the pyrolysis bed, vapor is passed through cyclones for char separation (10).
Circulating fluidized bed	This technology is a modified version of the bubbling fluidized bed where char and sand collected in the cyclones are transported to a combustion camera. In the combustion reactor char is combusted to generate heat for the pyrolysis process and the hot sand is recycled directly to bring the heat into the reactor (10).
Ablative reactors	Applied to large wood pieces. Heat transfer occurs between the reactor wall and the wood part in contact with the wall. The wood piece is under mechanical pressure, and, once this wood surface has been pyrolyzed, it is mechanically moved to allow the left un-pyrolyzed wood to attain contact with the hot reactor wall, until all wood has being pyrolyzed (10).
Entrained flow	Uses a gas as heat carrier medium. It has not been scaled up, most likely due to the limited heat transfer achieved by this technology (10).
Rotating cone	This technology uses centrifugal force to transport biomass upwards through a heated cone shaped reactor. Rotational speeds of around 600 rpm are applied to the cone for biomass transportation. This is a complex technology as rotating cones are joined with bubbling bed char combustors and risers for sand recycling for best energy usage (10).

Vacuum pyrolysis	Heat transfer is not as high as for the rest of fast pyrolysis technologies presented herein. However liquid yields are higher than those obtained by slow pyrolysis. Vacuum usage produces lower vapor residence times comparable with fast pyrolysis even when horizontal reactors with a moving bed of particles are employed. This technology is able to process larger particles than most fast pyrolysis reactors (10).

1.6 Bio-char Applications

The generic term “bio-char”, used to define the solid residue of pyrolysis processes, has now been linked to one of the possible applications of such material as a soil amendment and fertilizer. However, many applications of bio-carbon are now emerging and attracting the interests of the research community as well as of investors. If we were to define the solid co-product of pyrolysis with a more generic term, such as “bio-carbon”, applications with interesting potential include its use as:

1) Bio-coal, or coal substitute for combustion processes;
2) Bio-coke, for metallurgical applications;
3) Bio-char, for agricultural applications as soil amendment and fertilizer;
4) Bio-adsorbent, upon thermal and/or chemical activation;
5) Carbon sequestration technology;
6) a source of renewable carbon for Carbon-based advanced materials, such as carbon nanotubes, carbon fibers, and carbon-based composites and fillers.

In this thesis, two potential applications are explored: bio-carbon as bio-coal, and bio-carbon as bio-adsorbent. However, a very brief overview of the application of bio-char as a fertilizer and soil amendment is also provided, since this application is attracting a considerable attention worldwide.

1.6.1 Bio-char as Bio-coal

Biomass could be thought to be used directly instead of bio-char as a coal substitute. Biomass is an abundant, renewable, and inexpensive raw material. Problems with

biomass as a solid fuel are linked to the non-homogenous combustion characteristics, the low bulk density of the feedstock, the high affinity for water retention, the low energy content, and the perishable nature. Most of these problems are alleviated by applying mild pyrolysis, or Torrefaction, to biomass for obtaining bio-char. Torrefaction is the term designed to describe mild pyrolysis within a temperature range of 200-300 ^{o}C. Torrefaction adds to the energetic value of the biomass, gives homogeneity to the solid fuel, improves grindability, thus reducing comminution costs, and enhances combustion homogeneity, while substantially reducing the product water retention (12, 19, 21). This technology is subject of the research described in Chapters 2 and 4, which deal with Bio-char production and characterization as a substitute of coal.

1.6.2 Bio-carbon as Bio-char (soil amendment and fertilizer)

Bio-char production technologies partly resemble natural forest fires which are known as beneficial contributors to soil amendment through mineral enrichment. During forest fires, partly combusted and pyrolyzed biomass residues are produced and added naturally to the top layer of old soil, resulting in a natural process of re-fertilization. Such process is particularly evident in the Amazonian region of Brazil, where the practice of burning biomass and burying the residues has transformed a previously poor soil into a very fertile one, now known as “Terra Preta” (2). These findings have provided the motivation to investigate pyrolysis Bio-char as a soil amendment agent.

Agricultural practices have been using compost, manure, and chemical fertilizers applications on soils to enhance their productivity. Once a fertilizer is applied to a soil, the trend is its continuous use to meet productivity standards. Fertilizers, compost and manure applications generate pollution and have often detrimental effects, such as their contribution to greenhouse gas emissions by generation of methane, carbon dioxide and ammonia (15) or the dispersion of pathogens and heavy metals into the ground and the water system.

Bio-char used on soils can either release mineral nutrients to help plant development, or de-contaminate soils through pollutant adsorption to enhance plant growth by improving

soil quality. Use of bio-char can also avoid emission of global warming gases when applied to the soil (22).

1.6.3 Bio-char as a precursor of activated carbon

Biomass, Bio-char and its derivatives have been studied in an attempt to produce inexpensive adsorbents to cover the large demand of activated carbon for a broad range of environmental applications. This section reviews the background on the applicability of activated carbon, activated carbon production techniques and technologies, bio-char adsorption and bio-char as a precursor of activated carbon.

a. Activated carbon uses

Numerous applications are reported in the literature on the use of activated carbon from bio-char or biomass precursors. In Table 1-3, representative studies that have dealt with the particular application of activated carbon are summarized, along with the precursor material and the activation process type utilized.

Table 1-3. Application of activated carbon

Reference	**Feedstock**	**Process**	**Application**
(23)	Pine	Physical activation with flue gases.	For **thermo-catalytic decomposition of methane for hydrogen production**. Hydrogen is then used for energy production. In this study activated carbon is produced and regenerated with pyrolysis flue gases. The regeneration during the hydrogen production avoids frequent changes of catalyst due to poisoning.
(24, 25)	1.Palm shells 2. Solid	1.CO_2 physical activation. 2. KOH and	**H_2S removal** from a gas stream**.** H_2S is produced during coal gasification, in sewage treatment plants, in pulp and paper mills, refineries, and chemical plants. H_2S is also

	effluent for anaerobic digestion of dairy manure	H_2SO_4 Chemical activation 3. Steam physical activation	present in natural gas and petroleum deposits. OSHA has a ceiling concentration of 20 ppm and AIHA reports a maximum concentration of 30 ppm that a person can withstand for 1 hour without any permanent health damage. H_2S removal is also important for machinery, such as turbines, pipes, etc, as it is very corrosive.
(26)	Poultry Litter	Physical activation with steam	**Mercury adsorption** from flue gases. Mercury removal is needed to meet regulatory emissions from electric power plant boilers, natural gas and mercury cells used for chlorine production
(27, 28)	1.Oak Wood and Oak Bark 2. Oak cups pulp	1. Pyrolysis 2. Chemical activation with H_3PO_4 or $ZnCl_2$	**Chromium (IV) removal** from water streams. Persons and other living species can tolerate only a trace concentration of Cr (IV); higher concentrations are a cause of health problems. Cr (IV) is used in electroplating, metal finishing, magnetic tapes, pigments, leather tanning, wood protection, brass, electrical and electronic equipment. Wastewater streams from these industries will contain Cr (IV) in different quantities.
(29, 30)	Coffee residues	Physical activation	**Adsorption of formaldehyde** from air. Formaldehyde is found in paints, polymers, resins, adhesives, building material, and carpets. High concentrations cause health issues, with both chronic and temporal symptoms.

(30, 31)	1.Olive stones 2.Coconut shell	1.Chemical activation (H_3PO_4) under nitrogen Production of activated carbon discs 2. $ZnCl_2$ chemical activation + CO_2 physical activation	**Methane storage** for transportation fuels. Activated carbon from bio-char can store methane on its porous structure. Methane produces lower emissions of CO_2 than conventional fuels, is inexpensive, and reserves of large amounts previously un-exploited are now reachable with recent technology.
(32, 33)	1.Pecan 2.Shells Hazelnut	1.Chemical activation with H_3PO_4 under air 2. Chemical activation with H_2SO_4 under air	**Copper removal** from water streams. Copper is used in plating, electroplating, brass manufacture, mining, smelting, refineries, and agricultural chemicals. Waste water streams from these industries contain Cu (II) in different concentrations. Intake of copper by humans will cause health problems depending on its concentration. An acceptable concentration in drinking water, according to the WHO, is of less than 1.5 mg/l.
(28, 34)	1.Oak cups pulp 2. Rattan sawdust	1.Chemical activation with H_3PO_4 or $ZnCl_2$ 2. Pyrolysis + KOH chemical activation + CO_2 physical activation	**Phenol removal** from water streams. Phenols are found in wastewaters of petrochemical units, coal gasification, plastics and dyes manufacturing industries. Phenols are use in the production of epoxy and phenolic resins. They are harmful to humans at low concentrations and EPA regulation does not allow discharges of water streams with

			concentration higher than 1 mg/L. Phenols removal is also required in several processes, for example in the production of foods like molasses, vinegars and oils (35).
(28, 36)	1.Oak cups pulp 2.Sewage sludge	1.Chemical activation with H_3PO_4 or $ZnCl_2$ 2. pyrolysis or physical activation with CO_2	**Dye removal** from water. Dyes are found mainly in the effluents of the textile industry, and, in a lesser but still significant amount, in the wastewaters of leather, cosmetics, plastics, food, paper and pharmaceutical industries. These types of dyes are non-biodegradable, are stable, they generate an aesthetic problem, and some of them are toxic and carcinogenic (37, 38). Example of dyes are: Methylene Blue, Acid Red 111, Basic red 18, Brilliant blue, Rhodamine B, acid red 73, and reactive red 24.
(38, 39)	1.Baggase 2. Manure	1.CO_2 Physical activation, $ZnCl_2$, $MgCl_2$, and $CaCl_2$ chemical activation 2. Pyrolysis	**Lead adsorption** from water. Lead is poisonous. Maximum allow concentration in drinking water allowed by the EPA is of 15 ppb.
(40)	Rice husk	NaOH , KOH chemical activated carbons	**Hydrogen storage** for hydrogen to be applied in fuel cell for automotive transportation. Hydrogen is a cleaner fuel than conventional fuels. Physical adsorption onto activated carbon is being researched for a convenient and safe reversible uptake and release of H_2.
(40)	Rice husk	H_3PO_4 chemical activation	For manufacturing of **Electric double layer capacitors**. The efficiency of this products

			depends on the carbon content and on the porosity of the material.
(40)	Rice husk	CO_2 physical activation	**Catalytic support** for different applications.

Pollutant adsorption from gas and water stream onto activated carbon has great advantages among other available techniques. Activated carbon adsorption is a simple technology, easy to operate and implementable with inexpensive infrastructure. Additionally, activated carbon presents low sensibility for toxic substances decreasing as well extra operational costs.

Conventional activation processes are of two types: chemical and physical activation. Both techniques involve thermal treatment and an activation agent that promotes porosity formation. The main characteristics of these two processes are presented in Table 1-4, where difference and similarities between them are discussed.

Table 1-4. Comparison table between activation techniques

Physical Activation	**Chemical Activation**
- This is a two step process; 1st Biomass is pyrolyzed, 2nd Bio-char is activated. - Activation agents are: steam (41, 41), carbon dioxide, air, oxygen or their gas mixture. - Activation agents are added as injection of gases to the reactor at high temperature - Activation temperature is between 700 to 1000 °C - Clean technology; doesn't required recovery or	- This is a single step process; biomass is directly activated after its impregnation with a chemical substance (43) - Activation agents: phosphoric acid (H_2PO_4) (41), zinc chloride ($ZnCl_2$) (44), potassium hydroxide (KOH) (45) under nitrogen or air atmosphere (32) - H_2PO_4 and $ZnCl_2$ are dehydrating to the material promoting porous formation, while KOH causes gasification (46)

chemical disposal - The process parameters determining the product characteristics are: activation temperature, precursor nature (including carbonization history) and the oxidizing agent (42).	- Activation agents are added by impregnation before the thermal treatment. On occasions, impregnation agent is added while low temperature heating is applied (i.e. 85 °C, 160 °C (32)), this is to increase impregnation efficiency (30) - Activation temperature in the range of 400-600 °C. - Recovery and proper disposal of the activation agent is required for a sustainable process practice (i.e. recovery can be achieved by recycling the filtrate from the acid water wash done over the produced activated carbon onto the process as activated agent (28)) - Higher char yield, chemical impregnation reduces de production of tar (43) - The process parameters determining the product characteristics are: concentration impregnation-agent/feedstock, activation temperature and activation time (42).

Properties of the resulting activated carbon material are not only dependable on the process, but are as well dependant on the precursor material. Hence, there is some discrepancy in the literature about whether chemical or physical activation result in

mainly micro-porous or meso-porous distribution (47). Functional group formation onto the activated carbon surface could as well be affected by more than the type of activation used. This will certainly result in an effect on its adsorption performance.

As an example, two studies made with H_3PO_4 activation found contradicting results using different biomass; Dastqheib el al.(32) worked with pecan shells and found that the formation of oxygen acidic groups was satisfactory for copper adsorption, while Girgis et al. (44) worked with cotton stalks and did not find any significant change on the surface chemistry between the char and its activated form.

b. Activated Carbon technologies

Activation experimental set ups in laboratories are mainly done using horizontal (48, 49), vertical (50, 51) or rotary tubular furnaces (47, 52).

Higher scale production is done in rotary kilns (53) , rotary drums (44), steam gasifiers (54), and fluidized beds (55).

c. Bio-char as a pollutant adsorbent

A variety of studies are motivated on pyrolytic bio-chars adsorption for the removal of pollutants in gas and water streams without any further treatment. On this matter, the study by D. Mohan et al. (56) reports on the adsorption of Lead, Cadmium and Arsenic from water by oak and pine (wood and bark) Bio-chars, Liu et al. (57) focused on enhancing the phenol adsorption on rice-husk and corncobs Bio-chars by improving their production varying the residence time in a fast pyrolysis system, Mui et al. (58) worked with bamboo Bio-char on the adsorption of three different water dyes (Acid Blue 25, Acid Yellow and Methylene blue) concluding higher affinity of the produced Bio-char for Methylene Blue (58).

Many bio-char adsorption studies have focused on soil amendment applications. For example, Ying Yao et al. (59) carried out a comprehensive study on Sulfamethoxazle adsorption; this is a pharmaceutical pollutant found in waste water treatment, which has high mobility through ground water and it is toxic to aquatic life. In this study, Bio-char adsorption was evaluated on eight different activated carbons produced from four types

of biomass. His study reports efficiency of Bio-chars to retain this compound to different degrees, diminishing soil leachate. Xiang-Yang Yu et al. (60) studied the adsorption of insecticide acetamiprid on three different types of soil by a red gum wood Bio-char. Bio-char adsorption effectiveness and reduction of the dissipation of the pollutant through the soil was found to be dependable on the organic content on the soil, hence a higher effect upon adding Bio-char to the soil was reported in soils with lower organic content. These studies, and many others not mentioned here, make evident the existence of potential solutions on soil amendment through Bio-char incorporation in the soil and/or by Bio-char pollutant adsorption. A particular Bio-char should be produced with characteristics optimized depending on the soil kind and pollutant to be removed. A great compilation of these studies is found in the classic book by J. Lehmann's and S. Joseph, 2009 (15). However, research is needed to better relate feedstock chatacteristics, production operating conditions and final performance in any of the applications mentioned here.

d. Important Characteristics on an adsorbent

In testing the adsorption of pollutants, the first experimental phase consists in the verification of the adsorbent in an isolated medium. Adsorption capacity of an adsorbent with respect to a particular adsorbate is known to be influenced by available surface area, pore size distribution and surface chemistry of the absorbent as well as nature related characteristics of the adsorbate, as chemical structure and particle size. A comprehensive study on lead adsorption by Bagasse activated carbons done by Zhang et al. (38) shows mathematically the dependency of the properties mentioned above, proposing two different models for lead adsorption based on empirical data. This study, among similar ones, leaves us with very useful models that will allow improving efficiently the selection of adsorbents for particular applications. In real applications, however, isolated media are rarely found and performance of adsorbents are usually threatened by medium acidity or base characteristic (61), temperature, presence of other adsorbate species (62), etc, all parameters which lower the adsorbent performance and leave a broad field for further research.

Among the above mentioned properties influencing adsorption processes, the available surface area and the pore size distribution are, if not the main, two of the most important

required characteristics of an adsorbent for being considered suitable for profitable commercial applications. The next section discusses the surface area characterization of bio-chars and sets the background to consider bio-char as a suitable precursor for activated carbon production.

e. Bio-char: Surface area characteristics

Slow pyrolysis, fast pyrolysis and gasification studies have reported lower surface area values for their bio-char products in comparison to the surface areas of typical commercial activated carbon (found in the range of: 400 to1200 m^2/g) (63). There is a large body of literature discussing this observation, and only some of them are mentioned here:

The work of Brewer et al. (64) describes Bio-chars produced by three technologies: slow pyrolysis, fast pyrolysis and gasification, utilizing two feedstocks (switch grass and corn stover). The highest values of surface areas were found to be 50.2 m^2/g for switch grass and 20.9 m^2/g for corn stover, for bio-chars produced by slow pyrolysis (at 500 °C). Fast pyrolysis (at 500 °C) bio-char were reported to have areas from 7 to 21.6 m^2/g, while gasification at 730-760 °C produced bio-char products with areas from 23.9 to 31.4 m^2/g (64). A study by Marquez et al. (65) dealing with the activation of grape fruit skin, reports surface area of the pyrolyzed products of just 10 m^2/g, obtained under a pyrolysis of 700 °C with a holding time of 2 hours at that operating temperature (65).The work of D. Mohan et al.(56) reports bio-chars produced by fast pyrolysis at temperatures of 400 and 450 °C from oak wood, pine wood, oak bark and pine bark obtaining the following surfaces areas: 2.04, 2.73, 25.4 and 1.88 m^2/g, respectively. This study reveals the affinity for some of the produced Bio-chars to adsorb lead and in lesser quantity cadmium and arsenic; still these Authors recognize the need for activation practices to enhance the potential of the bio-chars analyzed for their adsorption characteristics for heavy metals as applied to soil remediation.

Even though practices of activation are popular over Bio-chars to enhance its low surface areas and there is high amount of literature on this topic, it has been reported by some authors the production of high surface area by just pyrolysis practices.

Y. Yao et al.(59) reported 336 m^2/g area for a digested sugar beet tailing Bio-char produced by slow pyrolysis at 600 °C with 2 h holding time, as opposed to the reported 2.6 m^2/g area for raw sugar beet tailing Bio-char produced under the same conditions and technology. The study suggests a significant dependency on the characteristics of the precursor material for final surface area development. A more recent study of Y. Yao et al. (59) shows that more feedstocks were found to have large surface area by only pyrolyzing them at a high temperature. In that case, Bio-chars were produced with the same technology and manufactured from brazilian peppers, bamboo, sugar Bagasse and hickory wood. Such Bio-chars produced at a temperature of 600 °C had areas of 234 m^2/g, 375.5 m^2/g, 388.3 m^2/g and 401.0 m^2/g , respectively, while Bio-chars produced at 450 °C had only areas in the range between 0.7 and13.6 m^2/g (59). Y. Chen et al. (66) investigated Bio-chars manufactured from cotton stalks, achieving surface areas between 94 and 224 m^2/g for Bio-chars produced by fast pyrolysis in the temperature range of 550-750 °C, using 30 min holding time. It could be mistakenly concluded from these studies that high temperature pyrolysis increase significantly surface areas of any Bio-char. However, it is important to remember that the examples aforementioned encounter low surface area using also high pyrolysis temperatures with different production technologies. This brief review highlights the importance of feedstock specific research on the adsorbent production field.

f. Characteristics of Bio-char as a precursor of activated carbon

The lack of an appropriate surface area development in Bio-char products makes them unsuitable for industrial and commercial applications. Nevertheless Bio-char presents important physical and chemical characteristics as a precursor of activated carbon, such as low inorganic content, high concentrated carbon, and a non-graphitable carbon structure (63).

Bio-chars also offer benefits related to the production cost of activated carbon by a renewable source (67). Bio-chars fulfill the requirements postulated by G. Crini (68) to characterize an inexpensive raw material for any process. According to G. Crini, the abundance of a feedstock material in nature, and the characterization of it as a waste by-product of an existent process or an up-coming process, makes a raw material

inexpensive and suitable for further valorization. In the case of thermal cracking technologies for energy and chemicals production (torrefaction, pyrolysis, gasification) bio-oil and syngas production are classified as potentially viable up-coming industries, and, therefore, Bio-char is been researched to overcome its status as waste by-product, and to consider it as a true co-product and as an inexpensive and renewable source of value-added products. The following table lists available reviews related to the production of activated carbon from agricultural material; all reviews presented in the table have a different study focus and include numerous studies made either with different activation techniques, different feedstocks and/or product comparisons according to a specific adsorptive application.

Table 1-5. Reviews on the production of activated carbon from agricultural material

Reference Year	**Number of Papers Included in the Review**	**Title**
(69)	185 (74 of which are on agricultural materials)	Adsorption of Methylene Blue on low-cost Adsorbents: A review
(70)	322	Utilization of Agro-industrial and Municipal Waste Material as Potential adsorbents for Water Treatment – A Review
(71)	469	Application of Low-cost Adsorbents for Dye Removal - A Review
(72)	96	Removals of Heavy Metal Ions from Wastewater by Chemically Modified plant waste as Adsorbents
(73)	109	Agricultural Residues as Precursors for Activated Carbon Production- A Review
(67)	153	Waste Materials for Activated Carbon Preparation and its use in aqueous treatment: A

		review
(68)	210	Non-conventional low-cost Adsorbents for Dye Removal: A review
(74)	68	Rice husk as a Potentially low-cost Biosorbent for Heavy Metals and Dye Removal: an Overview
(75)	100 (7 of which are on agricultural materials)	Low-cost Adsorbents for Heavy Metals Uptake from Contaminated Water: A Review
(76)	60	The Role of Sawdust in the Removal of Unwanted Materials from Water

In this thesis work, Chapter 3 presents the activation study conducted utilizing bio-char produced from birch bark and, specifically, its CO_2 activation. In Chapter 4, CO_2 activation is applied to several bio-chars produced from different representative biomass feedstocks. The comparative study is aimed at providing a better understanding of product characteristics according to the source material utilized as feedstock.

1.7 References

1. A. N. Phan, C. Ryu, V. N. Sharifi, J. Swithembank. Characterization of Slow Pyrolysis Products from Segregated Wastes for Energy Production. J. of Anal. and Appl. Pyrolysis 2008; 81 (1): 65-71.

2. J. Lehmann. Biochar for Environmental Management: Science and technology 2009.

3. S. Czernik, A. V. Bridgwater.Overview of Application of Biomass Fast Pyrolysis. Energy fuels 2004; 18 (2): 590-598.

4. P. Basu. Biomass Gasification and Pyrolysis Practical Design. Elsevier Inc 2010.

5. J. Gañan, J. F. González, C. M. Gonzáles - Garcia, E. M. Cuerda- Correa, A. Macias-García. Determination of the Energy Potential of Gases Produced in the Pyrolysis

Processes of the Vegetal Carbon Manufacture Industry. Bioresource Technology 2006; 97 (5): 711-720.

6. A. S. Pollard, M. R. Rover, R. C. Brown. Characterization of Bio-oil Recovered as Stage Fractions with Unique Chemical and Physical Properties. J. of Anal. and Appl. Pyrolysis 2012; 93: 129 -138.

7. S. Gust. Combustion Experiences of Flash Pyrolysis Fuel in Intermediate Size Boilers. Developments in Thermochemical Biomass Conversion 1997; 1: 481-488.

8. M. R. Pelaez-Samaniego, J. Mesa- Perez, L.A. B. Cortez, J. D. Rocha, C. G. Sanchez, H. Marin. Use of Blends of Gasoline with Biomass Pyrolysis-Oil Derived Fractions as Fuels in an Otto Engine. Energy for Sustainable Development 2011; 15 (4): 376 - 381.

9. D. Rennard, R. French, S. Czernik, T. Josephson, L. Schmidt. Production of Synthesis Gas by Partial Oxidation and Steam Reforming of Biomass Pyrolysis Oils. International Journal of Hydrogen Energy 2010; 35 (9): 4048 -4059.

10. A. V. Bridgwater. Review of Fast Pyrolysis of Biomass and Product Upgrading. Biomass and Bioenergy 2012; 38: 68-94.

11. M. P. McHenry. Agricultural Bio-char Production, Renewable Energy Generation and Farm Carbon Sequestration in Western Australia. Certainty, Uncertainty and Risk. Agriculture. Ecosystems and Environment 2009; 129 (1-3): 1–7.

12. D. Agar M. Wihersaan. Bio-coal, Torrefied Lignocellulosic Resources – Key Properties for its Use in Co-firing with Fossil Coal - Their Status. Biomass and Bioenergy. 2012; 44: 107-111.

13. A. Evans, V. Strezov, T. J. Evans. Sustainability Considerations for Electricity Generation from Biomass. Renewable and Sustainable Energy Reviews 2010; 14 (5): 1419-1427.

14. J. J. Chew V. Doshi. Recent Advances in Biomass Pretreatment - Torrefaction Fundamentals and Technology. Renewable and Sustainable Energy Reviews. 2011; 15 (8): 4212 - 4222.

15. J. Lehmann S. J. Bio-char for Environmental Management: Science and Technology 2009.

16. C. Di Blasi. Combustion and Gasification Rate of Lignocellulosic Chars. Progress in Energy and Combustion Science 2009; 35 (2): 121-140.

17. A. Ganesh R. Banerjee. Biomass Pyrolysis for Power Generation - A Potential Technology. Renewable Energy 2001; 22 (1-3): 9-14.

18. D. Chiaramonti, A. Oasmaa, Y. Solantausta. Power Generation Using Fast Pyrolysis Liquids from Biomass. Renewable and Sustainable Energy Reviews. 2005; 11 (6): 1056-1086.

19. M. J. C. Van der Stelt, H. Gerhauser, J. H. A. Kiel, K. J. Ptasinski. Biomass Upgrading by Torrefaction for the Production of Biofuels: A review. Biomass and Bioenergy 2011; 35 (9): 3748-3762.

20. M. J. Antal, K. Mochidzuki, L. S. Paredes. Flash Carbonization of Biomass. Industrial and Engineering Chemistry Research 2003; 42 (16): 3690-3699.

21. P. Rousset, C Aquiar, N. Labbe, J. M. Commandre. Enhancing the Combustible Properties of Bamboo by Torrefaction, Bioresource Technology 2011: 102 (17); 8225-8231.

22. C. J. Barrow. Biochar: Potential for Countering Land Degradation and for Improving Agriculture. Applied Geography 2012; 34: 21-28.

23. A. Celzard, V. Fierro, E. Martin, F. Broust, A. Zoulalian. Catalytic Decomposition of Methane Over a Wood Char Concurrently Activated by a Pyrolysis Gas. Applied Catalysis 2008; 346 (1-2): 164-173.

24. J. Guo, Y. Luo, A. C. Lua, R. Chi, Y. Chen, X. Bao, S. Xiang. Adsorption of Hydrogen Sulphide (H_2S) by Activated Carbons Derived from Oil-Palm Shell. Carbon. 2007; 45 (2): 330-336.

25. A. J. White. Development of an Activated Carbon from Anaerobic Digestion By-product to Remove Hydrogen Sulfide from Biogas [Dissertation]. University of Toronto 2010.

26. K. T. Klasson, I. M. Lima, L. L. Boihem Jr. Poultry Manure as Raw Material for Mercury Adsorbents in gas Application. J. Appl. Poult. Res. 2009; 18 (3): 562-569.

27. S. Rajput, V. K. Singh, P. H. Steele, C. U. Pittman Jr. Modeling and Evaluation of Chromium Remediation from Water Using Low Cost Bio-char, a Green Adsorbent. Journal of Hazardous Materials 2011; 188 (1-3): 319-333.

28. S. Timur, I. C. Kantarli, S. Onenc, J. Yanik. Characterization and Application of Activated Carbon Produced from Oaks Cups Pulp. J. of Anal. and App. Pyrolysis 2010; 89 (1): 129-136.

29. V. Boonamnuayvitaya, S. Sae-ung, W. Tanthapanichakoon. Preparation of Activated Carbons from Coffee Residue for the Adsorption of Formaldehyde. Separation and Purification Technology. 2005; 42 (2): 159-168.

30. M. Molina-Sabio, C. Almansa, F. Rodríguez-Reinoso. Phosphoric Acid Activated Carbon Discs for Methane Adsorption. Carbon 2003; 41 (11): 2113- 2119.

31. M. J. Darabi Mahboub, A. Ahmadpour, H. Rashidi. Improving Methane Storage on Wet Activated Carbons at Various Amounts of Water. Journal of Fuel Chemistry and Technology. 2012; 40 (4): 385-389.

32. S. A. Dastgheib, D. A. Rockstraw. Pecan Shell Activated Carbon: Synthesis, Characterization, and Application for the Removal of Copper from Aqueous Solution. Carbon 2001; 39 (12): 1849-1855.

33. E. Dermibas, N. Dizge, M. T. Sulak, M. Kobya. Adsorption Kicnetics and Equilibrium of Copper from Aqueous Solutions Hazelnut Shell Activated Carbon. Chemical Engineering Journal 2009; 148 (2-3): 480-487.

34. B. H. Hameed, A. A. Rahman. Removal of Phenol from Aqueous Solutions by Adsorption onto Activated Carbon Prepared from Biomass Material. Journal of Hazardous Materials. 2008; 160 (2-3): 576-581.

35. F. López, F. Medina, M. Prodanov, C. Güell. Oxidation of Activated Carbon: Application to Vinegar Decolorization. Journal of Colloid and Interface Science 2003; 257 (2): 173-178.

36. C. Jindarom, V. Meeyoo, B. Kitiyanan, T. Rirksomboon, P. Rangsunvigit. Surface Characterization and Dye Adsorptive Capacities of Char Obtained from Pyrolysis/Gasification of sewage Sludge. Chemical Engineering Journal 2007; 133 (1-3): 239- 246.

37. X. Xu, B.-Y. Gao, Q.-Y. Yue, Q.-Q. Zhong. Preparation and Utilization of Wheat Straw Bearing Amine Groups for the Sorption of Acid and Reactive Dyes from Aqueous Solutions. Journal of hazardous materials 2010; 182 (1-3) : 1-9.

38. K. Zhang, W. H. Cheung, M. Valix. Roles of Physical and Chemical Properties of Activated Carbon in the Adsorption of Lead Ions. Chemosphere 2005; 60 (8): 1129 - 1140.

39. X. Cao, L. Ma, B. Gao W. Harris. Dairy-Manure Derived Bio-Char Effectively Sorbs Lead and Atrazine. Environmental Science Technology 2009; 43 (9): 3285-3291.

40. Y. Chen, Y. Zhu, Z. Wang, Y. Li, L. Wang, L. Ding, X. Gao, Y. Ma, Y. Guo. Application Studies of Activated Carbon Derived from Rice Husks Produced by Chemical - Thermal Process - A review. Advances in Colloid and Interface Science 2011; 163 (1): 39- 52.

41. B. S. Girgis, A. M. Soliman, N. A. Fathy. Development of Micro-Mesoporous Carbons from Several Seed Hulls Under Varying Conditions of Activation. Microporous and Mesoporous Materials 2010; 142 (2-3): 518 - 525.

42. S. J. Allen, L. Whitten. The Production and Characterisation of Activated Carbon. A Review. Developments in Chemical Engineering and Mineral Processing. 1998; 6 (5): 231-261.

43. A. Ahmadpour, D. D. Do. The Preparation of Activated Carbon from Macadamia Nutshell by Chemical Activation. Carbon. 1997; 35 (12): 1723 - 1732.

44. B. S. Girgis, E. Smith, M. M. Louis, A. - N. A. El- Hendawy. Pilot Production of Activated Carbon from Cotton Stalk Using H_2PO_4. J. of Anal. and App. Pyrolysis 2009; 86: 180 - 184.

45. R. Azargohar. Bio-Char as a Precursor of Activated Carbon Applied biochemical Biotechnology 2006; 131 (1-3): 762 - 773.

46. G. P. Meisner, Q. Hu. High Surface Area Microporous Carbon Materials for Cryogenic Hydrogen Storage Synthesized Using New Template - Based and Activation - Based Approaches. Nanotechnology 2009; 20 (20); 204023.

47. G. San Miguel, G. D. Fowler, C. J. Sollars. A Study of the Characteristics of Activated Carbon Produced by Steam and Carbon Dioxide Activation of Waste Tyre Rubber. Cabon 2003: 41 (5); 1009-1016.

48. M. Molina-Sabio, M. T. Gonzalez, F. Rodriguez - Reinoso, and A. Sepulveda. Effect of Steam and Carbon Dioxide Activation in the Micropore Size Distribution of Activated Carbon. Carbon. 1996; 34 (4): 505 - 509.

49. A. M. Warhurst, G. L. McConnachie. Characterisation and Applications of Activated Carbon Produced from Moringa Oleifera Seed Husks by Single - Step Steam Pyrolysis. Water Research 1997; 31 (4): 759-766.

50. C. Sentorun - Shalaby, M. G. Ucak - Astarliog, L. Artok, C. Sarici. Preparation and Characterization of Activated Carbons by One - Step Steam Pyrolysis / Activation from Apricot Stones. Microporous and Mesoporous Materials 2006; 88 (3): 126 - 134.

51. R. Azargohar, A.K. Dalai. Steam and KOH Activation of Biochar: Experimental and modeling Studies. Microporous and Mesoporous Materials 2008; 110 (2-3): 413–421.

52. V. Minkova, S. P. Marinov, R. Zanzi, E. Bjornbom, T. Budinova, M. Stefanova, L. Lakov. Thermochemical Treatment of Biomass in a Flow of Steam or in a Mixture of Steam and Carbon Dioxide. Fuel Processing Technology 2000; 62 (1): 45-52.

53. I. M. Lima, A. McAloon, A. A. Boateng. Activated Carbon from Broiler Litter: Process Description and Cost of Production. Biomass and Bioenergy 2008; 32 (6): 568 - 572.

54. A. Garcia-Garcia , A. Gregorio, C Franco, F. Pinto, D. Boavida, I. Gulyurtlu. Unconverted Chars Obtained During Biomass Gasification on a Pilot Scale Gasifier as a Source of Activated Carbon Production. Bioresource Technology 2003; 88 (1): 27 - 32.

55. I. Martin-Gullon, M. Asensio, R. Font, A. Marcilla. Steam- Activated Carbon from a Bituminous Coal in a Continuous Multistage Fluidized Bed Pilot Plant. Carbon. 1996; 34 (12): 1515-1520.

56. D. Mohan, C. U. Pittman Jr., M. Bricka, F. Smith, B. Yancey, J. Mohamed, P.H. Steele, M. F. Alexandre-Franco, V. Gomez-Serrano, H. Gong. Sorption of Arsenic, Cadmium and Lead by Chars Produced from Fast Pyrolysis of Wood and Bark During Bio-Oil Production. Journal of colloid and interface science 2007; 310 (1): 57-73.

57. W. - J. Liu, F. - X. Zeng, H. Jiang, X. - S. Zhang. Preparation of High Adsorption Capacity Bio-Chars from Waste Biomass. Bioresource Technology 2011; 102 (17): 8247 - 8252.

58. E. L. Mui, W. H. Cheung, M. Valix, G. McKay. Dye Adsorption onto Char from Bamboo. Journal of Hazardous Materials 2010; 177 (1-3): 1001 -1005.

59. Y. Yao, B. Gao, H. Chen, L. Jiang, M. Inyang, A.R. Zimmerman, X.Cao, L. Yang, Y. Xue, H. Li. Adsorption of Sulfamethoxazole on Bio-Char and its Impact on Reclaimed Water Irrigation. Journal of Hazardous Materials 2012; 209-210: 408-413.

60. X. Y. Yu, C. L. Mu, C. Gu, C. Liu, X. J. Liu. Impact of Woodchip Bio-Char Amendment on the Sorption and Dissipation of Pesticide Acetamiprid in Agricultural Soils. Chemosphere 2011; 85 (8): 1284-1289.

61. Y. S. Al-Degs, M. I. El-Barghouthi, A. H. El Sheikh, G. M. Walker. Effect of Solution PH, Ionic Strength, and Temperature on Adsorption Behaivor of Reactive Dyes on Activated Carbon. Dyes and Pigments 2008: 77 (1); 16-23.

62. C. Pelekani, V. L. Snoeyink. Competitive Adsorption Between Atrazine and Methylene Blue on Activated Carbon: the Importance of Pore Size Distribution. Carbon. 2000; 38 (1): 1423 - 1436.

63. H. Marsh FR. Activated carbon. Elsevier Ltd; 2006.

64. C. E. Brewer, K. Schmidt-Rohr, J. A. Satrio, R. C. Brown. Characterization of Bio-char from Fast Pyrolysis and Gasification Systems. Environmental Progress & Sustainable Energy 2009; 28 (3): 386-396.

65. F. Marquez-Montesinos, T. Cordero, J. Rodríguez-Mirasol, J. J. Rodríguez. CO_2 and Steam Gasification of a Grapefruit Skin Char. Fuel 2002; 81(4): 423 - 429.

66. Y. Chen, H. Yang, X. Wang, S. Zhang, H.Chen. Biomass-Based Pyrolytic Polygeneration System on Cotton Stalk Pyrolysis: Influence of Temperature. Bioresource Technology. 2012; 107: 411-418.

67. J. M. Dias, M. C. M. Alvim-Ferraz, M. F. Almeida, J. Rivera-Utrilla, M. Sánchez-Polo. Waste Materials for Activated Carbon Preparation and its Use in Aqueous-Phase Treatment: A review. Journal of environmental management. 2007; 85 (4): 833-846.

68. G. Crini. Non-conventional Low-Cost Adsorbents for Dye Removal: A Review. Bioresource Technology 2006; 97 (9): 1061-1085.

69. M. Rafatullah, O. Sulaiman, R. Hashim, A. Ahmad. Adsorption of Methylene Blue on Low-Cost Adsorbents: A Review. Journal of Hazardous Materials 2010; 177 (1-3): 70 - 80.

70. A. Bhatnagar. Utilization of Agro-Industrial and Municipal Waste Materials as Potential Adsorbents for Water Treatment - A review. Chemical Engineering Journal 2010; 157 (2-3): 277 -296.

71. V. K. Gupta. Application of Low - Cost Adsorbents for Dye Removal - A Review. Journal of Environmental Management 2009; 90 (8): 2313 - 2342.

72. W. S. Wang Ngah, M. A. K. M Hanafiah. Removals of Heavy Metal Ions from Wastewater by Chemically Modified Plant Waste as Adsorbents. Biosresource Technology 2008; 99 (10): 3935 - 3948.

73. O. Ioannidou. Agricultural Residues as Precursors for Activated Carbon Production-A review. Renewable and Sustainable Energy Reviews 2007; 11 (9): 1966 - 2005.

74. T. G. Chuah, A. Jumasiah, I. Azni, S. Katayon, S. Y. Thomas Choong. Rice Husk as a Potentially Low-Cost Biosorbent for Heavy Metal and Dye Removal: An Overview. Desalination 2005; 175 (3): 305-316.

75. S. Babel, T. A. Kurniawan. Low-cost Adsorbents for Heavy Metals Uptake from Contaminated Water: A Review. Journal of Hazardous Materials. 2003; 97 (1-3): 219 - 243.

76. A. Shukla, Y.- H. Zhang, P. Dubey, J. L. Margrave, Shyam. The Role of Sawdust in the Removal of Unwanted Materials from Water. Journal of Hazardous Materials. 2002; 95 (1-2): 137-1352.

2. Chapter 2: Bio-coal Production from the Torrefaction of Maple Wood Biomass

2.1 Introduction

Substituting conventional fuel with biomass for combustion has raised a large interest to date in attempt to achieve sustainable energy production. According to a 2010 survey of energy resources, 10 % of the total 2008 global energy demand was covered by biomass and 87 % of this biomass percentage was cover by woody type of biomass. It's estimated that the world energy demand quantities will rise for 2015 and biomass will have a greater contribution without a fixed specification on the biomass type covering this future demand (1). While biomass has a large potential as a fuel to replace coal for electricity production, the fuel characteristics of biomass varies widely. A consistent biomass supply is critical to ensure maximum combustion efficiency (2). Biomass has other problematic properties such as hygroscopicity, low heating value, non-homogeneous moisture content and non-homogeneous behavior during combustion. Hygroscopic fuels lead to storage problems, decrease in calorific value and increased transportation costs. A method to eliminate these problems is the thermal upgrade of biomass by torrefaction. Torrefaction is the low temperature (200-300 ^{o}C) thermal conversion (i.e. mild pyrolysis) of biomass. This technique provides a means to remove oxygen from biomass and decompose hemicellulose to ultimately produce a fuel with increased energy density (3). Lignin and cellulose can also decompose in the torrefaction temperature range, to a lesser degree (4).

Recently Chen and Kuo (5) studied the effect of torrefaction temperature on five specific constituents of biomass: hemicellulose, cellulose, lignin, xylan and dextran. At a torrefaction temperature of 230 ^{o}C, the authors did not observe any significant impact on the biomass properties as only some moisture and light volatiles were released. At 260 ^{o}C, hemicellulose was partially pyrolyzed while lignin and cellulose remained relatively unaffected. Lastly, it was found that large amounts of hemicellulose and cellulose were destroyed at torrefaction temperatures of 290 ^{o}C, resulting in a large consumed mass. Chen and Kuo (6) conclude that the ideal properties of torrefied biomass would be achieved at 260 ^{o}C without compromising mass. In addition, torrefaction of a blend of

hemicellulose, lignin and cellulose was studied and no interactions were observed. Thus weight loss from torrefaction could be predicted from the superposition of the weight losses of the separate constituents (5,6).

Recently, van der Stelt et al. (3) provided a comprehensive review of torrefaction technology. The products of torrefaction are solid (bio-coal), liquid (bio-oil) and gaseous (bio-gas), as with the thermal treatment of biomass at temperatures above the torrefaction range. It should be noted that the solid product is also referred to as bio-char and bio-coal is used when the objective is to produce a coal substitute. The properties of the products depend on biomass type and torrefaction conditions such as residence time and reaction temperature (3). There has been significant progress recently in the torrefaction technique and Table 2-1 highlights some interesting studies found in the literature.

Table 2-1. Overview: torrefaction in the literature

Reference and year	Biomass	Temperatures ($^{\circ}$C)	Characterizations
(7) 2008	Eucalyptus	240, 260, 280	TGA analysis, grindability, proximate and ultimate analyses, gross calorific values
(5) 2011	Lauan	220, 250, 280	TGA analysis, grindability, proximate, elemental and fiber analyses, heating value
(8) 2005	wood briquettes	220, 250, 270	proximate analysis and heating value, moisture and hydrophobic characteristics, elemental analysis
(9) 2012	corn stover	200, 250, 300	proximate and ultimate analyses, heating value

(10) 2012	Beech	200, 230, 245, 270, 300	NMR, EPR, elemental analysis
(11) 2012	cotton stalk, prosopis, sugarcane bagasse	300	proximate analysis, gross calorific values, bulk density, moisture content
(12) 1990	wood (type not given)	250-260 and 260-270	proximate and ultimate analyses, smoke and combustion tests, density
(13) 2011	clean pine chips, and Southern yellow pine logging residue chips	225, 250, 275, 300	moisture content, grindability, particle size, bulk and particle densities, heat content, proximate and ultimate analyses, chemical composition
(14) 2006	beech, willow, larch, straw	230-300 (10 ºC increments)	proximate and ultimate analyses, heating value,
(15) 2011	Bamboo	220, 250, 280	gross calorific value, proximate and ultimate analyses, heating value, FTIR
(16) 2011	Beech	220, 250, 280	NIRS
(17) 2009	wheat straw, rice straw, cotton gin waste	260, 315	moisture, pH, heating value, ash content, fixed carbon
(18) 2011	empty fruit bunches, mesocarp fiber, kernel shell	220, 250, 300	elemental analysis, heating values, moisture content

(19) 2011	white leadtree (*Leucaena leucocephala*)	200, 225, 250, 275	proximate and ultimate analyses, heating value, TG-MS

The upgrading of biomass by torrefaction is not only important when the product is used for combustion purposes. In gasification, pre-treatment of biomass (wood) by torrefaction can lead to gasifier designs with higher efficiency than those using untreated biomass for gasification (20). Untreated wood, although a clean fuel, is highly probable to produce undesirable condensable tars in gasifiers as it is thermally unstable. These tars produce down-stream blockages of engines, turbines, piping, etc (21). The other known disadvantages of untreated wood with respect to gasification include its high moisture content and high O/C ratio. Low gasification efficiencies can be explained from the fact that the optimal gasification temperature of wood is around 700 °C, however, higher gasification temperatures are practically required to avoid tars. These higher gasification temperatures lead to the over-oxidation of wood in the gasifier, ultimately causing thermodynamic losses. In addition, the high chemical exergy of the wood is not fully used during gasification. In contrast, torrefied biomass, with its low moisture content and low O/C ratio, was shown to reduce thermodynamic losses when used in a gasifier (20). Prins et al. (20) presented a design which recycles energy from the gasification stage to the torrefaction pre-treatment stage and showed this arrangement to be thermodynamically favorable for a lab-scale setup. In addition, Wannapeera et al. (19) showed that torrefaction reduces tar production due to cross-linking reactions, which alter the structure of the original feedstock biomass. These cross-linking reactions increase with torrefaction holding time, resulting in increased bio-char yield and decreased tar yields. In pyrolysis, pre-treatment of biomass by torrefaction can also provide more bio-oil of better quality. Specifically, M. Klaas (22) found that the highest amount of original biomass energy was contained in bio-oil produced by pyrolysis when biomass torrefaction was used as a pre-treatment.

An important bio-coal characterization is the determination of its hygroscopic behavior. Hygroscopy was measured in various studies (8,13, 23, 24) without a common methodology. Borrega and Kärenlampi (23) studied the hygroscopicity of heat-treated

spruce wood and investigated the mechanisms that affect it. The authors reported the hygroscopicity of the heat treated wood in terms of the equilibrium moisture content as a function of mass loss occuring during thermal treatment at setup temperatures of 150 ^{o}C and 170 ^{o}C. Borrega and Kärenlampi (23) found a decrease in hygroscopicity with increasing mass loss at both setup temperatures, but the data formed two different groups. It was hypothesized that hygroscopy could not be explained by mass loss alone and that irreversible hydrogen bonding (i.e. a hornification mechanism) had to be considered. Felfli et al. (8) studied the hydrophobic characteristics of torrefied briquettes by direct immersion in water and determined the moisture content by measuring the change in briquette weight. The weight change due to water absorption was reported as a function of immersion time and torrefaction temperature. The authors found that after a 70 minute immersion time, the absorbed moisture did not exceed 10 % and the structure of the torrefied briquette remained intact. In comparison, an untreated briquette disintegrated after an immersion time of 10 minutes. After immersion in water for 17 days, Felfli *et al.* (8) observed a significant increase in moisture (116 %) in the briquettes torrefied at 220 ^{o}C, but their structure remained intact. This phenomenon resulted from the dissolution of impregnated tar in the briquettes. In contrast, no dissolution of impregnated tars was observed with the briquettes torrefied in the range of 250-270 ^{o}C and their final moisture content was reported as 28 %. These briquettes also remained intact. For all the torrefaction temperatures, the torrefied briquettes had an increase in moisture content within minutes of water exposure. Phanphanich and Mani (13) observed a decrease in water absoprtion capacity with increasing torrefaction temperature. The authors hypothesized that the loss of hydroxyl groups from biomass during the torrefaction process results in the decrease in water absorption capacity.

Recently, Li et al. (25) measured the hygroscopicity of torrefied sawdust in a controlled moisture environment. Specifically, the moisture absorption rates were measured after the samples resided in an atmosphere with 90 % relative humidity for 48 hours at 30 ^{o}C. The results indicated a reduction of 40 wt% moisture absorbance capacity between biomass and torrefied biomass (25). Hemicellulose degradation has been related to moisture changes by Sadaka and Negi (17). The torrefaction of three feedstocks with different hemicellulose contents was studied: wheat straw (28-39 % hemicellulose), rice

straw (4-39 % hemicellulose) and cotton gin waste (19-36 % hemicellulose). The largest reduction in hygroscopicity was observed with the wheat straw, which have the largest in hemicellulose content (17). The effect of hemicellulose decomposition on hydrophobicity is also mentioned by Li et al. (25).

The objective of the present work is the production of bio-coal samples from maple wood biomass under carefully controlled operating conditions and the investigation of their applicability as a coal substitute by carrying out a comprehensive characterization of their properties.

2.1 Methods

2.1.1 Biomass selection

Woody biomass was selected for the present study since woody biomass has a higher energy yield than herbaceous biomass. For example, Bridgeman et al. (26) compared willow biomass, wheat straw and red grass canary biomass and found a higher energy yield with torrefied willow biomass. Accordingly, woody biomass seemed to represent an optimal choice with respect to bio-coal production for combustion applications.

2.1.2 Equipment description

The torrefaction experiments are conducted in a batch Inconel mechanically fluidized reactor (MFR) having an inside diameter 9 cm, a height of 13 cm and a volume capacity of 815 ml. The reactor volume capacity is defined as the total chamber volume of the reactor subtracted by the volume occupied by the agitator. A diagram of the MFR is given in Figure 2-1 and a detailed schematic of the entire MFR setup is given in Figure 2-2.

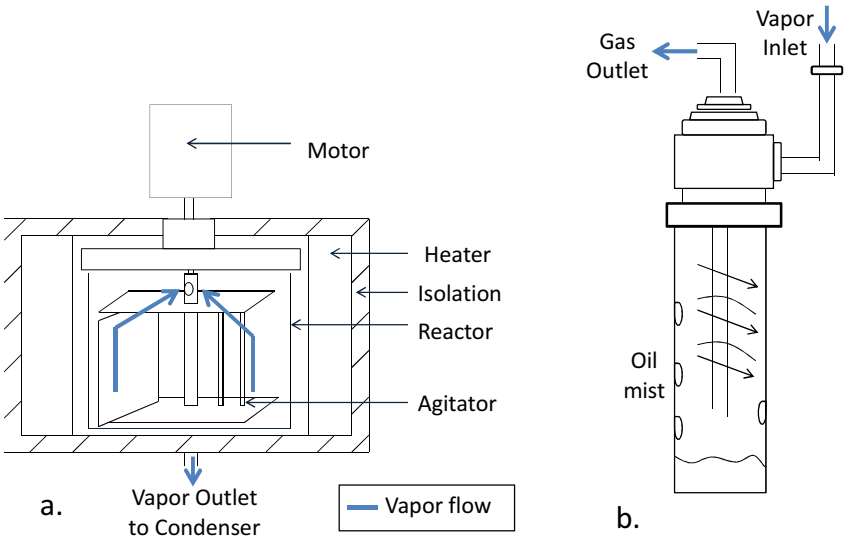

Figure 2-1. (a) MFR Reactor; (b) Condenser

Reactor heating is provided by means of a radiant ceramic heater and ceramic fibers of 1 ½ in were used for insulation. The system is tuned to a PID controller (EZ Zone PM from WATLOW). A thermocouple is placed inside the reactor on the top part of the chamber, acting as the sensor of the control system. Two more thermocouples are also used (A and B, as shown in Figure 2-2): A. is located between the reactor wall and the heater and its purpose is to follow the heating cycles and provide an indication of the energy consumption; B. is located on top of the reactor near the seal and its purpose is to monitor the seal temperature ultimately verifying the efficiency of the water cooling coil located near the seal. The seal is made of graphite cord and a gasket marker N°27 from Permatex which has a temperature limit of 345 ^{o}C.

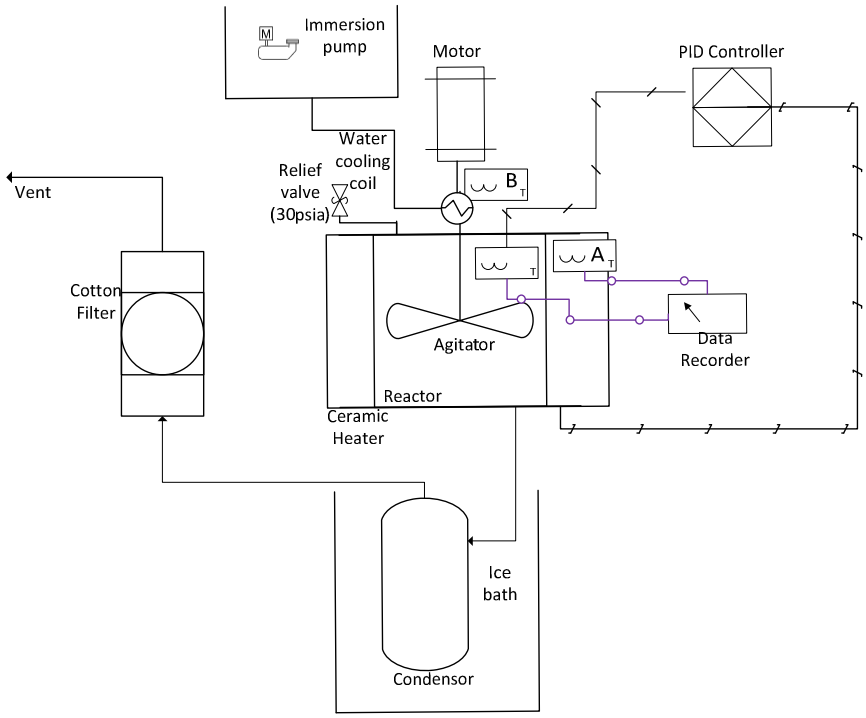

Figure 2-2. Detailed schematic of the MFR reactor

Drawbacks on temperature measurements are detected and fixed through a set of calibration experiments covering the experimental temperature range of this work. Drawbacks are a consequence of the inability for thermocouple sample immersion in the system caused by the use of an agitator. Figure 2-3 provides the relation between the top thermocouple and sample temperature according which data is fixed on this study.

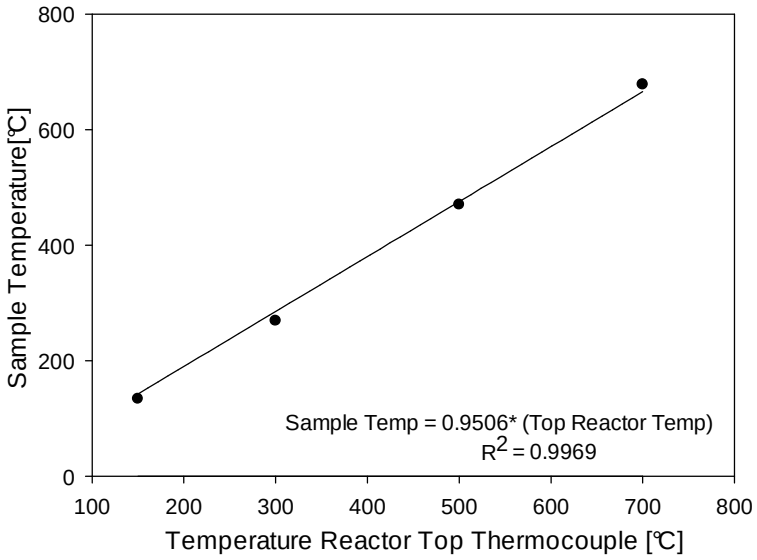

Figure 2-3. Relationship between the sample temperature and the thermocouple reading at the top of the reactor

The biomass is ground to a sieve diameter of less than 1 mm (when required) before loading into the reactor. To ensure appropriate conditions for agitation, the maximum load capacity of the reactor with loose raw material is 80 % of the reactor volume capacity, to avoid entrainment of char and tar. The agitation system is designed to maintain a homogeneous temperature within the reactor, avoid dead zones and enhance heat transfer. As shown in Figure 2-1a, the agitator is composed of two paddles with adjustable scrappers to clean the bottom and wall of the reactor.

During operation, the vapors produced inside the reactor chamber flow to the upper part of the chamber, pass through the holes located at the top of the agitator central tube and proceed down the tube on their way to the condenser (indicated by the arrows in Figure 2-1a). The condenser (Figure 2-1b) is directly connected to the reactor as illustrated in Figure 2-2. The input flow into the condenser enters tangentially in order to create a vortex inside the condenser. This increases the efficiency of bio-oil collection. The condenser volume is 130 ml and its temperature is maintained by submergence in an ice bath. The remaining vapors and non-condensable gases leave the condenser and pass through a cotton filter prior to being vented to the exhaust line. Safety measures include a

pressure gauge on the reactor and a relief valve to monitor reactor pressure and avoid reactor overpressure and damage.

2.1.3 Torrefaction experiments

For this study, 100 g of maple wood sawdust was used as received for each run, occupying 58 % of the reactor volume (loose). Maple sawdust was obtained from Murphy Forest Products from biomass collected in Pennsylvania USA. The feedstock was used with its natural moisture content of 7.1 wt% for all runs. The sawdust has a loose bulk density of 212 kg/m^3 and a compact bulk density of 255 kg/m^3. To determine the feedstock particle size distribution, a stack of sieves was used for the fraction above 850 μm and a Sympatec Helos laser diffraction sensor was used for the fraction bellow 850 μm, resulting data was added together to calculate a Sauter mean diameter of 663.6 μm and the size distribution given on Figure 2-4.

A typical experiment involves loading the feedstock biomass into the MFR and sealing the reactor. The agitator is then set to 49.5 rpm and the heater is turned on and controlled by PID system. Once the desired reaction temperature is reached, this temperature is maintained for the desired holding time. At this point the heater is shut off and the reactor is quenched in ice until 100 ^{o}C is reached. It is then left to gradually cool down to room temperature without any additional ice bath cooling.

Experiments were done at various reaction temperatures covering the ranges traditionally associated with both torrefaction and pyrolysis. (143 °C, 190 °C, 238 °C, 285 °C, 333 °C, 380 °C, 428 °C, 475 °C, 570 °C and 665 °C; sample temperature). A heating rate of 12 °C/min and holding times of 30 min or 50 min were used. The value of holding time was selected in order to obtain a representative product at each temperature. Mass yields of bio-oil, bio-coal and non-condensable gases were calculated on a dry basis. The yields were calculated from the ratio between the mass of the obtained product and mass of the feed biomass material, as shown in Eq. 2-1 where X is the component (bio-coal or bio-oil), Y_X is the yield of the component, M_X is the mass of the component and M_{feed} is the dry mass of the biomass feed. In the case of the non-condensable gases, the yield is determined by subtracting $Y_{bio\text{-}coal}$ and $Y_{bio\text{-}oil}$ from 100 %.

$$Y_X = \frac{M_X}{M_{feed}} * 100 \quad \text{Eq. 2-1}$$

Unless otherwise mentioned in the rest of this manuscript, the holding time was 30 min and the biomass loading was 100 g.

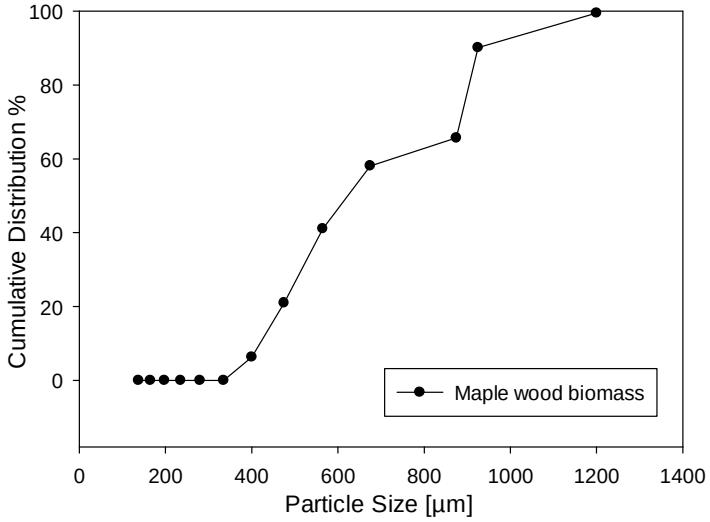

Figure 2-4. Maple wood cumulative particle size distribution as feed in the reactor

2.1.4 Characterization

The bio-char produced was characterized by ultimate (elemental) analysis, ash analysis, calorific analysis (high heating value), FTIR and hygroscopicity. All tests were done after pre-drying samples over 2 hours in an oven at 100 ^{o}C.. Ultimate analysis was performed using an AN634 Flash 2000 CHN Analyzer. Vanadium Oxide (catalyst for sulfur content detection) was used during CHN analysis. Oxygen content was calculated by difference accounting for the ash content in the sample. The ash content was determined according the ASTM D1102-84 standard (Standard Test Method for Ash in Wood) using nickel crucibles (30 mL). High heating values were obtained using an IKA C200 Calorimeter. Pre-drying was used to ensure the HHV was independent of the ambient humidity and/or any water uptake by the sample. FTIR was performed using a Thermo Scientific Nicolet 6700 mid infrared spectrometer (with scans of 2 cm^{-1}/s for a range of 400-4000 cm^{-1}) using the Attenuated Total Reflectance (ATR) accessory. For pH measurements all Bio-coal samples were pre-grinded using a mortar and pestle. On each test 0.2 g of pre-

grinded Bio-coal samples were mixed with 8ml of distillated water in essay tubes. Samples were left soaking on the essay tubes during 3 hours. Finishing 3 hours pH determinations were carried out using a pH-meter from Thermo Scientific; Onion 2 star. Standards solutions with pH of 2, 4 and 7 were used to verify correct calibration on the pH-meter.

Hygroscopicity experiments were performed in a highly controlled environment. First, 3-5 g of bio-coal (or biomass) was loaded onto an aluminum dish that was placed inside an airtight container (307 ml). Each container was filled with water to half its volume capacity to saturate the existent air in the containers, as illustrated in Figure 2-5, then sealed closed so that the dish with the biomass would float on water. A humidity indicator was used to verify that the air was saturated with humidity. The containers containing the bio-coal and water were placed in an enclosure with a temperature set at 15 °C during the time of the test. Samples were taken from the fridge at specific times between 2 days and 23 days for moisture content measurements. A halogen moisture analyzer HB43-S (Mettler Toledo) was used for this purpose; the equipment was programmed to dry 1 g of sample to 100 °C and to report the moisture content when the weight of the sample stabilized. Bio-coal samples were compared with biomass and coke samples. Coke was selected for comparison since it is a product from coal pyrolysis and has similar properties to bio-coal including a low amount of impurities, high carbon content and high energy density. Replicate experiments were performed to validate the acquired data.

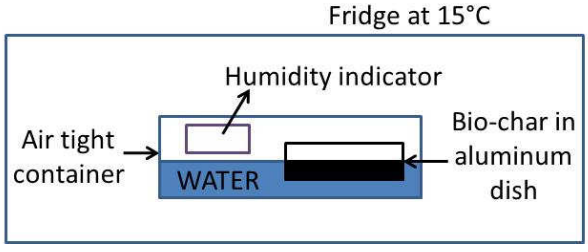

Figure 2-5. Set up for hygroscopy measurement in a controlled saturated atmosphere

As mentioned above, the samples were placed inside containers and a humidity indicator was used to determine when saturated conditions were met. The moisutre data

collected from the humidity indicator data logger located in one of the sample containers in the fridge is given in Figure 2-6. The humidity graph (Figure 2-6a) shows that the atmosphere in the airtight container reached saturated conditions after 100 min. The temperature and dew point graphs (Figure 2-6b) verified that the system reached the saturated temperature or dew point, hence fulfilling the condition of a saturated atmosphere. Exposing the bio-coals to this extreme condition provided a reproducible and consistent means to study their ability to attract and hold water molecules, through mechanisms of either adsorption or absorption.

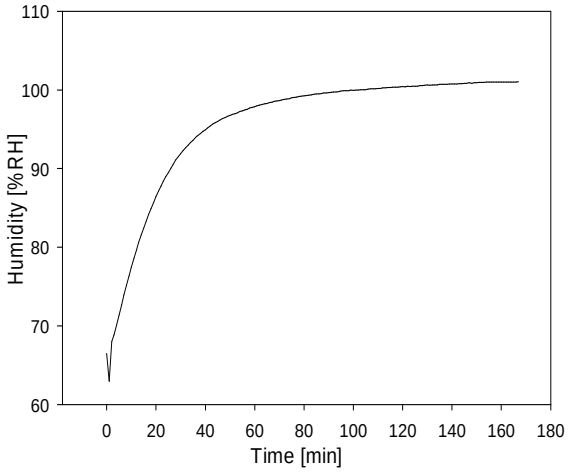

(a)

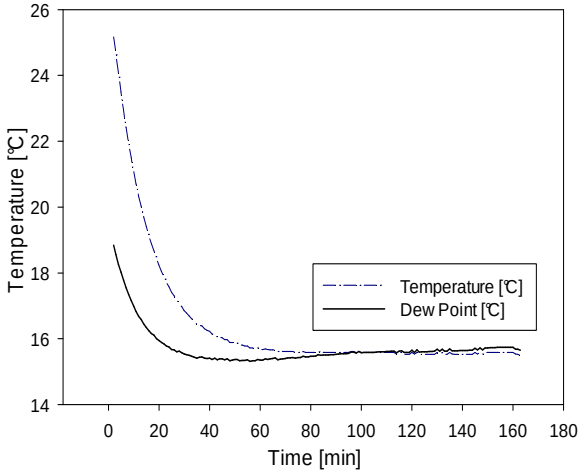

(b)

Figure 2-6. Humidity indicator graphs on hygroscopy set up; (a) Relative Humidity and (b) Temperature reaching Dew point

2.2 Results and Discussion

2.2.1 Yields

The variation of the mass yields of bio-coal, bio-oil and non-condensable gases with reaction temperature are given in Figure 2-7. The biomass load, holding time, heating rate and agitator velocity were 100 g, 30 min, 12 ^{o}C/min and 49.5 rpm, respectively. The trend lines for the data were determined using Table curve 2D^{TM}.

As observed in Figure 2-7a, the mass yield of bio-coal decreased significantly with reaction temperature and stabilized at about 22 %. A decrease to 35 % in mass yield was observed between 190 to 238 ^{o}C, followed by a decrease of 21 % to 26 % between 238 to 285 ^{o}C. After 285 °C, the bio-coal mass yield decreased by 3 % to 6 % reaching a final value of 22.3% at the highest evaluated reaction temperature of 665 ^{o}C. Figure 2-8 shows the various degrees in charring of the bio-coals produced. The products at 143 and 190 ^{o}C resembled the original biomass (only a slight change in color) and similar observations were made by Chen and Kuo (6). The product color darkened only starting at 238 °C, resembling the regular appearance of char and thus indicating a change in composition. The trend in bio-coal mass yield shown in Figure 2-7a is similar to the one observed by Sharma et al. (27) in a pectin bio-char study.

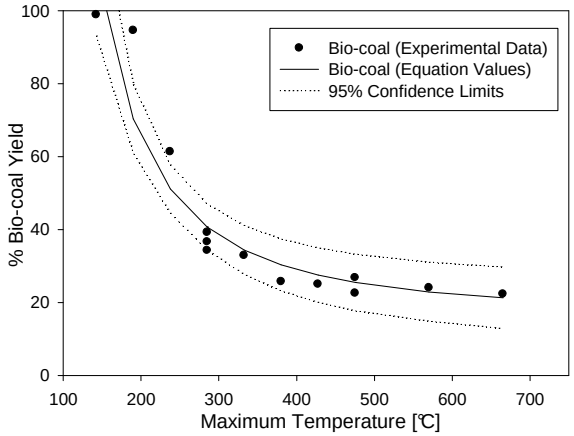

(a)

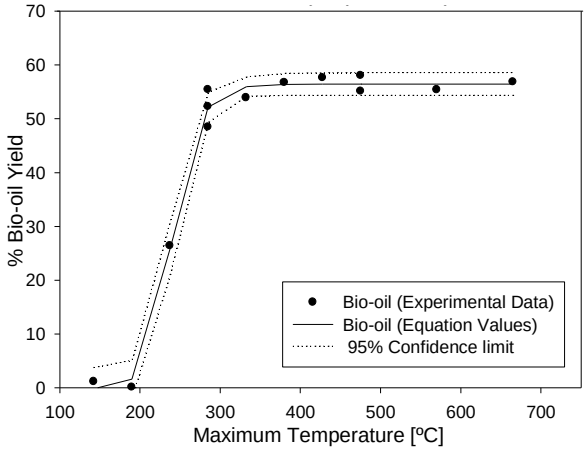

(b)

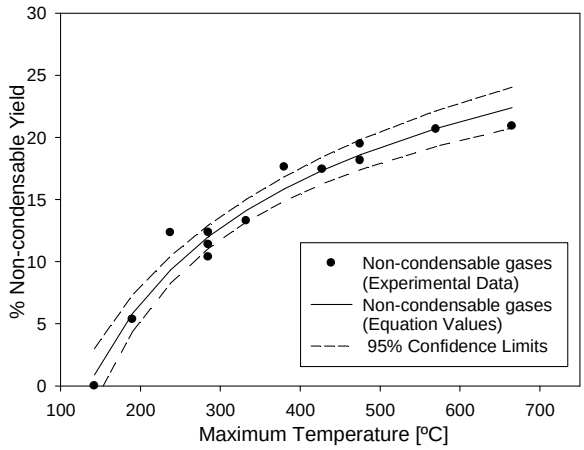

(c)

Figure 2-7. Yields at various reaction temperatures (a) bio-coal; (b) bio-oil; and (c) non-condensable (biomass load = 100 g; holding time = 30 min; heating rate = 12 ^{o}C/min; agitator velocity = 49.5 rpm)

Figure 2-8. Bio-coal products at the various temperatures studied

As shown in Figure 2-7b, the bio-oil mass yield increased significantly between 190 to 285 °C, after which the yield values were relatively constant at a value of

approximately 54 %. This trend for bio-oil yield is in accordance with slow pyrolysis processes as studied by Di Blassi (28). A similar trend was observed with the non-condensable gas yield (Figure 2-7c), which also increased with temperature and reached a value of 20 %. Yield values showed a moderate change between 1.5 % to 3.47 % with each 50 °C increase in temperature. In general , the bio-coal, bio-oil and non-condensable gas yields in the MFR reactor followed the same trends as the reported yields from slow pyrolysis in the study done by Di Blassi (28).

2.2.2 Effect of holding time on mass yields

The effects of holding time on bio-coal, bio-oil and non-condensable gas mass yields are given in Figure 2-9a, 9b and 9c, respectively. An increase in holding time from 30 to 50 min resulted in a decrease in bio-coal mass yield for a given reaction temperature. This is shown in Figure 2-9a for temperatures of 238 °C, 333 °C and 475 °C. The decrease in bio-coal yield results from the fact that further reactions occurred during the additional time. As illustrated in Figure 2-9b, higher amounts of oil were collected with longer holding times at the same reaction temperatures specified above. This results partly from the decrease in bio-char yield due to further reactions. This data might also be a consequence from a reduction in the velocity of the vapor phase leaving the reactor since the volumetric flow rate is smaller (velocity = volumetric flow/transversal area). Such a decrease in vapour velocity would increase the residence time through the condenser, resulting in a higher collection efficiency in the condenser. The non-condensable gas yield remained relatively unchanged as the holding time was raised from 30 to 50 min, as shown in Figure 2-9c.

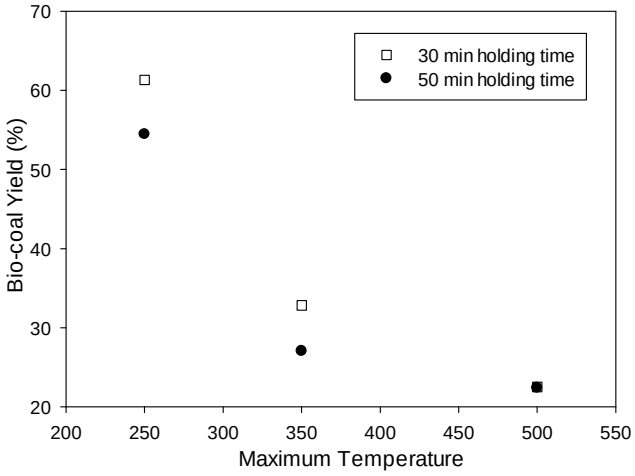
70
60
50
40
30
20
200
250
300
350
400
450
500
550
Bio-coal Yield (%)
Maximum Temperature
30 min holding time
50 min holding time

(a)

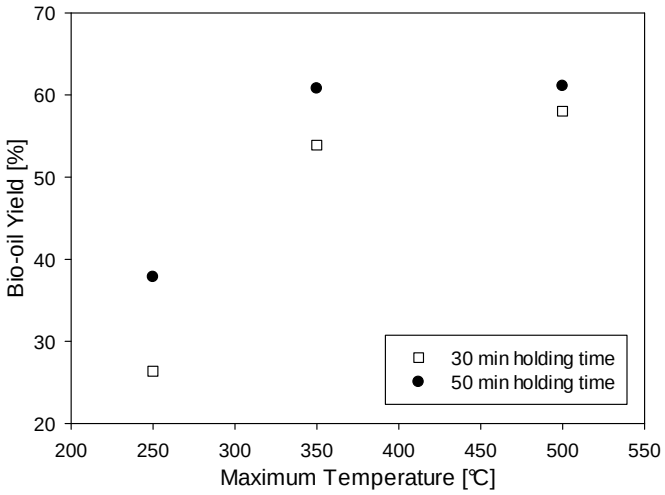
70
60
50
40
30
20
200
250
300
350
400
450
500
550
Bio-oil Yield [%]
Maximum Temperature [℃]
30 min holding time
50 min holding time

(b)

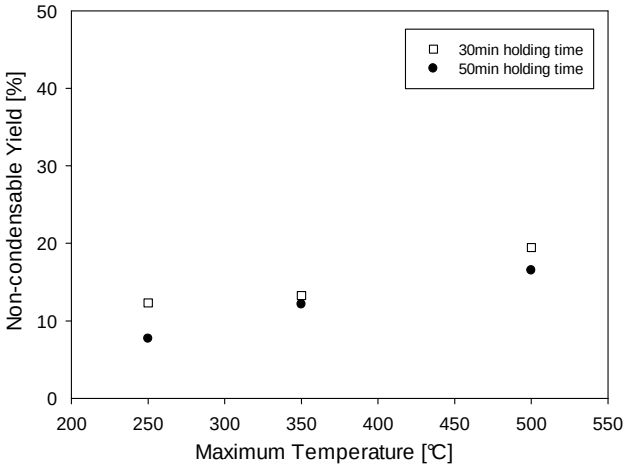

(c)

Figure 2-9. Yield variations at 30 min (square) and 50 min (circle) holding times at the maximum pyrolysis temperature for (a) bio-coal; (b) bio-oil; and (c) non-condensable gases (biomass load = 100 g; heating rate = 12 ^{o}C/min; agitator velocity = 49.5 rpm)

2.2.3 Calorimetry Results

The effect of reaction temperature on the high heating value (HHV, on a dry basis) of the bio-coal produced with a holding time of 30 min is shown in Figure 2-10. The energy recovery in the bio-coal produced, which was calculated using Eq. 2, is plotted as a function of reaction temperature in Figure 2-11 (the mass yield of bio-coal is also re-plotted in Figure 2-11 for comparison). It should be noted that Eq. 2 was proposed in (29, 30). In both graphs the data point at 25 ^{o}C corresponds to the original biomass. Two opposing effects are observed: the HHV increased with reaction temperature up to 380 ^{o}C, while the percentage energy recovery in the bio-coal (i.e. energy yield) decreased with increasing reaction temperature. Thus high energy bio-coal products can be obtained, but at the expense of their mass and energy yields. The energy yield was greater than the mass yield for every reaction temperature studied, following the same trend found by Bridgeman et al. (26). The optimal reaction temperature is therefore the maximum temperature at which the biomass has been sufficiently upgraded to increase its energetic value without greatly reducing the mass yield. This occurs over a range of reaction temperatures between 190 °C and 285 °C (i.e. in the torrefaction temperature range).

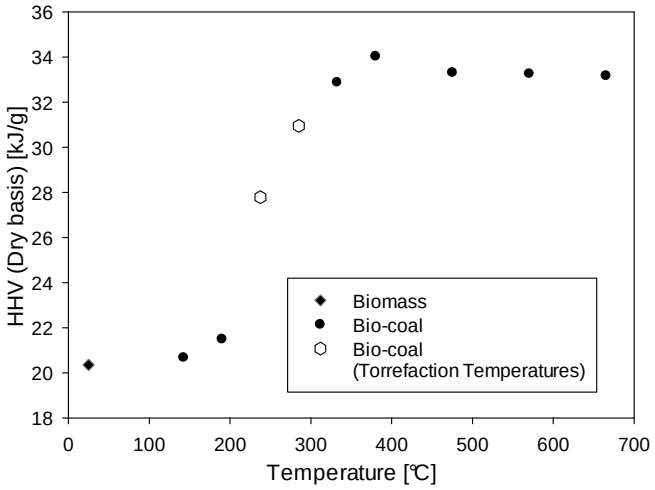

Figure 2-10. High heating values on a dry basis (biomass load = 100 g; holding time = 30 min; heating rate = 12 ^{o}C/min; agitator velocity = 49.5 rpm)

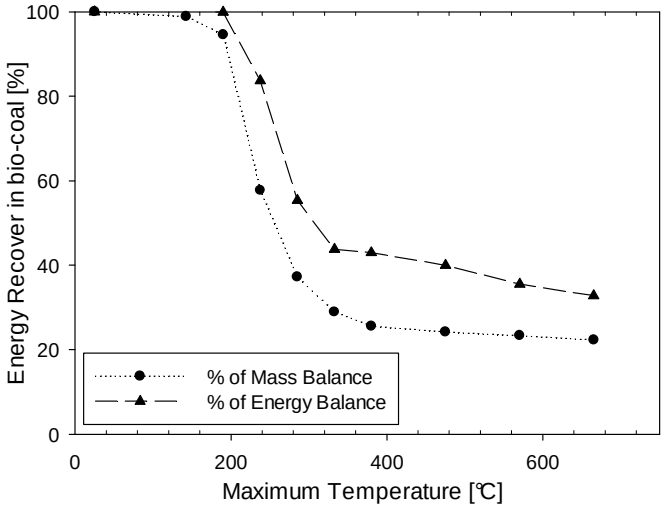

Figure 2-11. Percentage energy recovery in bio-coal (biomass load = 100 g; holding time = 30 min; heating rate = 12 ^{o}C/min; agitator velocity = 49.5 rpm)

$$\%_{\substack{\boldsymbol{Energy\ Recover} \\ \boldsymbol{in\ the\ Bio-char}}} = \boldsymbol{Y_{Bio-char}} * \frac{\boldsymbol{HHV_{Biochar}}}{\boldsymbol{HHV_{Biomass}}} * \mathbf{100} \qquad \text{Eq. 2-2}$$

2.2.4 Ultimate Analysis and and Ash Content

The elemental and ash compositions of the maple wood biomass used in this study are given in Table 2-2 and trends in the elemental composition (namely carbon, hydrogen and oxygen) with reaction temperature are shown in Figure 2-12.

Table 2-2. Biomass Composition (dry basis)

	% C	*% N*	*% O*	*% H*	*% Ash*
Biomass (Maple Wood)	46.74	0.14	46.86	5.88	0.39

During pyrolysis, the carbon content is concentrated given that the hydrogen and oxygen contents diminish. For the entire span of reaction temperature studied, the nitrogen content varied between 0.06 to 0.2 %, the ash content varied between 0.39 and 1.63 %, and the sulphur content was negligible. The trends in the elemental compositions shown in Figure 2-12 are in agreement with the visual change in appearance of the biomass and bio-coal products illustrated in Figure 2-8 it is only at a temperature of 238 °C where changes in composition became detectable.

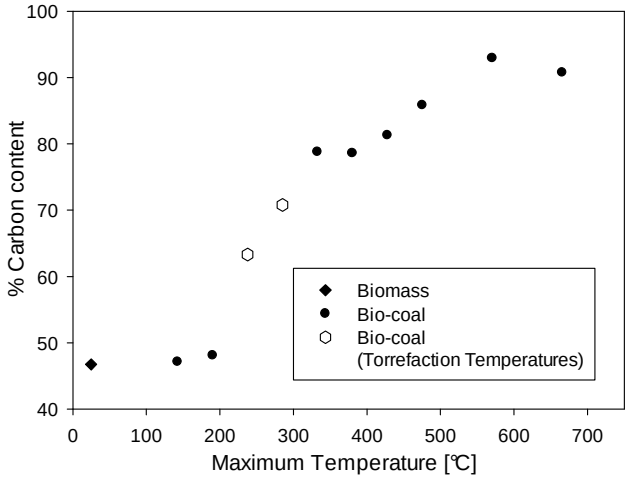

(a)

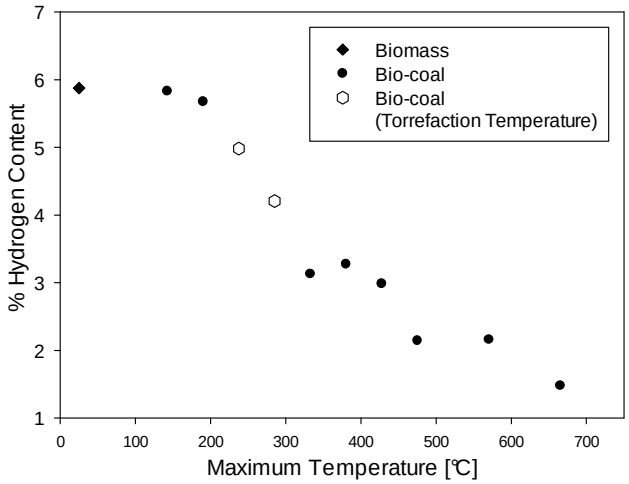

(b)

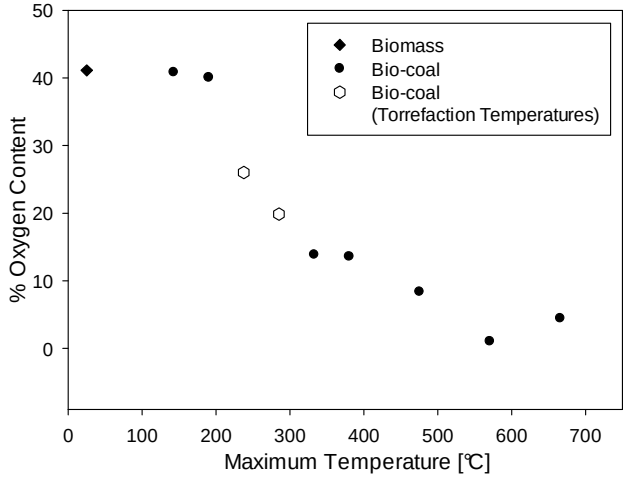

(c)

Figure 2-12. Variation of (a) carbon; (b) hydrogen and (c) oxygen composition with maximum reaction temperature

The elemental composition was also used to calculate the HHV, based on an empirical correlation proposed by Channiwala and Parikh (31) and given in Eq. 3 where C, H, O, S, N, and A respectively represent the carbon, hydrogen, oxygen, sulphur, nitrogen and ash contents of the sample, expressed in mass percentages on a dry basis. The greatest changes in the samples composition observed in the present study were on carbon, oxygen and hydrogen, which correspond to the first three terms of the correlation.

$$\boldsymbol{HHV}\ \left[\frac{\boldsymbol{KJ}}{\boldsymbol{g}}\right] = \mathbf{0.3491} * \boldsymbol{C} + \mathbf{1.1783} * \boldsymbol{H} - \mathbf{0.1034} * \boldsymbol{O} - \mathbf{0.0211} * \boldsymbol{A} + \mathbf{0.1005} * \boldsymbol{S} - \mathbf{0.0151} * \boldsymbol{N} \quad \text{Eq. 2-3}$$

The HHV is most dependant on the carbon content (88-93 %), followed by hydrogen (7.3-37 %) and oxygen (0.9-26.3 %). This confirms that pyrolysis, as a carbon concentrating process, increased the HHV of the bio-coal product. In addition, oxygen and hydrogen removal during the process also contributed to the increase in calorific value of the product. Results found with Eq. 3 for HHV are in relatively good agreement with calorific values calculated with the bomb calorimeter as illustrated in Figure 2-13 and trends are similar. The increase in the amount of atomic carbon and decrease in atomic hydrogen and oxygen resulting from the heating process in the torrefaction temperature range is similarly observed in other studies such as the one by Medic et al. (3). The reduction in hydrogen and oxygen content and overall mass loss resulted in a torrefied product having an increased energy density in comparison to the raw biomass, as observed in the present study and in (3)

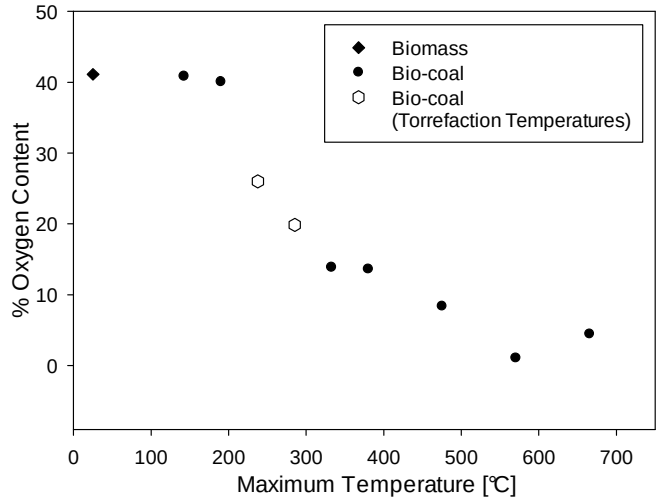

Figure 2-13 Comparison between bomb calorimeter bio-coal's HHV values and bio-coal's HHV calculated from elemental composition

The Van Krevelen diagram is given in Figure 2-14 by plotting the molecular ratios of hydrogen/carbon vs oxygen/carbon. It can be observed in Figure 2-14 that the major changes in the elemental composition occured at torrefaction temperatures (200-

300 ^{o}C). The Van Krevelen diagram provides a better way to visualize the changes in the elemental composition that influence the HHV.

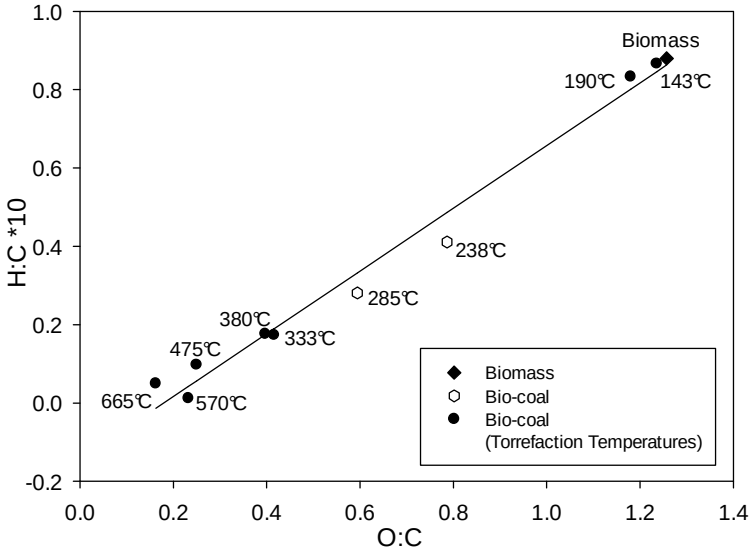

Figure 2-14. Van Krevelen diagram; variation on elemental composition

2.2.5 FTIR

Analysis of the feedstock biomass and selected bio-coals by Fourier transform infrared spectroscopy (FTIR) was performed to determine the changes in the chemical structure of the samples and is given in Figure 2-15. The reduction in oxygen and hydrogen content, which was observed in the elemental analysis, was also reflected in the FTIR spectra by the reduction, disapperance or formation of specific peaks in comparison to the biomass spectrum. The spectra for the bio-coal produced at 428 °C and 570°C show a lack of funtional group peaks, which were initially present in the maple wood biomass feedstock. These funtional groups include OH^- and H^+ originating from alcohol and phenols observed in the 3100-3600 cm^{-1} region and a C-O span originating from alcohol, phenols, ester or ethers observed between 1000-1300 cm^{-1}. These results are in agreement with the decrease in hydrogen and oxygen content observed from the elemental analysis of the bio-coals.

Another observation is an inclination angle on the baseline in FTIR analysis. This angles were removed from Figure 2-15 for comparison purposes but for the record their tendency to increase was related with the rise in the sample pyrolytic temperature. The appearance of this incline could be explained by an increase in aromatic carbon content with higher reaction temperatures (27). Sharma et al. (27) observed similar inclines in the FTIR spectra of pectin bio-chars and comfirmed by NMR analysis the presence of aromatic carbon.

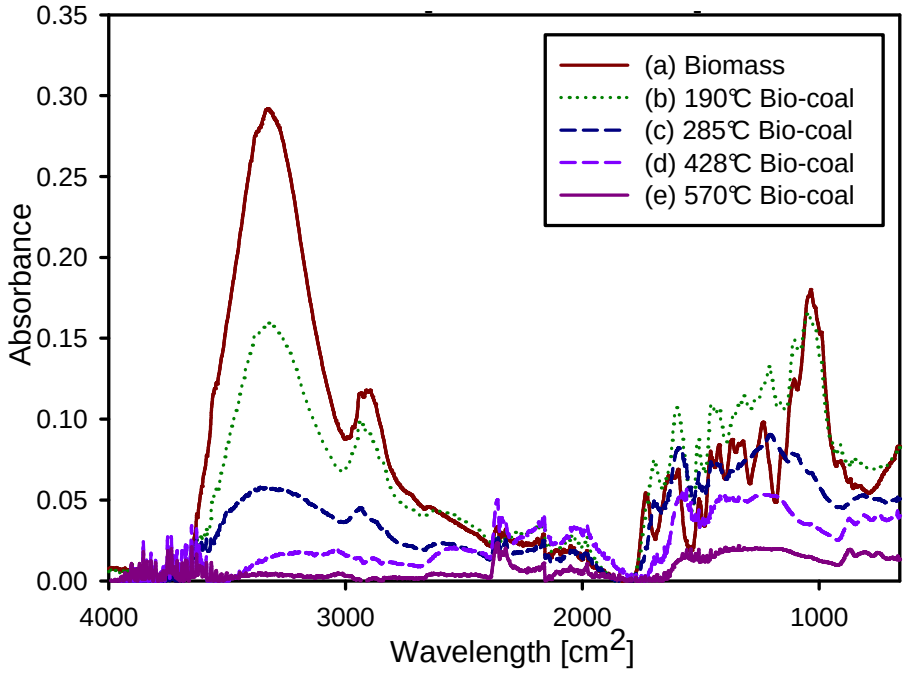

Figure 2-15. FTIR spectra for (a) feedstock biomass; and bio-coals produced at reaction temperatures of (b) 190 ˚C, (c) 285 ˚C, (d) 428 ˚C and (e) 570 ˚C

2.2.6 Hygroscopicity

The change in the moisture content of the samples plotted with time, given in Figure 2-16. shows interesting hygroscopic results. As expected, the biomass data (circle) showed higher values of moisture content under a water-saturated atmosphere in comparison to the bio-coal and coke samples. The bio-coals produced at 238 °C (square) and 285 °C (upside-down triangle) had the lowest moisture values of all samples. Coke (shaded diamond) showed a medium hygroscopicity value among all data. The results

indicate that biomass can double or triple the water retention capacity of bio-coals produced in the torrefaction temperature range (200-300 °C). These bio-coals are thus suitable to avoid water uptake.

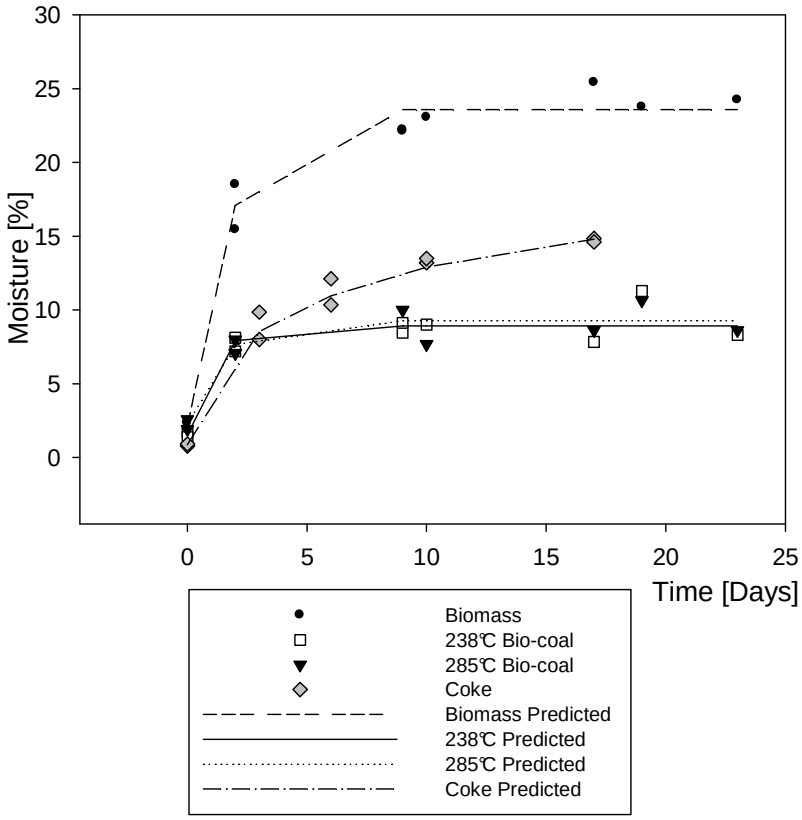

Figure 2-16. Hygroscopy of biomass, torrefied bio-coals and coke, reported in units of moisture at different tested times

The reduction in hygroscopicity of the thermally treated biomass has been related with hemicellulose decomposition, since hemicellulose has a hydrophilic character (24). Hemicellulose decomposes directly after water vaporization, at temperatures between 200-380 °C (32). This temperature range corresponds to the lowest thermal decomposition range among main wood components (i.e. hemicellulose, cellulose and lignin), and covers the torrefaction temperature range. Hardwoods as maple wood typically contain 40-50 % cellulose, 25-35 % hemicellulose and 20-25 % lignin.

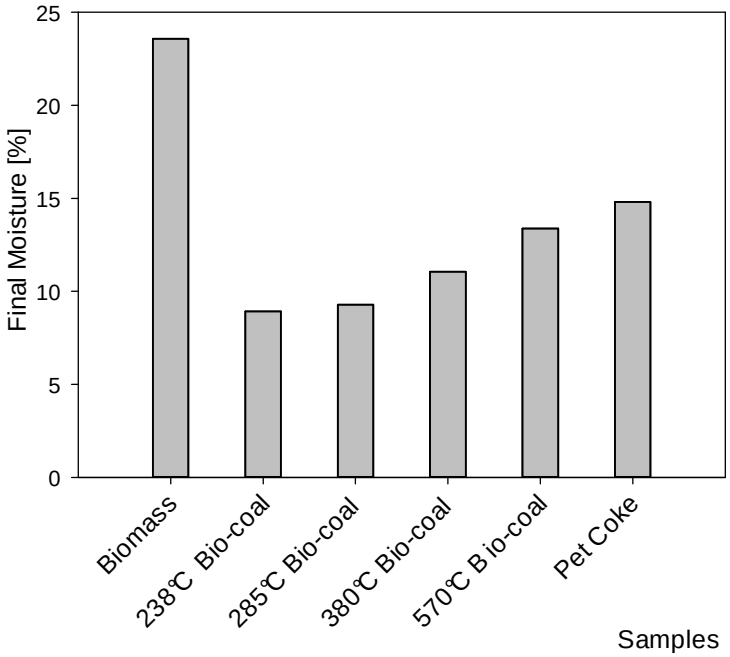

Figure 2-17 Asymptotic hygroscopic values, reported in units of moisture when it has stabilized with time

Hygroscopy values of Bio-coals are on a range of 8.9-13.3 % of water retention in saturated water conditions (Figure 2-17). It's still not very clear why an increase of temperature generates a slightly more hydrophilic sample. In fact higher pyrolysis temperature disintegrates a higher amount of polar sites on a carbon surface. J. Pastor-Villegas identified polar sites as oxygen containing groups found on the carbon surface (33), and as shown above with elemental analysis and FTIR the tendency of these groups is to disappear with an increment on process temperature.

2.2.7 pH

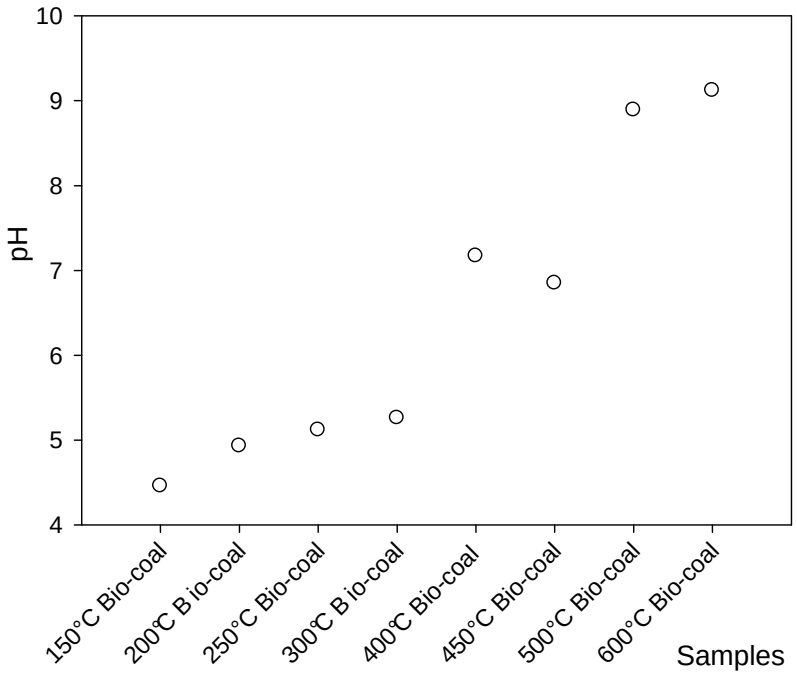

Figure 2-18. pH of Bio-coal samples produced at different maximum temperature

When measuring Bio-coal pH samples by soaking them in water for a set period of time, it is noticeable that higher pH samples are found at higher pyrolytic temperature. Figure 2-18 reinforces the FTIR analysis and is in agreement with studies as the one J. Pastor-Villegas made on Bio-chars (33); phenols and alcohols groups are disintegrated with temperature and are part of the acidic oxygen groups available on the carbon surface. Basic groups and ashes are stronger to disintegration and remain on the Bio-char surface.

2.3 Conclusions

Thermal heat treatment of Maple wood biomass is achieved in a MFR at temperatures ranging from 143 to 665 ^{o}C. The yields of the products from the heat treatment, namely bio-coal, bio-oil and non-condensable gases are determined experimentally. Fuel-related characteristics such as energy recovery, calorific values and hygroscopy are determined for all bio-coal products. In addition, elemental composition and FTIR analyses are presented in this study to provide further understanding of

pyrolytic changes in the product. A novel hygroscopicity study indicates that the lowest value of water uptake is obtained with bio-coal produced at a temperature of 238 °C, which falls in the torrefaction temperature range. This bio-coal has a water uptake of 8.9 wt% when exposed to a saturated atmosphere for 23 days. In contrast, Maple wood biomass has a water uptake of 23.6 wt% after 23 days. Bio-coals produced at higher temperatures and coke all have higher water uptakes when compared to bio-coal produced at 238 °C. The benefits of torrefaction at 238 °C include an increase of 7.44 kJ/g in calculated high heating value of bio-coal produced at this temperature when compared to raw biomass. This increase represents 58 % of the total calorific increase achieved from pyrolysing biomass to a maximum temperature of 665 °C. Thermal treatments at temperatures lower than 238 °C are found unattractive since the products are not sufficiently upgraded in terms of calorific content. The mass yield of bio-coal produced at 238 °C is 61.3 %, corresponding to a 38.7 % mass loss when compared to the original biomass. Pyrolysis at higher temperatures results in further mass losses, up to a maximum mass loss of 77.7 % at a process temperature of 665 °C. The energy recoveries of bio-coal produced at 238 and 665 °C are 83.7 % and 32.8 %, respectively, illustrating similar tendencies as the mass yields. The results observed here clearly show that there is an optimal treatment temperature corresponding to the maximum temperature at which the biomass is sufficiently upgraded to increase its energetic value and decrease its hygroscopicity, without greatly reducing the mass yield and energy recovery. It is shown in the present work that this optimal occurs at 238 °C for Maple wood biomass, making torrefaction a viable upgrading method.

2.4 References

1. World Energy Council. Survey of Energy Resources 2010.

2. Bioindustrial Innovation Centre. Assessment of Agricultural Residuals as a Biomass Fuel for Ontario Power Generation 2010.

3. M.J.C. Van der Stelt, H. Gerhauser, J.H.A. Kiel, K.J. Ptasinski. Biomass Upgrading by Torrefaction for the Production of Biofuels: A Review. Biomass and Bioenergy 2011; 35 (9); 3748-3762.

4. P.T. Williams, S. Besler. The Influence of Temperature and Heating Rate on the Slow Pyrolysis of Biomass, Renewable Energy 1996; 7 (3): 233–250.

5. W.-H. Chen, H. Hsu, K. Lu, W. Lee, T. Lin. Thermal Pretreatment of Wood (Lauan) Block by Torrefaction and its Influence on the Properties of the Biomass. Energy 2011; 36 (5): 3012-21.

6. W.-H. Chen, P.-C. Kuo. Torrefaction and Co-Torrefaction Characterization of Hemicellulose, Cellulose and Lignin as well as Torrefaction of some Basic Constituents in Biomass. Energy 2011; 36 (2): 803-811.

7. B. Arias, C. Pevida, J. Femoso, M. G. Plaza, F. Rubiera, J. J. Pis. Influence of Torrefaction on the Grindability and Reactivity of Woody Biomass, Fuel Processing Technology Fuel Processing Technology 2008; 89 (2): 169-175.

8. F.F. Felfli, C. A. Luengo, J. A. Suarez, P. A. Beaton. Wood Briquette Torrefaction, Energy for Sustainable Development 2005; 9 (3): 19-22.

9. D. Medic, M. Darr, A. Shah, B. Potter, J. Zimmerman. Effects of Torrefaction Process Parameters on Biomass Feedstock Upgrading. Fuel 2012; 91 (1): 147-54.

10. T. Melkior, S. Jacob, G. Gerbaud, S. Hediger, L. Le Pape, L. Bonnefois, M. Bardet. NMR Analysis of the Transformation of Wood Constituents by Torrefaction. Fuel 2012; 92 (1): 271-280.

11. B. Patel, B. Gami, H. Bhimani. Improved Fuel Characteristics of Cotton Stalk, Prosopis and Sugarcane Bagasse through Torrefaction, Energy for Sustainable Development. Energy for Sustainable Development 2012; 15 (4): 372-375

12. R. Pentananunt, A. N. M. Rahman, S. C. Bhattacharya Upgrading of Biomass by Means of Torrefaction. Energy. 1990; 15 (12): 1175-1179.

13. M. Phanphanich, S. Mani. Impact of Torrefaction on the Grindability and Fuel Characteristics of Forest Biomass. Bioresource Technology 2011; 102 (2): 1246-1253.

14. M.J. Prins, K. J. Ptasinski, F. J. J. G. Janssen. Torrefaction of Wood: Part 2. Analysis of Products. J. of Anal. and Appl. Pyrolysis 2006; 77 (1): 35-40.

15. P. Rousset, C. Aguiar, N. Labbe, J. - M. Commandre. Enhancing the Combustible Properties of Bamboo by Torrefaction, Bioresource Technology 2011: 102 (17): 8225-31.

16. P. Rousset, F. Davrieux, L. Macedo, P. Perre. Characterisation of the Torrefaction of Beech Wood using NIRS: Combined Effects of Temperature and Duration. Biomass and Bionenergy. 2011; 35 (3): 1219-1226.

17. S. Sadaka, S. Negi. Improvements of Biomass Physical and Thermochemical Characteristics via Torrefaction Process. Environmental Progress & Sustainable Energy. 2009; 28 (3): 427-34.

18. Y. Uemura, W. N. Omar, T. Tsutsui, S. B. Yusup. Torrefaction of Oil Palm Wastes. Fuel 2011; 90 (8): 2585-2591.

19. J. Wannapeera, B. Fungtammasan, N. Worasuwannarak. Effects of Temperature and Holding Time during Torrefaction on the Pyrolysis Behaviors of Woody Biomass. J. of Anal. and Appl. Pyrolysis. 2011; 92 (1): 99-105.

20. M. J. Prins, K. J. Ptasinski, F.J.J.G. Janssen. More Efficient Biomass Gasification via Torrefaction. Energy 2006; 31 (15): 3458–3470.

21. L. Devi, K. J. Ptasinski, F. J.J.G. Janssen. A review of the Primary Measures for Tar Elimination in Biomass Gasication Processes Biomass and Bioenergy. 2003; 24 (2): 125-140.

22. M. Klaas. Investigating Potential Pathways to Optimize the Effectiveness of the Pyrolysis Process [Dissertation]. The University of Western Ontario 2011.

23. M. Borrega , P. P. Kärenlampi. Hygroscopicity of Heated-Treated Norway Spruce (Picea Abies) Wood. Eur. J. Wood Prod 2010; 68 (2): 233-235.

24. J. Bourgois, R. Guyonnet. Characterization and Analysis of Torrified Wood. Wood Science and Technology. 1988; 22 (2): 143-155.

25. H. Li, X. Liu, R. Legros, X. T. Bi, C. J. Lim, S. Sokhansanj. Torrefaction of Sawdust in a Fluidized Bed Reactor. Bioresource Technology 2012; 103 (1): 453-458.

26. T.G. Bridgeman, J.M. Jones, I. Shield, P.T. Williams. Torrefaction of Reed Canary Grass, Wheat Straw and Willow to Enhance Solid Fuel Quantities and Combustion of Properties. Fuel 2008; 87: 844-856.

27. R.K. Sharma, J.B Wooten, V.L. Baliga, M.R. Hajaligol. Characterization of Chars from Biomass - Derived Materials: Pectin chars. Fuel 2001; 80 (12): 1825-1836.

28. Colomba Di Blasi. Combustion and Gasification Rate of Lignocellulosic Chars. Progress in Energy and Combustion Science. 2009; 35: 121-140.

29. P.C.A. Bergman, A. R. Boersma, J.H.A. Kiel, M.J.Prins, K.J. Ptasinski, F.J.J.G. Janssen. Torrefaction for Entrained - Flow Gasification of Biomass. Energy Research Centre of the Netherlands (ECN) 2005.

30. P.C.A. Bergman, A. R. Boersma, J.H.A. Kiel, M.J.Prins, K.J. Ptasinski, F.J.J.G. Janssen. Torrefaction for Entrained - Flow Gasification of Biomass. The 2nd World Conference and Technology Exhibition on Biomass for Energy, Industry and Climate Protection 2004.

31. S. A. Channiwala P. P. Parikh. A Unified Correlation for Estimating HHV of Solid, Liquid and Gaseous Fuels. Fuel 2001; 81 (8): 1051-1063.

32. L. Gašparovič, Z. Korenová and L'udovít Jelemenský. Kicnetic Study of Wood Chips Decomposition by TGA. 36th International Conference of SSCHE. 2009: 178p.

33. J. Pastor-Villegas, J. Meneses Rodriguez, J. M. Pastor-Valle, J.F. Rouquerol J. Denoyel, R. Garcia - Garcia. Adsorption - Desorption of Water Vapour on Chars Prepared from Common Wood Charcoals, in Relation to their Chemical Composition,

Surface Chemistry and Pore Structure. J.of Anal. and Appl. Pyrolysis. 2010; 88 (2): 124-133.

3. Chapter 3: Pyrolysis of Birch Bark Biomass and Production of Char by CO_2 Activation

3.1 Introduction

White Birch is a hardwood tree species found commonly in eastern Canada, and more specifically north of Lake Superior and across northeastern Ontario. According to the Ecology and Management of White Birch Wood proceedings, the multiple uses of this tree are not fully commercially developed (1). Bark from birch wood is consider a waste product of tree de-barking when wood pulp is separated to be used either for lumber or pulp and paper (2). Bark is currently burnt for energy. Pyrolysis presents a potential alternative to convert birch bark to higher value products (3).

Bio-char produced by pyrolysis of birch bark and birch bark bast was studied by Kuznetsov et al. (4).This study found high reactivity of bio-chars to steam activation and that activation could be carried out on birch bark and birch bark bast (sub-product on tannin extraction from birch bark) feedstock at moderate temperatures obtaining iodine adsorption capacities comparable with commercial powder adsorbents.

Bio-oil from the pyrolysis of birch bark has potential uses. There is archaeological evidence of the use of birch bark bio-oil as an adhesive in weapons and ceramic artifacts, as well as a chewing material resembling a gum (5-7). Present interest has focused on the extraction of betulin from birch bark bio-oil. Betulin, found in a percentage of 25-30 %, depending on the birch bark specie (8), has a number of potential pharmaceutical applications as antitumoral agent, anti HIV precursor, and melanoma prevention agent. A good compilation of betulin patents is presented by Chatham Biotec LTD (9). Betulin extraction is achieved either by chemical extraction with methanol or by sublimation through pyrolysis (10). Pyrolysis has been proven not to destroy betulin during birch bark processing, and, with the right pyrolysis conditions, betulin can be completely extracted from the bio-oil. Advantages of sublimation over chemical techniques are its lower cost and lower toxicity (11, 12).

There has been no systematic study of the production of high value activated carbon from the bio-char that is a byproduct of the production of betulin from birch bark, with the exception of the study by Kuznetsov et al. (4), which used steam activation. Other studies (13-19), using other biomass feedstocks, have obtained good results with carbon dioxide as the activation agent. The first objective of this study was, therefore, to test the use of carbon dioxide to activate chars made from birch bark.

Most studies of bio-char activation have used a fixed bed reactor (20-22). Characteristics of fixed bed reactors are relatively poor heat and mass transfer between the gas and the particles, and pronounced radial temperature profiles; these reactor characteristics are thought to be detrimental for char activation (13). The second objective of this study was, therefore, to compare activated char produced in a traditional fixed bed reactor to chars produced in a new reactor, the Mechanically Fluidized Reactor (MFR), which ensure a uniform temperature and excellent particle to gas heat and mass transfer.

3.2 Method

3.2.1 Equipment set up

The Mechanically Fluidized Reactor (MFR) presented in Chapter 2 was modified to perform pyrolysis and activation in the same reactor. The main modifications are indicated in bold in Figure 3-1. The reactor has been modified so that it could be supplied with either inert nitrogen, for the pyrolysis step, or carbon dioxide for the activation step (Figure 2a). The gas flow entering the reactor is controlled by a pressure regulator upstream of a calibrated sonic nozzle (Appendix 1). N_2 flows are calibrated for values between 0.6 to 2.7 L/min, while CO_2 flows are calibrated for values of 0.59-2.2 L/min. The four inlet ports for the introduction of either nitrogen or carbon dioxide into the reactor chamber are illustrated in the image in Figure 2b.

The PID controller used to control the reactor temperature in this study is an Omega model CN7623. This model is different from the one used for the project described in chapter 2 and provides an overall better performance; it allows for auto-tuning, and

changes of up to 100 °C with potential control without any need of changing PID parameters.

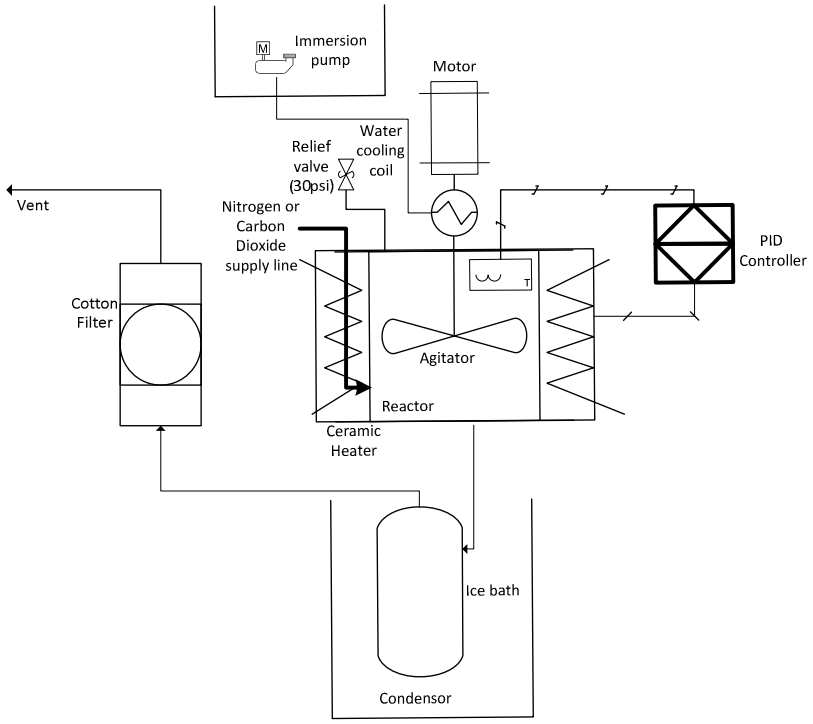

Figure 3-1. MFR; General reactor diagram

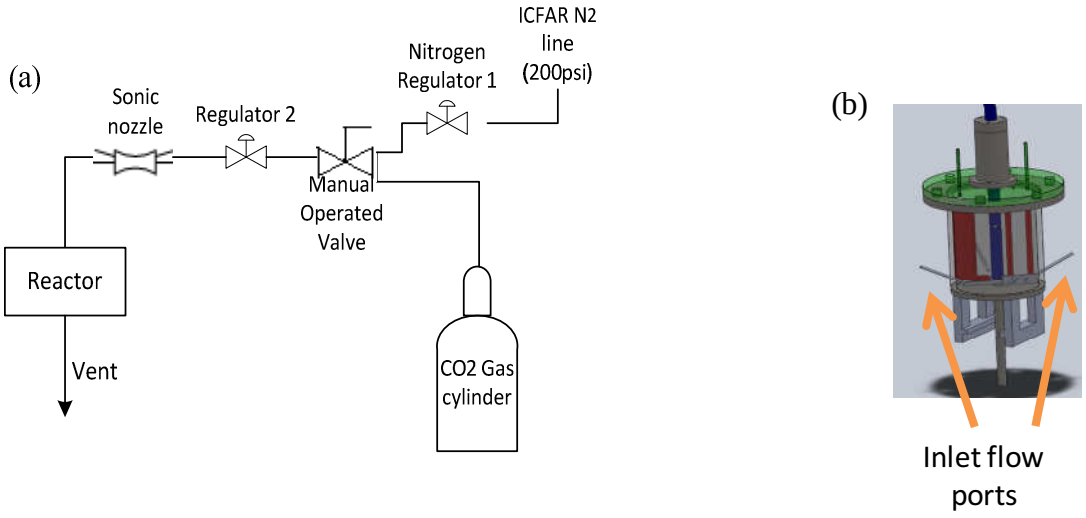

Figure 3-2. Detail of the MFR flow feeding system

Activation experiments carried out in the MFR were compared with activation products obtained with a conventional fixed bed reactor. The fixed bed reactor is designed with a chamber of 59.5 mL in volume, 0.27 m long cylindrical chamber, with an inner diameter of $2.5x10^{-2}$ m, which can process up to 10 g of sample (Figure 3-3). A spiral tube is used to preheat the carbon dioxide supplied to the reactor by inserting both the spiral tube and reactor chamber inside of an electrically heated tubular furnace. Temperature is regulated with the same PID controller as the one used for the MFR, with a different set of parameters values.

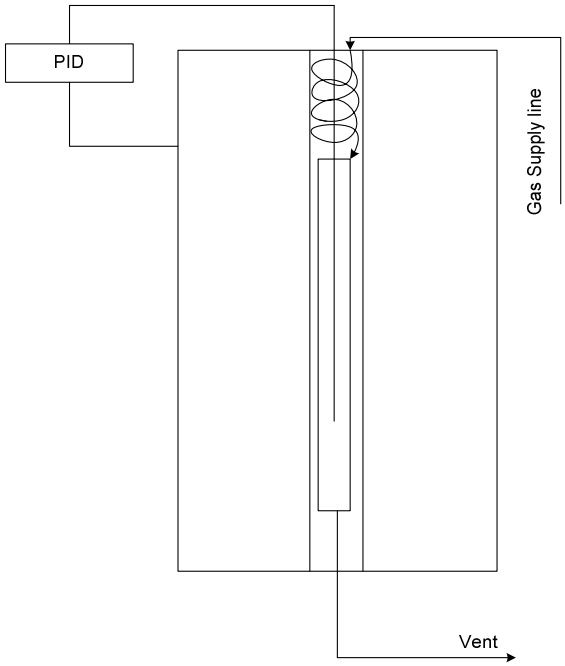

Figure 3-3. Fixed bed reactor diagram in a tubular furnace (1093 °C, 110 V, 8 Amp)

3.2.2 Characterization

The size distribution of the birch bark particles was measured through sieving. The compacted bulk density of the biomass was determined by weighing a sample of biomass powder and determining its volume after compacting the powder by placing its container in a vibrator.

Surface areas were measured with nitrogen isotherms, using the Tristart II 3020 surface analyzer from Micromeritics. 5 point Isotherms were constructed at 77.35 K in a liquid

nitrogen bath. Data were interpreted with a dedicated software through BET for surface area determination.

For pH measurements, all bio-chars and activated carbons samples were pre-ground using a mortar and pestle. Grinding provides a greater exposure of the particle surface to water and allows for more consistent results. For each test, 0.2 g of pre-grinded Bio-coal samples were mixed with 8 ml of distilled water in test tubes where they were left soaking for 3 hours. The pH of the resulting solution was then determined with a pH-meter from Thermo Scientific (Onion 2 star).

3.3 Experiments

Bark from White Birch was provided by the Forintek division of FPinnovations (Quebec City area) in sawdust form (Figure 3-4). Each MFR experiment used 100 g of birch bark biomass. For each experiment in the fixed bed reactor, 7 to 10 g of MFR bio-char were used as feedstock. The biomass had a moisture content of 6.58 wt% and was used without any further drying. Table 3-1 shows the elemental composition of the birch bark sawdust. Its particle size distribution is shown in Figure 3-5; its Sauter-mean diameter was 345 µm.

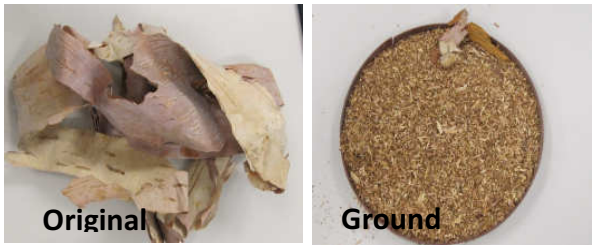

Figure 3-4. Feedstock; Birch bark biomass

Table 3-1. Feedstock elemental composition

	Ash [%]	C [%]	N [%]	H [%]	O [%]
Birch bark Biomass	1.8	58.5	0.6	7.2	31.95

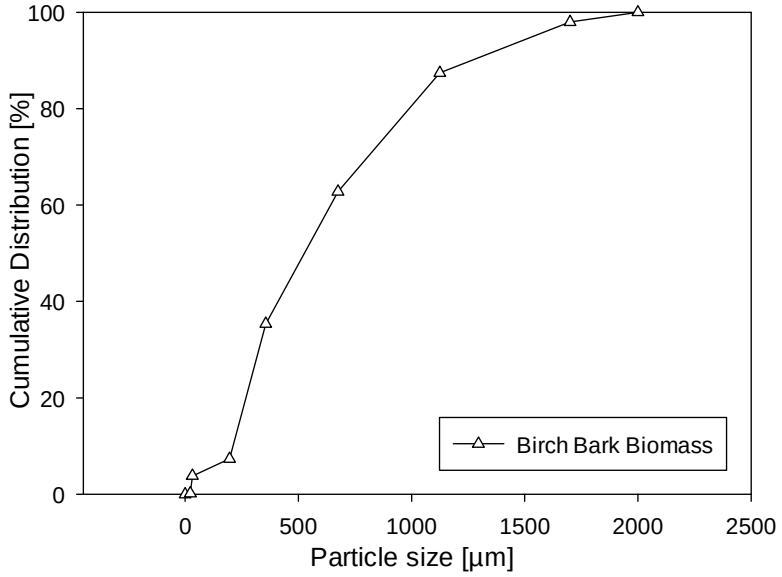

Figure 3-5.Birch bark biomass cumulative particle size distribution as feed in the reactor

3.3.1 Bio-char Production

Pyrolytic bio-chars were produced in the MFR over a wide range of temperatures. The operating conditions selected for the bio-char production were as follows: a biomass load of 100 g, a heating rate of 12 °C/min, an agitation speed of 49.5 rpm, and holding times of 30 or 10 min at the maximum pyrolysis temperature.

3.3.2 Process and Activation Technology Comparison Experiments

Figure 3-6 illustrates the temperature history for 4 experiments performed in the MFR: 1 pyrolysis experiment and 3 consecutive pyrolysis-activation experiments.

All experiments have been carried out at the maximum process temperature of 665 °C. The operating conditions were: for pyrolysis, a 30 min holding time at the maximum temperature, and, for activation, 0.59 L/min of CO_2 flow, with activation times of 30, 60 or 90 minutes.

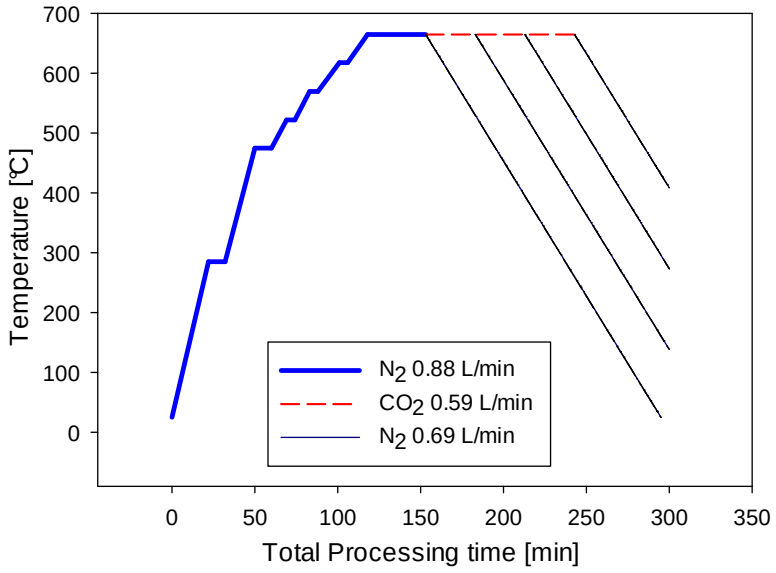

Figure 3-6. Temperature history for the consecutive Pyrolysis – Activation Experiments at 665°C carried out in the MFR (holding times during activation of: 30min, 1h, 1h:30min, , CO_2 injection 0.59 L/min).

Figure 3-7 shows the process diagram description for the two-stage activation experiments. Bio-char is produced by MFR pyrolysis with a max temperature of 665 °C and 30 min holding time. Activation is carried in the fixed bed reactor using the MFR bio-char as feedstock.

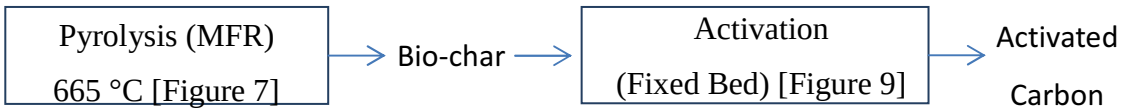

Figure 3-7. Process by stages for production of activated carbon: MFR pyrolysis experiment and activation in the fixed bed reactor (Figure 3-8). Activation done under equal conditions as MFR activation (Figure 3-6)

Activation in the fixed bed reactor is done under the same conditions as the MFR activation: a maximum process temperature of 665 °C with a CO_2 flow of 0.59 L/min, and activation times of 30, 60 or 90 minutes (Figure 3-8).

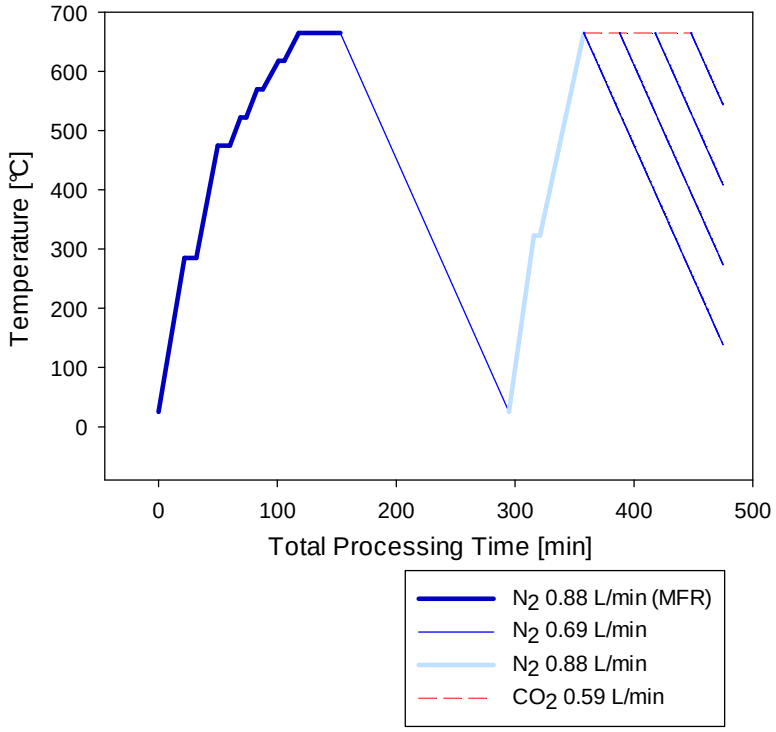

Figure 3-8. Temperature history for MFR bio-char production (with a maximum temperature of 665 °C) followed by fixed bed activation at 665 °C (holding times during activation of: 30min, 1h, 1h:30min, , CO_2 injection 0.59 L/min).

3.4 Results and Discussion

3.4.1 Bio-char Yields and Surface Areas

Figure 3-9 shows the bio-char mass yield obtained with the MFR pyrolysis production tests expressed on a biomass dry basis. As expected, the bio-char yield decreased with increasing temperature. At high temperatures, the holding time effect on the bio-char yield is negligible. An extensive discussion of these results can be found in Chapter 2.

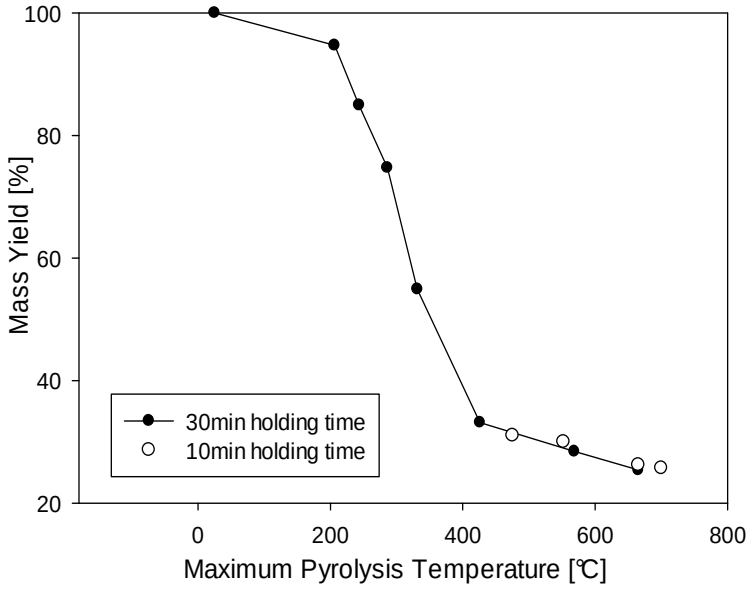

Figure 3-9. Bio-char Mass Yields at Different Maximum Process Temperatures in the MFR (Biomass load:100 g, Holding Time at a Maximum Temperature: 10 or 30 min, Agitator velocity: 49.5 rpm)

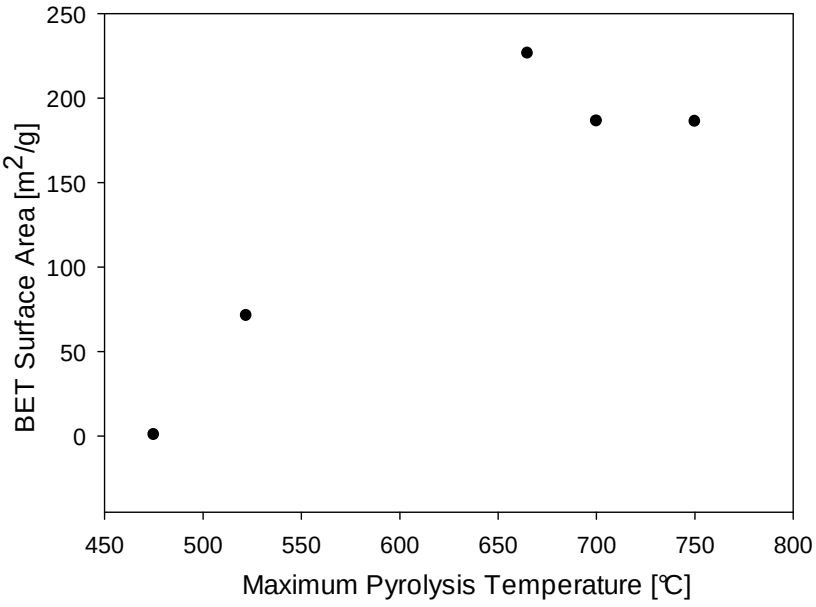

Figure 3-10. Bio-char Surface Areas at Different Maximum Pyrolysis Temperatures

Figure 3-10 presents the surface areas of bio-chars produced at different maximum temperatures.

The surface area generally increases with increasing pyrolytic temperature. The surface area peaks at a pyrolysis temperature of 665 °C with a value of 226.5 m^2/g. For temperatures above 665 °C, the bio-char surface area decreases slightly to 186 m^2/g at 750 °C. Yu et al. (23) found similar surface area trends with corn cob bio-chars processed with microwave pyrolysis: the surface area increased with increasing pyrolysis temperature up to a process temperature of 600 °C, above which the surface area was slightly reduced. Yu et al.(23) explained the increase as related to the release of volatile matter during the pyrolysis, and the slight decrease after 600 °C as a result of blockage of pores due to deposits formation at high temperature. In this study, activation was performed on bio-char obtained from pyrolysis with a maximum processing temperature of 665 °C, since these conditions provided the pyrolytic bio-char with the largest surface area.

3.4.2 Activated Carbon Production using Different Technologies

The activated carbon mass yield is calculated as:

$$\textbf{Activated Carbon Mass Yield } [\%] = \frac{\textbf{Mass of Activated Carbon}}{\textbf{Mass of Dry Birch Bark Biomass}} * \textbf{100} \qquad \text{Eq. 3-1}$$

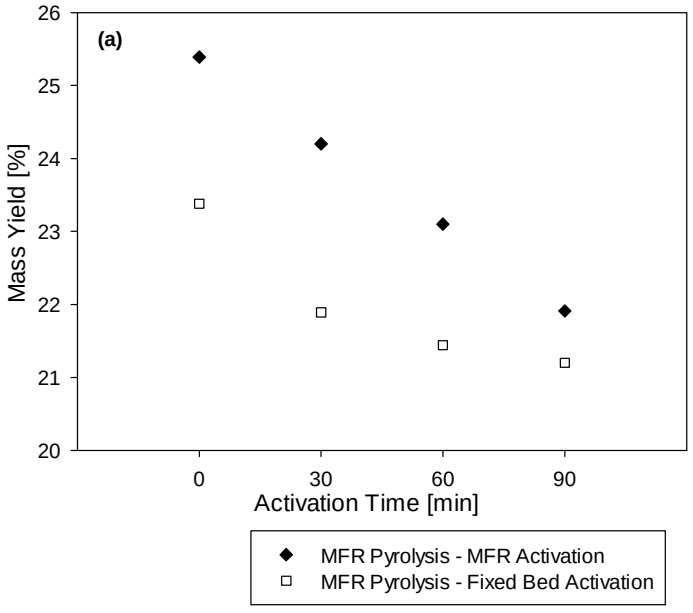

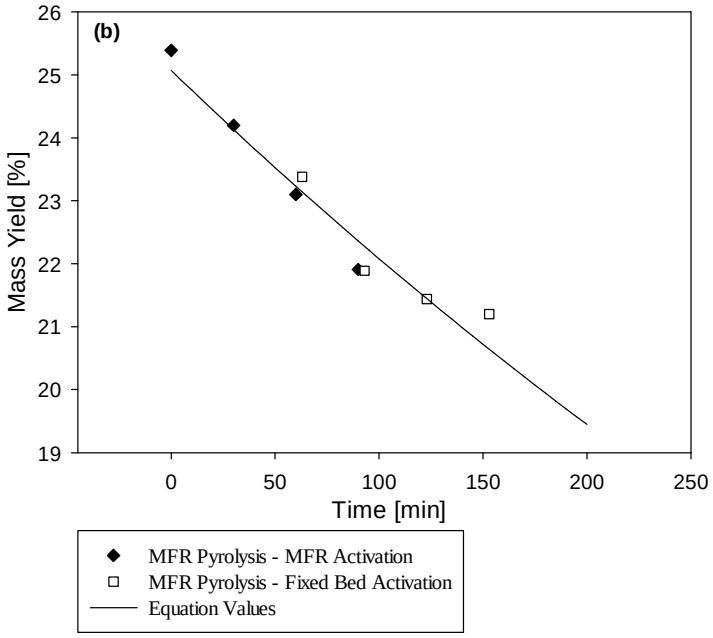

Figure 3-11. (a) Activated Carbon Mass Yield from a Consecutive Pyrolysis - Activation in the MFR (Figure 3-6) and pyrolysis in the MFR with Activation in the Fixed Bed (Error! Reference source not found.) (Activation Temperature: 665 °C, CO_2 injection 0.59 L/min, holding times during activation of: 30min, 1h, 1h:30min) (b) Activated Carbon Mass Yield Presenting all data from Figure 3-11(a), Shifting Time on the x-axis for the Fixed Bed Activation

Figure 3-11a presents the activated carbon mass yield obtained by the two processes. A lower yield is obtained by utilizing the two stage process: MFR pyrolysis under nitrogen, cooling under nitrogen and then reheating under nitrogen in the fixed bed before activation with carbon dioxide (Figure 3-8). Figure 3-11b was obtained by taking the data of Figure 3-11a and shifting the times for the MFR – fixed bed runs by 63 minutes. Reheating the pyrolytic bio-char in the fixed bed, under nitrogen, before performing the activation in the fixed bed seems to be roughly equivalent, as far as the yield is concerned, to activating the bio-char under carbon dioxide in the MFR for 63 minutes. As shown by Figure 3-11b, the yield data from both types of activation can be fitted with the same equation:

$$\frac{x_0 - x}{x_0 - x_\infty} = 25.07 * \exp(-0.001t) \quad \text{Eq. 3-2}$$

This equation suggests that the minimum yield is 0 %. This behavior is different from the linear relationship that was reported by J.L. Figueiredo (24) for CO_2 activation.

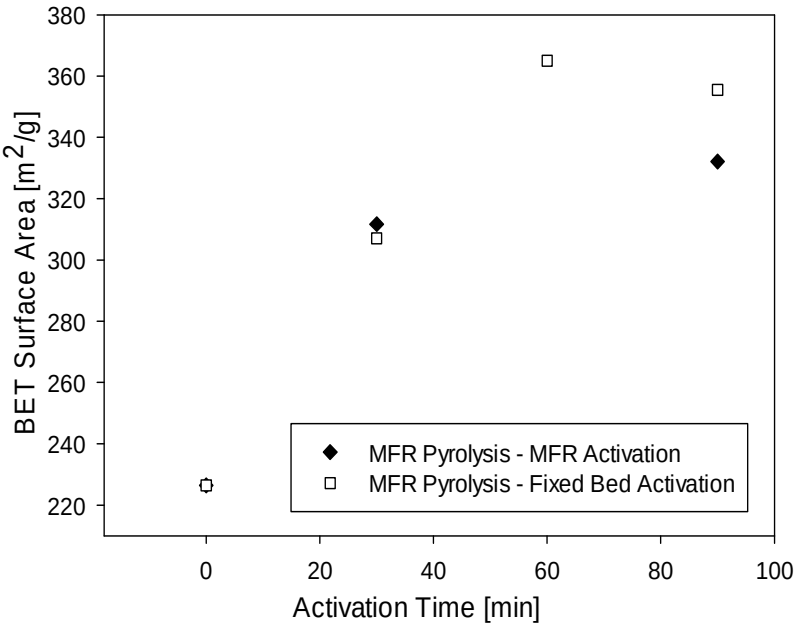

Figure 3-12. Activated Carbon Surface Areas with Consecutive Pyrolysis - Activation in the MFR (Figure 3-6) and Activation in the Fixed Bed (Figure 3-8) (Activation Temperature: 665 °C, CO_2 injection 0.59 L/min, holding times during activation of: 30min, 1h, 1h: 30min)

Activated carbon surface areas are presented in Figure 3-12. Similar surface areas were obtained with both activation reactors. It seems that the surface area of the activated char depends mainly on the duration of the activation under carbon dioxide. Comparing these results with those illustrated in Figure 3-11a and 11b, it appears that the main difference between the two types of activation reactors is the yield: activating with the fixed bed reactor requires an additional reheating step, under nitrogen, during which additional pyrolysis occurs, reducing the overall yield without creating additional pores.

The highest surface area for carbon activated at 665 °C was 355 m^2/g, obtained for an activation time of about 60 minutes. Activation at 665 °C, therefore, increases the surface area by nearly 60 %.

Although activation in the MFR gave slightly higher yields of activated char than activation in the fixed bed, similar surface areas were obtained with both technologies. Studies for the optimization of the production of activated carbon was, therefore, performed with the more traditional fixed bed reactor.

3.4.3 Optimization of Activation in the Fixed Bed Reactor

Figure 3-13 shows the two production and activation procedures used to compare two production runs. In the first run (Figure 3-13a), the carbon dioxide is applied as soon as the bed temperature reached 323 °C, while, in the second run (Figure 3-13b), it was only applied after the bed reached 665 °C.

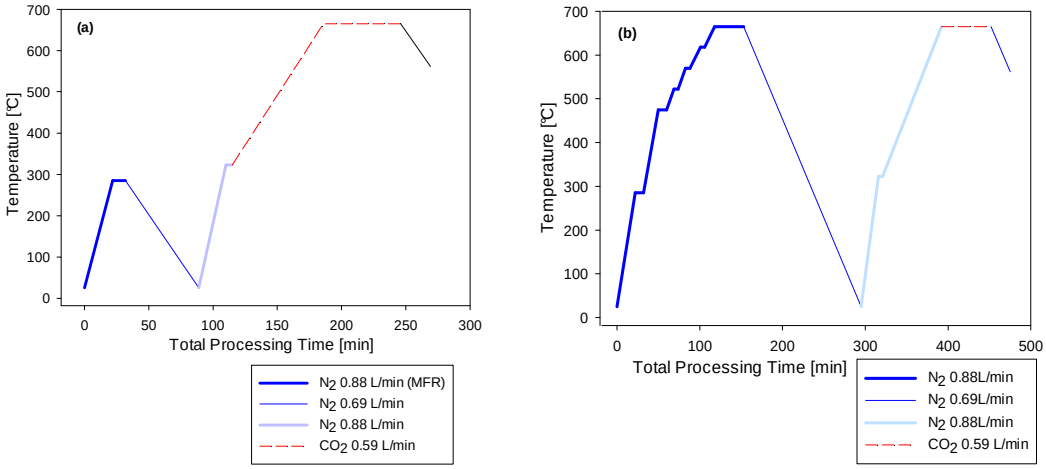

Figure 3-13. Activation Experiments Description; CO_2 Injection from a Low Temperature and CO_2 Injection only at a Maximum Process Temperature for Activation (Fixed Bed Reactor) (Maximum activation Temperature: 665 °C, CO_2 injection 0.59 L/min)

Mass loss during activation is calculated during the time of CO_2 injection in the system, in relation to the Mass yield of the bio-char produced just before activation starts (Eq. 3-3).

$$\textbf{Mass Loss During Activation } [\%] = \frac{\textbf{Mass of Biochar at 665°C} - \textbf{Mass of Activated Carbon}}{\textbf{Mass of Biochar at 665°C}} * \mathbf{100} \quad \text{Eq. 3-3}$$

Results of surface areas and mass loss during activation are presented in the following table.

Table 3-2. Surface Area and Mass Loss Values for Activation Experiments with CO_2 Injection at Different Temperatures, description of the experiment shown in Figure 3-13

Activation Process	**Surface Area [m^2/g]**	**Mass Loss During Activation**
CO_2 injection from a low temperature, 323°C, up to a maximum activation temperature of 665 °C	380	50.25%
CO_2 injection only at a maximum process temperature of 665 °C	365	8.35%

Table 3-2 shows that starting to apply carbon dioxide at lower temperatures does not make any significant change in the activated char surface area, since the two surface areas are within experimental error of the BET tests. This indicates that, for birch bark bio-chars, no significant activation occurs before a temperature of 665°C. Cao et al. (25), which performed a thermogravimetric analysis of the activation of a mixture of barks (fir, spruce and larch) with steam, found similar results.

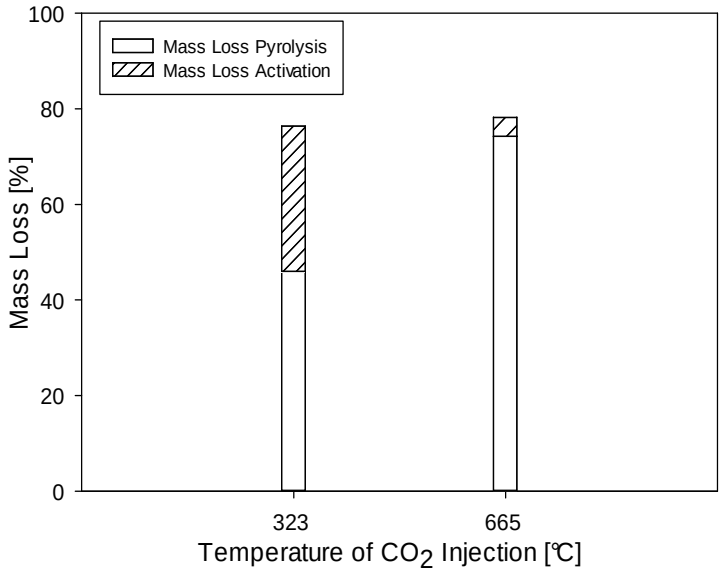

Figure 3-14. Overall Mass Loss during Pyrolysis and Activation with CO_2 Injection Points at different Temperatures (Figure 3-13)

Figure 3-14 compares the mass losses obtained when starting the carbon dioxide flow at 323 °C or at 665 °C. The results show that the overall mass loss is essentially the same with both procedures.

Figure 3-15 shows how char was activated with carbon dioxide at different temperatures in the fixed bed reactor. In all cases, activation was performed at a constant temperature, i.e. the maximum temperature reached by the char sample during its production.

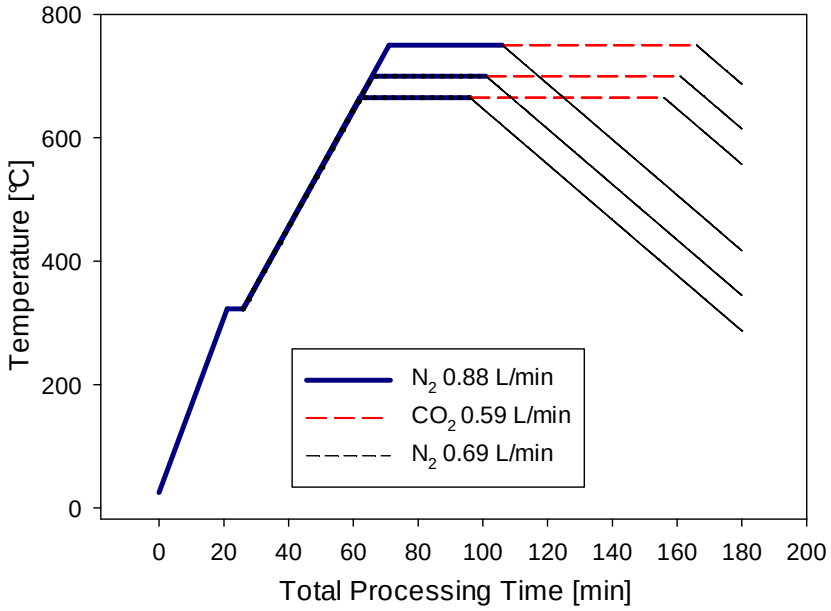

Figure 3-15. Pyrolysis and Activation Experiments Description at Different Temperatures (Fixed Bed Reactor, activation holding time 1h, injection 0.59 L/min)

Figure 3-16 shows the impact of the maximum temperature on the BET surface areas obtained for the pyrolytic bio-char and the activated char. In the absence of carbon dioxide activation, the surface area decreases slightly with the maximum temperature.

On the other hand, with carbon dioxide activation, the surface area increased slightly with the maximum temperature.

Figure 3-16 clearly shows the great benefits of performing the carbon dioxide activation, since it nearly doubles the surface area. Figure 3-16 suggests that activating with carbon dioxide at temperatures higher than 750 °C would bring only minor additional increases in surface area.

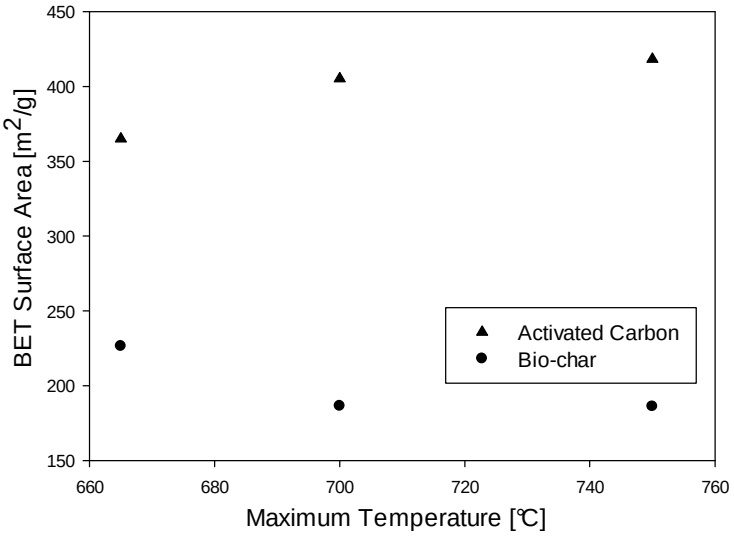

Figure 3-16. Activated carbons and bio-chars surface areas at different temperatures (Pyrolysis; maximum temperature holding time: 30 min, Activation; 1 h holding time at maximum temperature, 0.059 L/min CO_2, Figure 3-15)

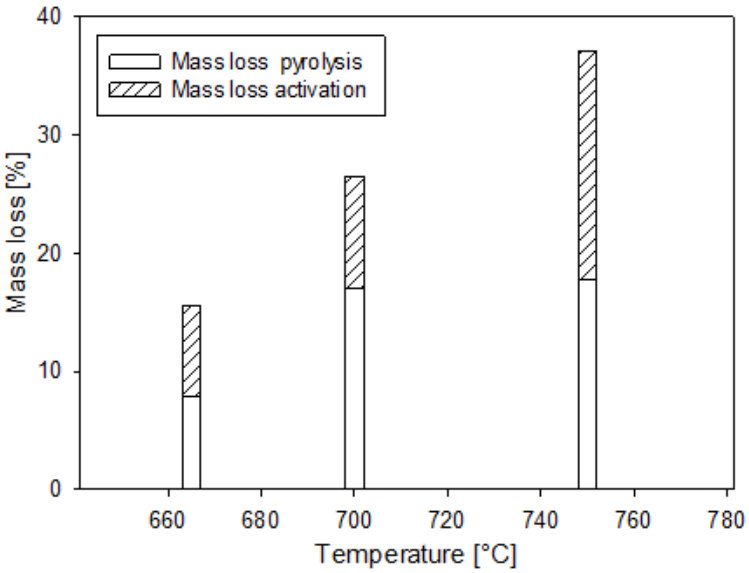

Figure 3-17. Mass loss distribution on the fixed bed reactor; during pyrolysis and activation

Figure 3-17 shows that increasing the activation temperature greatly increases the total mass loss. Actually, combining the results from Figure 3-16 and 17 indicates that increasing the activation temperature actually reduces the surface area when expressed in m^2 per unit mass of original biomass. Judging solely by the surface area parameter, 700 °C would likely be the preferred activation temperature as it results in a high value of surface area (405 m^2/g) without excessive mass loss of the product.

3.4.4 pH of bio-chars and activated carbons

Activated carbon pH is an important characteristic for determination of adsorption applications. The high (basic) bio-char pH has been related to the beneficial performance of the char as a soil amendment of acid soils (26).

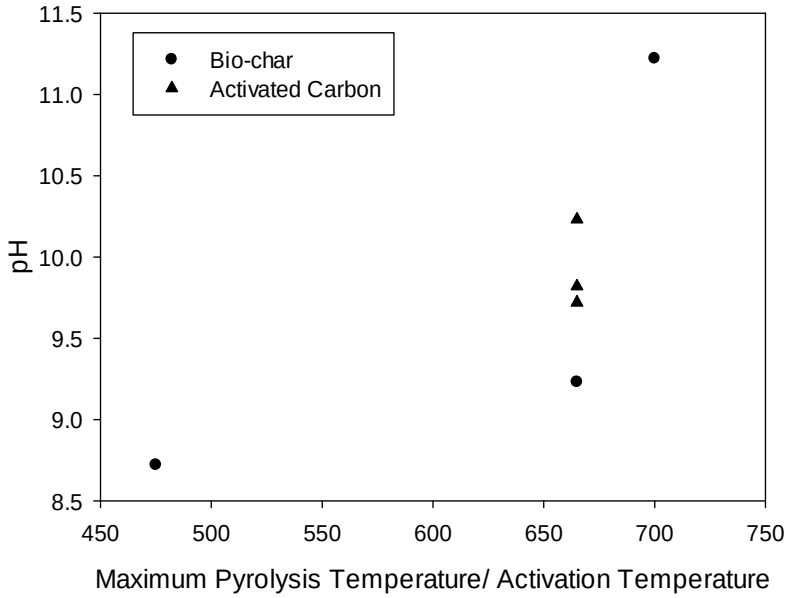

Figure 3-18. Representative pH Values of high temperature bio-chars and activated carbon production at 665 °C (For different activation times: 30min, 1h, 1h 30min, 0.59 L/min CO_2)

Figure 3-18 shows that the bio-char pH increases slightly with increasing pyrolysis temperature. This had already been observed in the work reported in Chapter 2. The pH of bio-char and activated carbons produced at a temperature of 665 °C ranges from 9.2 to 10.3. Results herein are in agreement with the results reported by Faust et al. (27), who concluded that carbons processed at high temperatures will form alkali oxides.

3.5 Conclusions

- Birch bark bio-char surface areas are found to increase with pyrolysis temperatures to a maximum of 226 m^2/g achieved at 665 °C. Pyrolytic temperatures higher than 665 °C reduce the surface areas values.
- Activating bio-char produced at 665 °C with carbon dioxide at 665 °C increased the surface area by nearly 60 %.
- Performing both the pyrolysis and the activation in the same Mechanically Fluidized Reactor (MFR), instead of the performing the activation in a more traditional fixed bed reactor, does not change the surface area. However, it significantly increases the mass yield of activated carbon.

- The surface area of activated carbon increases with activation temperature, topping at 420 m^2/g for an activation temperature of 750 °C. The optimal temperature for production of birch bark activated carbon with CO_2 is about 700 °C since it combines a surface area of 405 m^2/g with a lower mass loss than that achieved at 750 °C.
- Both pyrolytic bio-char and CO_2 activated carbon from birch bark are alkaline.

3.6 References

1. H. Chen, A. Luke, W. Bidwell, Editors. NEST Workshop Proceedings. Ecology and Management of White Birch Workshop 2000.

2. R. Patt, O. Kordsachia, J. Fehr . European Hardwoods vs. Eucalyptus Globulus as a Raw Material for Pulping. Water Science and Technology 2006; 40: 39-48.

3. A. Demirbas, Editor. Biorefineries for Biomass Upgrading Facilities (Green Energy and Technology). London: Springer-Verlag 2010.

4. B. N. Kuznetsov, T. V. Ryazanova, M. L. Shchpko, S. A. Kuznetsova, E. V. Veprkova, N. A. Chuprova. Optimisation of Thermal and Biochemical Methods for Recovery of Wastes from Extraction Processing of Birch Bark. Chemistry for Sustainable Development 2005; 13: 439–447.

5. K. Tiilikkala, L. Fagernas, J. Tiilikkala. Hystory and Use of Wood Pyrolysis Liquids as Bioide and Plant Protection Product. The Open Agriculture Journal 2010; 4: 111-118.

6. P.P.A. Mazza, F. Martini, B. Sala, M. Magi, M. P. Colombini, G. Giachi, F. Landucci, C. Lemorini, F. Modugno, E. Ribechini. A New Palaeolithic Discovery; Tar-Hafted Stone Tools in a European Mid-Pleistocene Bone-Bearing Bed. J. of Archeol Sci. 2006; 33 (9): 1310-1318.

7. K. Evans. Glue, Disinfectant and Chewing Gum: Natural Products Chemistry in Archaeology. Chem. Ind . London. 1993; (12): 446-449.

8. B.N. Kuznetsov, T.V. Ryazanova, M. L. Shchipko, S.A. Kusznetsova, E.V. Veprikova, N.A. Chuprova. Optimization of Thermal and Biochemical Methods for Recovery of Wastes from Extraction Processing of Birch Bark. Chemistry for Sustainable Development 2005; 13: 439-447.

9. Chatham Biotec LTD. Betulin Industry Skateholders Analysis 2007.

10. P. Jääskeläinen. Betulinol and its Utilisation 1981; 63 (10): 599-603.

11. M.-F. Guidoin, J. Yang, A. Pichette, C. Roy. Betulin Isolation from Birch Bark by Vacuum and Atmospheric Sublimation. A Thermogravimetric Study. Thermochimica Acta 2003; 398 (1-2): 153-166.

12. J. Népo Murwanashyaka, C. Roy, H. Pakdel. Extraction of Betulin by Vacuum Pyrolysis of Birch Bark. Journal of Wood Chemistry and Technology 2002; 22 (2-3): 147-155.

13. V. Minkova, S. P. Marinov, R. Zanzi, E. Bjornbom, T. Budinova, M. Stefanova, L. Lakov. Thermochemical Treatment of Biomass in a Flow of Steam or in a Mixture of Steam and Carbon Dioxide. Fuel Processing Technology 2000; 62 (1): 45-52.

14. M. Ahmedna, W.E. Marshall, R.M. Rao. Production of Granular Activated Carbons from Select Agricultural Byproducts and Evaluation of their Physical, Chemical and Adsorption Properties. Bioresource Technology 2000; 71 (2): 71-113.

15. A. C. Lua, T. Yang, J. Guo. Effects of Pyrolysis Conditions on the Properties of Activated Carbons Prepared from Pistachio-Nut Shells. J. of Anal. Appl. Pyrolysis 2004; 72 (2): 279 - 287.

16. T. Zhang, W. P. Walawender, L. T. Fan, M. Fan, D. Daugaard, R. C. Brown. Preparation of Activated Carbon from Forest and Agricultural Residues through CO_2 Activation. Chemical Engineering Journal 2004; 105 (1-2): 53-59.

17. F. Rodriguez-Reinoso, M. Molina-Sabio. Activated Carbons from Lignocellulosic Materials by Chemical and/or Physical Activation: An Overview. Carbon. 1992; 30 (7): 1111-1118.

18. M. L. Sekirifa, M. Hadj-Mahammeda, S. Pallier, L. Baameur, D. Richardb, A. H. Al-Dujaili. Preparation and Characterization of an Activated Carbon from a Date Stones Variety by Physical Activation with Carbon Dioxide J. of Anal. and Appl. Pyrolysis 2012 (In press)

19. P. J. M. Carrott, Suhas, M. M. L. Ribeiro, C. I. Guerrero, L. A. Delgado. Reactivity and Porosity Development during Pyrolysis and Physical Activation in CO_2 or Steam of Kraft and Hydrolytic Lignins. J. of Anal. and Appl. Pyrolysis 2008; 82 (2): 264-271.

20. A. C. Lua, J. Guo. Activated Carbon Prepared from Oil Palm Stone by One-Step CO_2 Activation for Gaseous Pollutant Removal. Carbon 2000; 38 (7): 1089 - 1097.

21. A. Ahmadpour, D. D. Do. The preparation of Active Carbons from Coal by Chemical and Physical Activation. Carbon 1996; 34 (4): 471 - 479.

22. H. Demiral, I. Demiral, B. Karabacakoglu, F. Tumsek. Production of Activated Carbon from Olive Bagasse by Physical Activation. Chemical Engineering Research and Design. 2011; 89 (2): 206 - 213.

23. F.Yu, P. H. Steele, R. Ruan. Microwave Pyrolysis of Corn Cob and Characteristics of the Pyrolytic Chars. Energy Sources. 2010; 32 (5): 475-484.

24. J. L. Figueiredo. Evaluation of the Efficiency of Activation in the Production of Carbon Adsorbents. Carbon 1996; 34 (5): 679

25. N. Cao, H. Darmstadt, F. Soutric, C. Roy. Thermogravimetric Study on the Steam Activation of Charcoals Obtained by Vacuum and Atmospheric Pyrolysis of Softwood Bark Residues. Carbon 2002; 40 (4): 471 - 479.

26. C. Steiner. Slash and Char as Alternative to Slash and Burn - Soil Charcoal Amendments Maintain Soil Fertility and Establish a Carbon Sink [Dissertation].

Bayreuth, Germany: Institute of Soil Science and Soil Geography, University of Bayreuth; 2006.

27. S.D. Faust. Chemistry of Water Treatment. Lewis publishers, editor 1998.

4. Chapter 4: Analysis of the Production of Bio-coal and Activated Carbon from Different Biomasses

4.1 Introduction

About 20 % of above-ground agricultural residual biomass can be sustainably harvested and utilized for a variety of different purposes, based on the preservation of soil organic matter and the prevention of soil erosion (1). Although this number was derived for the Province of Ontario in Canada, it would apply to many of the top producing agricultural regions around the world. According to the World Energy Council, forestry and agricultural residues have the potential to provide energy at a level of about 100 EJ/year, worldwide (2).

Biomass presents a potential alternative for coal substitution in electrical power production. Raw biomass, however, has serious drawbacks, such as high hygroscopy, low heating value, and non-homogeneous moisture content causing non-homogeneous behavior during combustion. Torrefaction of biomass can improve these properties and provide a product more suitable for coal substitution (3). Char from biomass pyrolysis also has potential as a feedstock for the production of high-value activated carbon, using either physical activation or mild gasification with carbon dioxide (4).

The biomasses selected for this study are representative of typical residual feedstocks and span a wide range of properties to identify the types of feedstocks that would be most suitable for the production of either bio-coal or activated carbon. They include a wood, a bark, two agricultural residues and a grass. They are maple wood, birch bark, corn stalk, coffee pulp and switch grass. Maple wood is the woody representative biomass of our study. It is a hardwood that is already used in wood manufacture, with broad commercialization. Bark is a residue from wood processing and wood manufacturing industry, which is produced as a co-product after pulp extraction (5). Commercial applications of this residue are restricted due to its chemical composition (6). Pyrolysis of birch bark has been studied for the extraction of high-value chemical products from its bio-oil, while bio-char has been proposed as a precursor for activated carbon (7).

Corn stalk is an abundant aboveground agricultural residue from corn crops. Globally 520 Tg of corn is produced per year, from which North America is a major contributor (8). USDA estimated that production of corn stover (corn stalks, leaves, cobs and husks) were of 243 Mt per year from which 82 Mt per year could be sustainably collected (9). There is large interest on pyrolysis research as a technology for the utilization of this biomass (10-14).

Coffee pulp is a waste generated from the wet processing of coffee cherries to obtain coffee beans (15). The production of coffee pulp is approximately equal to 1 tonne for every 2 tonnes of raw feedstock material (16). Coffee pulp represents an environmental pollution problem as its sugar, protein and mineral content, and its high water retention creates an ideal environment for rapid growth of microorganisms. As a result, it must immediately be treated after production (17). The use of coffee pulp as animal feed has been pursued in the past, but its contents of caffeine, chlorogenic acid, tannins, and abundant potassium has led to poor results (16). Coffee pulp adversely affects the economics of coffee production and ends up being disposed as a residue instead of being used (17).

Switch grass is a perennial grass that has multiple advantages over other bioenergy crops (18): it can be cultivated on marginal land that has poor soil quality and undesirable characteristics, eliminating competition with food crops, it is easy and cheap to grow, it does not require irrigation, and it has been shown to improve soil conservation. Switch grass is also considered as a potential feedstock for second generation bioethanol production (19). The potential use of grass pellets for combustion has been studied through TGA techniques and compared to wood combustion (20), and pyrolysis applications have been analyzed, although application for either bio-coal or activated carbon production have never been investigated (21).

4.2 Methods

4.2.1 Equipment and Production Experiments

Batch pyrolysis experiments have been conducted in a batch Inconel Mechanically Fluidized Reactor (MFR) having an inner diameter of 0.09 m, a height of 0.13 m and a

volume capacity of 0.81 L (22). Figure 4-1 shows a diagram of the MFR. Reactor heating is provided by means of a radiant ceramic heater, and regulated with a PID controller (Omega model CN7623). A thermocouple placed in the top part of the reactor, acts as the sensor of the control system. A previous calibration relates the measured temperature to the temperature of the reacting biomass particles in the MFR bed, as described in Chapter 2.

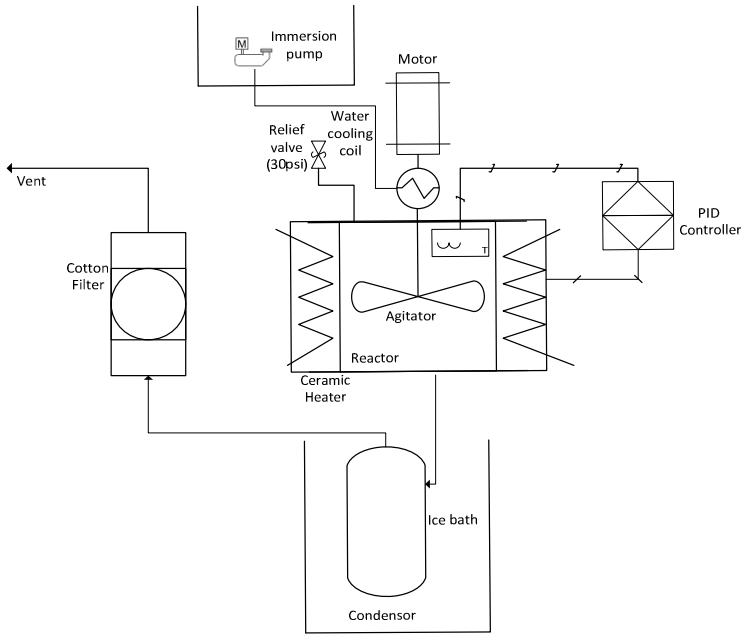

Figure 1

Figure 4-1. MFR diagram

Biomass was ground to a sieve diameter of less than 1 mm (when required) before loading into the reactor. The maximum load capacity of the reactor with loose raw material is 80% of the reactor volume capacity, to avoid entrainment of char and tar. All experiments were done with an agitation velocity of 49.6 rpm, a heating rate of 12 °C/min and 30 min holding time at the maximum pyrolysis temperature, which ranged from about 200° to 570 °C. Yields were calculated from the ratio of the mass of product to the mass of the biomass feedstock on a dry basis.

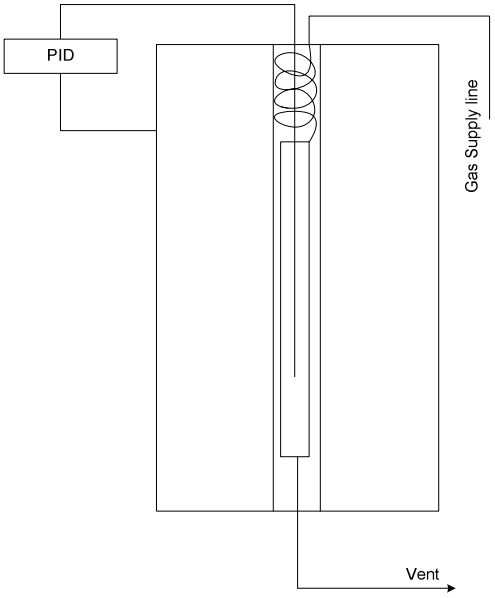

Figure 4-2. Fixed bed reactor in a tubular furnace (1093 °C, 110V, 8 Amp)

Activation experiments were carried in a batch fixed bed reactor Figure 4-2. Char produced in the MFR was activated with carbon dioxide in the fixed bed reactor at 750°C for 1 hour. The fixed bed reactor is a 0.27 m long cylindrical chamber, with an inner diameter of $2.5*10^{-2}$ m. It can process about 10 g of char. Both a spiral tube that is used to preheat the carbon dioxide entering the reactor and the actual reactor are heated in a tubular furnace (Figure 4-2). The reactor temperature is regulated with the same PID controller that has been used with the MFR with different set of control parameters values.

4.2.2 Characterization

The different biomasses were characterized by moisture content, elemental analysis, ash content and calorific value. Bio-chars were characterized by their yield, calorific value and hygroscopy. Representative bio-chars and activated carbons were characterized by BET surface areas.

Elemental analysis, ash content, calorific value and hygroscopy measurements were performed on samples that had been dried over 2 hours in an oven at 100 ^{o}C. Elemental analysis was performed using an AN634 Flash 2000 CHN Analyzer. Vanadium oxide

(catalyst for sulfur content detection) was used for the CHN analysis. Oxygen content was calculated by difference, accounting for the ash content in the sample. The ash content was determined according the ASTM D1102-84 standard (Standard Test Method for Ash in Wood) using nickel crucibles (30 mL). High heating values were obtained using an IKA C200 Calorimeter.

Hygroscopicity experiments were performed in a humidity-controlled environment. First, 3-5 g of bio-coal (or biomass) were loaded onto an aluminum dish that was placed inside an airtight container (0.3 L). Each container was filled up with water to half its volume capacity to saturate the existent air in the containers, with the dish floating over the water. A humidity indicator was used to verify that the air was saturated with humidity. The containers containing the bio-coal and water were placed in a wine-cooler with a temperature controlled at 15 C. A halogen moisture analyzer HB43-S (Mettler Toledo) was used to measure the moisture content of the samples. Replicate experiments were performed to validate the acquired data.

4.3 Results and Discussion

4.3.1 Feedstock characterization

Table 4-1. Feedstocks Main Characteristics; Moisture Content, Elemental Composition, Ash Content, and High Heating Value

Feedstock	Moisture Content [%]	Ash content [Dry %]	C [Dry %]	N [Dry%]	H [Dry%]	O [Dry%]	O/C	H/C	HHV [J/g]
Maple wood	7.1	0.39	46.74	0.14	5.88	46.9	1.00	0.13	20340
Birch bark	7.13	1.81	58.5	0.6	7.2	31.95	0.55	0.12	22420
Coffee pulp	4.5	8.85	43.04	1.81	8	38.3	0.89	0.19	17080
Corn stalk	8.01	4.31	45.76	1.41	7.24	41.27	0.90	0.16	16770
Switch grass	8.21	5.51	44.68	1.76	7.34	40.7	0.91	0.16	16770

Table 4-1 presents the results of the biomass characterization. As expected, the ash content is low for maple wood and birch bark. Coffee pulp has the highest ash content. Carbon, hydrogen and oxygen contents are in a similar range for all types of biomass,

with birch bark having a higher oxygen content and a lower carbon content than the other biomasses. Birch bark and maple wood have higher heating values than the other biomasses.

Table 4-2. Feedstock Main Components; Content of Cellulose, Hemi-cellulose and Lignin taken from Literature

Feedstock	Cellulose	Hemi-cellulose	Lignin
Coffee pulp (23)	63 ±2.5	2.3±1	17.5±2.2
Switch grass (21)	32	19.2	18.8
Switch grass (20)	30.2 ±0.98	19.83 ±2.06	
Hardwood (17)	42	24-33	23-30
Corn stalk (24)	38.02	21.1	24.65
Corn stalks(10)	42.2	29.6	21.7
	Homo-cellulose		Lignin
Birch bark(5)	49.8		27.9

Hemi-cellulose, cellulose and lignin contents reported in the literature are shown in Table 4-2. Hardwood values are used as representative of maple wood.

4.3.2 Pyrolysis Product Mass Yield

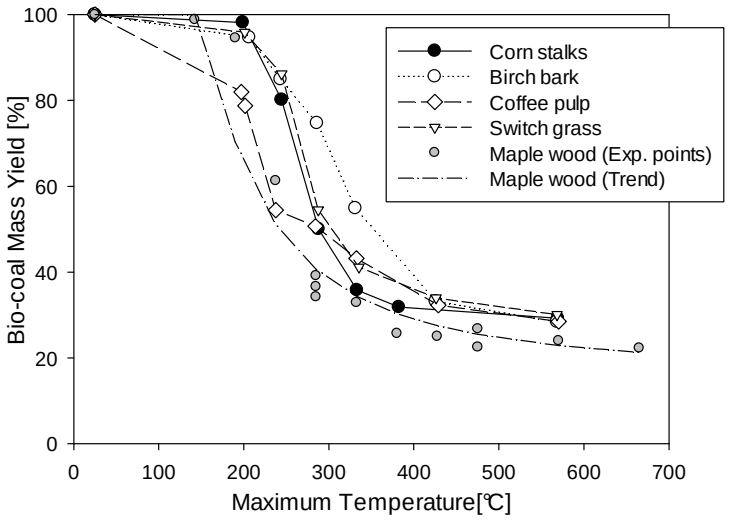

Figure 4-3 Bio-coal Mass Yields from Different Biomasses

The mass yield of bio-coal decreases for all biomasses with increasing maximum pyrolysis temperature (Figure 4-3). There is a sharp drop in bio-coal yield at a temperature that ranges from about 200 °C for maple wood to 300 °C for birch bark. Replicate experiments conducted with maple wood show that the results were reproducible.

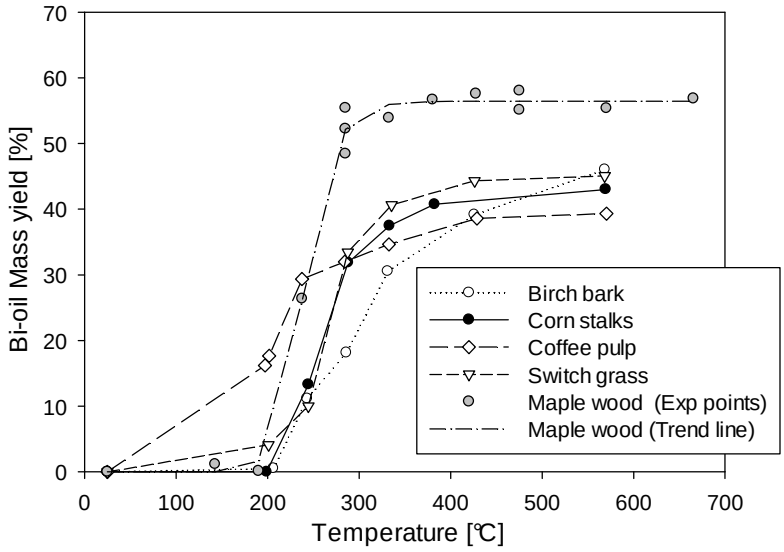

Figure 4-4 Bio-oil Mass Yields from Different Biomasses

Bio-oil, which is obtained by condensing the vapors evolving during the batch pyrolysis, is a valuable co-product of bio-coal production; it may be the source of chemicals or be used to fuel the pyrolysis process Figure 4-4. shows that the bio-oil yield increases with increasing maximum pyrolysis temperature, reaching a plateau at temperatures ranging from 300 to 400 °C, depending on the biomass. The maximum bio-oil yield that can be obtained from maple wood (57 wt%) is significantly higher than the maximum bio-oil yields obtained from the other biomasses, which ranged from 38 to 46 wt%. Replicate experiments conducted with maple wood show that the results were reproducible (Figure 4-4).

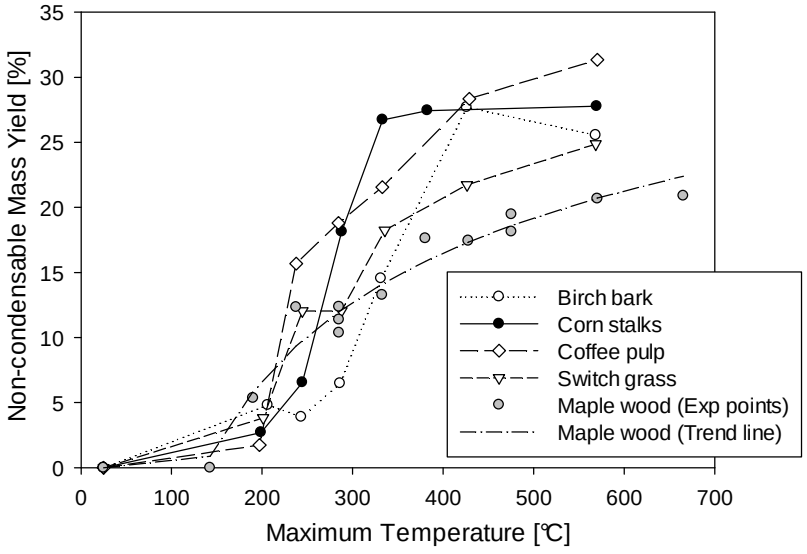

Figure 4-5. Non–condensable Gases Mass Yield from Different Biomasses

Non-condensable gases, consisting of carbon monoxide, carbon dioxide, methane, hydrogen and traces of other light gases, can be used to fuel the pyrolysis process. The yield of non-condensable gases increases with increasing maximum pyrolysis temperature (Figure 4-5). For the highest maximum pyrolysis temperature of 570 C, it ranges from 20 wt%, for maple wood, to 31 wt%, for coffee pulp. Replicate experiments conducted with maple wood show that the results were reproducible (Figure 4-5).

Table 4-3. Bio-oil Water Content (From Bio-oil Production with a Maximum Pyrolysis temperature of 570°C)

Feedstock	Bio-oil water content [%] (from production at 570°C)
Switch Grass	72.8
Coffee Pulp	86.7
Maple Wood	52.1
Birch Bark	68.9
Corn Stalk	60.4

Table 4-3 compares the water content of bio-oils produced with a maximum pyrolysis temperature of 570 °C for all biomasses. Coffee pulp gives bio-oil with the highest water content, although its initial moisture is the lowest (Table 4-3). Coffee pulp is the biomass with the largest cellulose content (Table 4-2), and the highest ash content (Table 4-1). The principal pyrolysis product of cellulose is Levoglucosan and ash acts as a catalyst for the degradation of levoglucosan into compounds of lower molecular weight, including water (25). Grey et al. (26) report the formation of water product in high ash feedstocks. Oudenhoven et al. (27) proposed utilizing the acid aqueous phase of the bio-oil to wash and demineralize the biomass by removing the ashes, to reduce the degradation of levoglucosan; this may be applied to coffee pulp residue to reduce the production of pyrolytic water.

4.3.3 Calorimetry Results

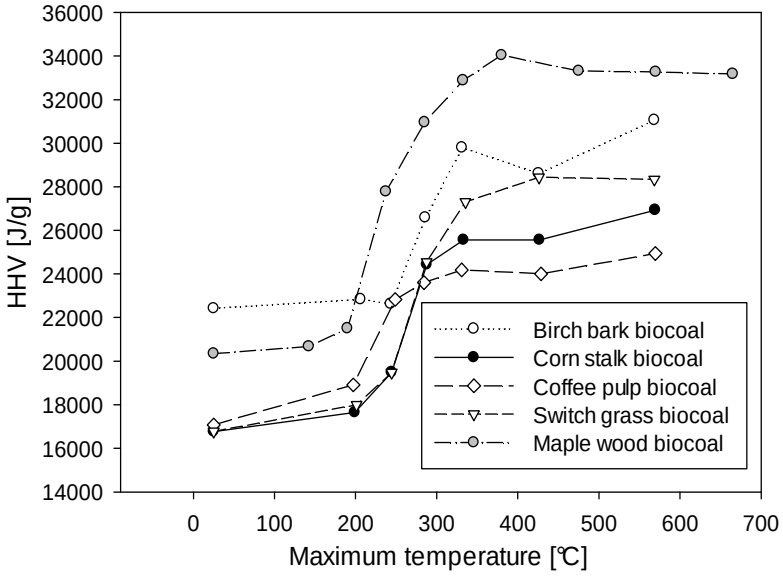

Figure 4-6 Biomass and Bio-coal High Heating Values for Different Biomasses

Figure 4-6 displays the high heating value (HHV) of bio-coals produced from the different feedstocks. The heating value of the char can reach a value that is nearly double that of the original biomass. Pyrolyzing above 350 °C does not improve the heating value. Maple wood and birch bark are the biomasses with the highest HHV as well as the

biomasses with the highest lignin content and the highest original heating values of the raw feedstock. Baker (28) reported that the heating value of cellulose is lower than the heating value of lignin, while Demirbas (29) found that the heating value of biomasses can be directly related to their lignin content.

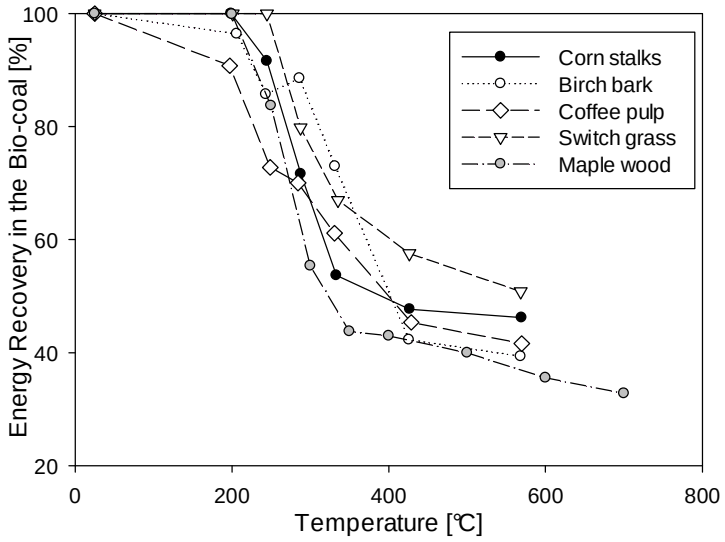

Figure 4-7 Percentage of Energy Recovery in Bio-coal from Different Biomasses

The energy recovery in the Bio-char can be calculated as follows:

$$\%_{\substack{\textbf{Energy Recover}\\ \textbf{in the Bio-char}}} = \mathbf{Y_{Bio-char}} * \frac{\mathbf{HHV_{Biochar}}}{\mathbf{HHV_{Biomass}}} * \mathbf{100} \quad \text{Eq. 4-1}$$

Figure 4-7 shows the energy recovery values of the Bio-chars calculated by Eq.4-1. Energy recovery decreased with increasing the maximum pyrolysis temperature. Trends and values are similar for all feedstocks. The actual maximum pyrolysis temperature to be selected for the production of bio-coal will be the result of a compromise between the loss in energy shown in Figure 4-7 and the enhancement in heating value shown in Figure 4-6. Another factor will also be the desired hygroscopic characteristics of the bio-coal.

4.3.4 Hygroscopicity

Figure 4-8 to 4-12 shows the hygroscopy graphs for the various biomass feedstocks and the corresponding bio-coals produced at different temperatures. All the biomasses and bio-coals reached stable moisture content after 20 days. Bio-coal has always a lower equilibrium moisture content than the original biomass, with the largest relative reductions observed with maple wood (Figure 4-8) and birch bark (Figure 4-9). The equilibrium moisture content was reduced by about two thirds for maple wood and by about half for birch bark. The bio-coal hygroscopy seems to be related to the lignin content of the original biomass, but definite conclusions would require the measurement of the lignin content of the actual feedstocks that were used for this study.

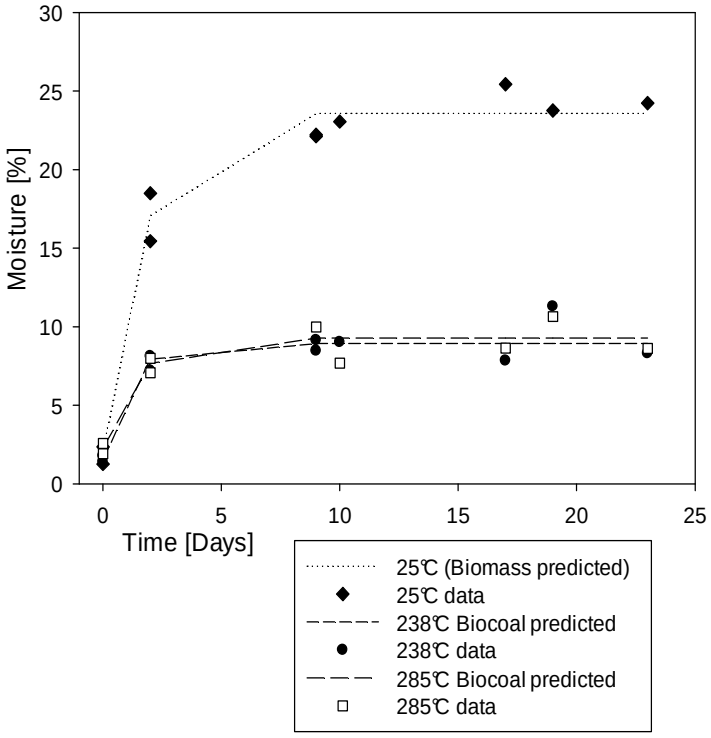

Figure 4-8. Maple wood biocoal – biomass hygroscopy, presented in moisture units reported at different tested times

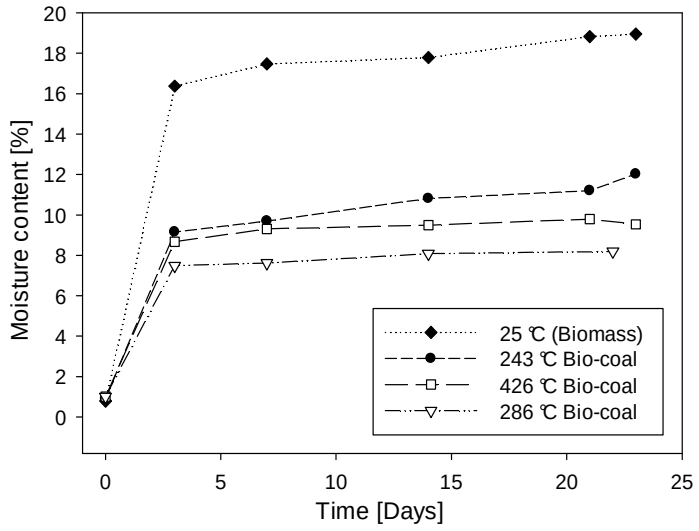

Figure 4-9. Birch bark bio-coal – biomass hygroscopy, presented in moisture units reported at different tested times

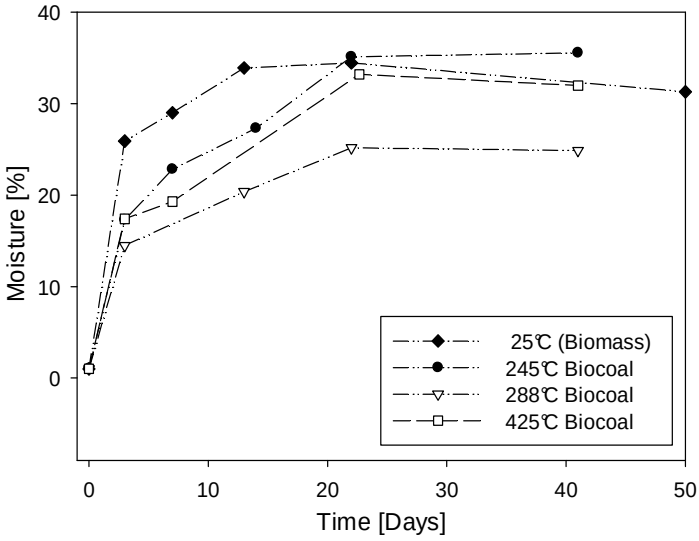

Figure 4-10**.** Corn stalk bio-coal – biomass hygroscopy, presented in moisture units reported at different tested times

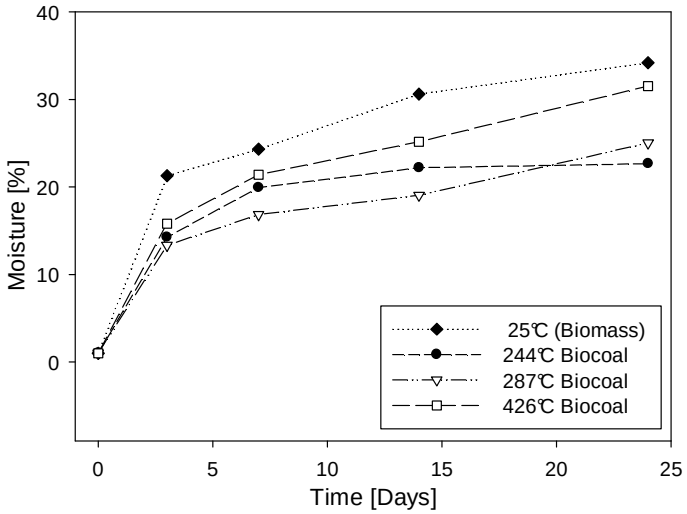

Figure 4-11. Switch grass bio-coal – biomass hygroscopy, presented in moisture units reported at different tested times

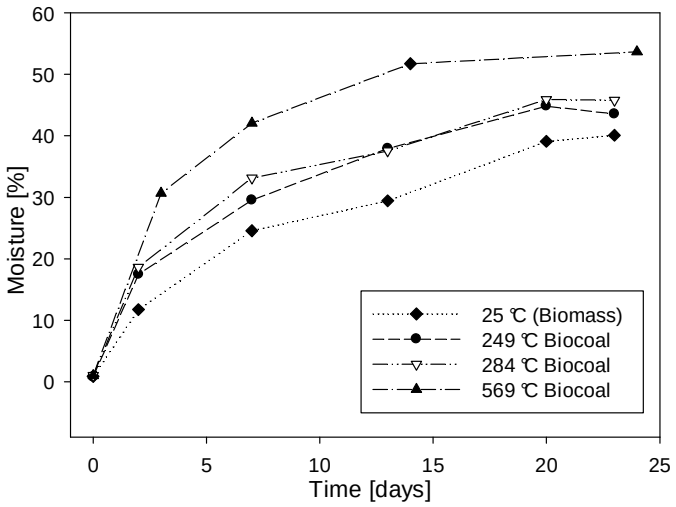

Figure 4-12. Coffee pulp bio-coal – biomass hygroscopy, presented in moisture units reported at different tested times

Figure 4-13. Microbial activity over bio-chars from coffee pulp, presented in moisture units reported at different tested times

Low hygroscopy of the bio-coals is of great importance to the industry for its preservation and to avoid degradation via biological organisms. Biological degradation is a common problem when biomass is directly used as coal replacement. This problem is particularly severe when the materials are stored under humid conditions (30). Coffee pulp fails to have or develop hydrophobic structures with thermal treatment. Microbial growth was evident on the 300 °C pyrolysis bio-coal from coffee pulp (Figure 4-13); these samples developed microbial growth within 30 days under saturated humidity conditions at 15 °C. With coffee pulp, a maximum pyrolysis temperature of 600 °C was required to avoid any microbial growth, but the energy and mass yield of the bio-coal obtained under such conditions were unattractive.

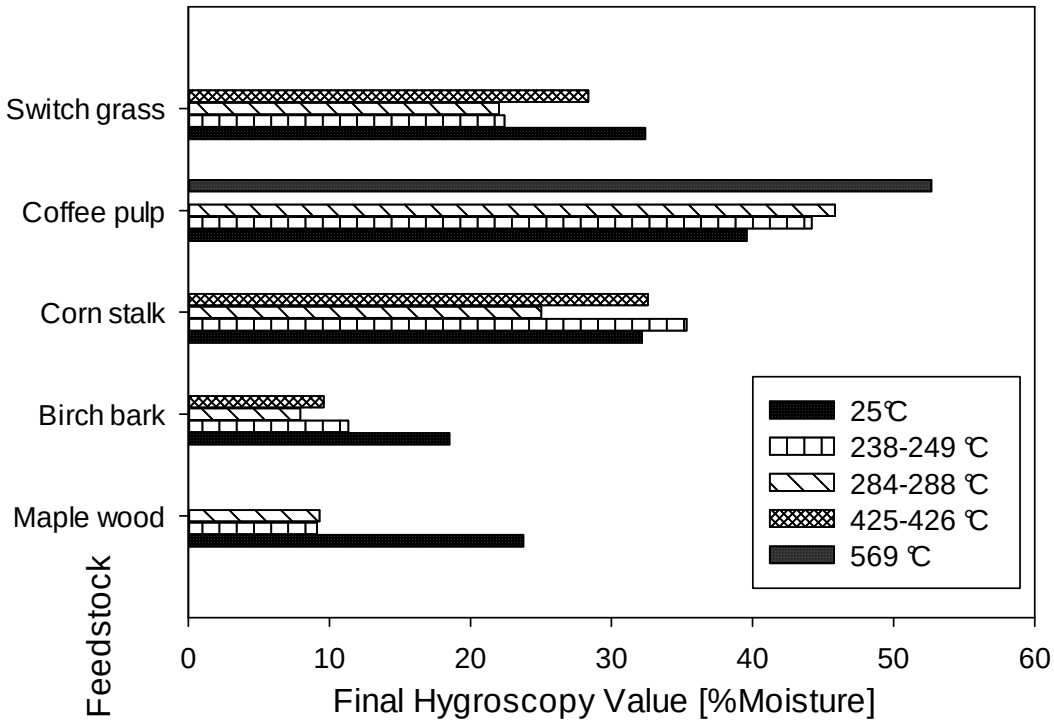

Figure 4-14 Final hygroscopy values for biomass and bio-coal produced at different temperatures and from different feedstocks (units of final hygroscopy are given as equilibrium moisture percentage of samples exposed to saturated atmosphere)

Figure 4-14 compares the equilibrium moisture contents for various bio-coals. Bio-coals produced from maple wood and birch bark are the most attractive.

Table 4-4. Main bio-coal characteristics of samples with lowest hygroscopy for each feedstock

Maximum Pyrolysis Temperature	Feedstock	Hygroscopy [Moisture %]	Energy Recovery [%]	HHV bio-coal [J/g]	Bio-coal Mass Yield
286°C	Birch bark	7.9	88.6	26583	74.7
288°C	Corn stalk	25	71.6	24434	49.9
Biomass [25°C]	Coffee pulp	39.6	100	17079	100
238°C	Maple wood	9.1	83.7	27782	61.3
285°C	Maple wood	9.3	55.4	30950	34.2
287°C	Switch grass	20.2	79.8	24552	54.5

Table 4-4 summarizes, for each biomass, the characteristics of the least hygroscopic bio-coal. Maple wood and birch bark seem to be the most attractive feedstocks.

4.4 Activation Results

Figure 4-15 shows that the activated chars with the highest surface areas were obtained from birch bark and maple wood, the feedstocks with the highest lignin content. Apaydin-Varol et al. (12) reported that a high lignin content of the original biomass results in a high char surface area.

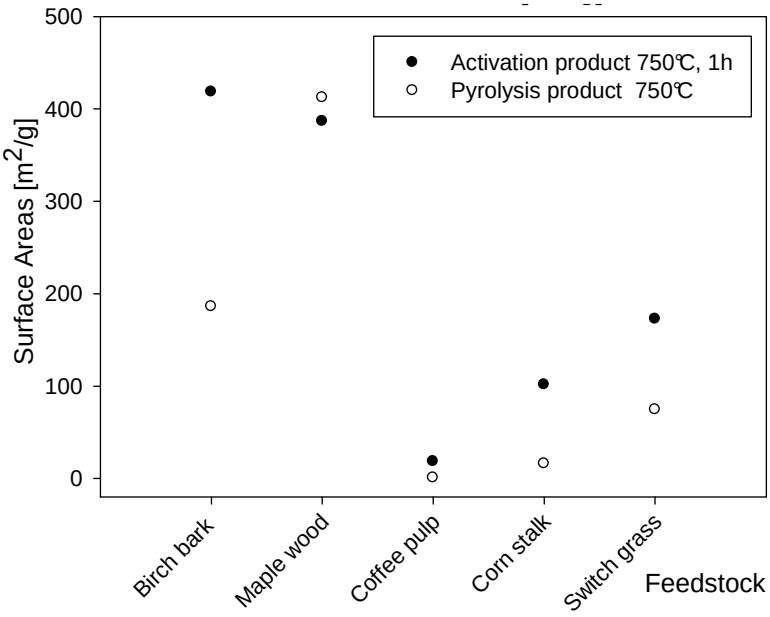

Figure 4-15. Bio-char and activated carbon surface areas for different processed biomasses

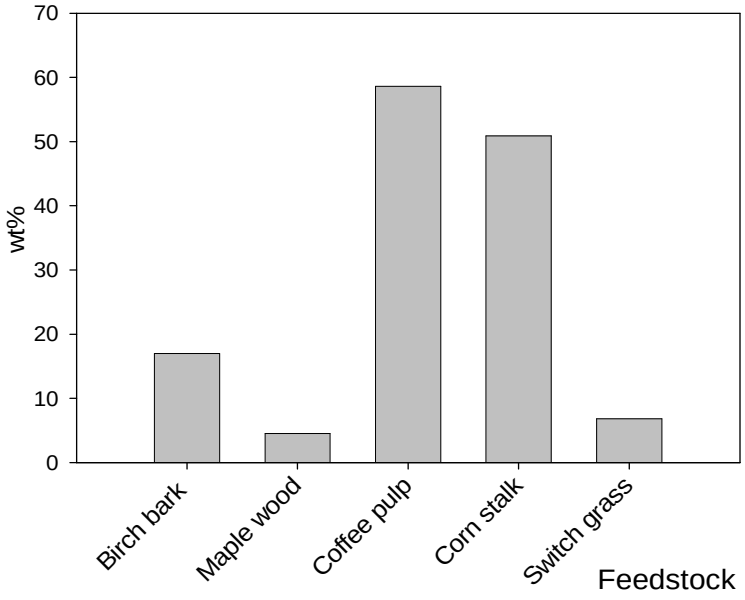

Figure 4-16. Mass loss during activation for different feed biomasses

Carbon dioxide activation is effective with chars from birch bark, corn stalk and switch grass, but is completely ineffective with char from maple wood (Figure 4-15). Figure 4-15 shows the fraction of material lost during activation depends greatly on the char that is activated. Figure 4-15 confirms that char from maple wood is not affected by carbon dioxide activation.

4.5 Conclusions

- Switch grass, corn stalk and coffee pulp gave relatively poor bio-coals and activated carbons, when compared to maple wood and birch bark.
- Optimal conditions for bio-coal production range from a top temperature of 238 °C for maple wood to 286 °C for birch bark. Converting these feedstocks to bio-coal reduces hygroscopy by about 60 % and increases the heating value by 20 to 36 %. In both cases, 84 to 89 % of the energy of the original biomass is recovered in the bio-coal.

- Only birch bark and maple wood provide activated carbon with a high surface area of about 400 m^2/g. Carbon dioxide activation greatly increases the surface area of birch bark char, but does not have a significant effect on maple wood char.
- Feedstocks with a high lignin content are more likely to produce a bio-char with a high surface area through batch pyrolysis.

4.6 References

1. Bioindustrial Innovation Centre. Assessment of Agricultural Residuals as a Biomass Fuel for Ontario Power Generation . November 2010.

2. World Energy Council. 2010 Survey of Energy Resources.

3. J. J. Chew, V. Doshi. Recent Advances in Biomass Pretreatment - Torrefaction Fundamentals and Technology. Renewable and Sustainable Energy Reviews. 2011; 15 (8): 4212 - 4222.

4. R.C. Bansal, M. Goyal. Activated Carbon Adsorption. Boca Raton: Taylor & Francis; 2005.

5. I. Miranda, J. Gominho, I. Mirra, H. Pereira. Fractioning and Chemical Characterization of Barks of Betula Pendula and Eucalyptus Globulus. Industrial Crops and Products. 2013; 41: 299 - 305.

6. S. Sensoz. Slow Pyrolysis of Wood Barks from Pinus Brutia Ten. and Product Compositions. Bioresource Technology. 2003; 89 (3): 307 - 311.

7. B. N. Kuznetsov, T. V. Ryazanova, M. L. Shchipko, S. A. Kusznetsova, E.V. Veprikova, N. A. Chuprova. Optimization of Thermal and Biochemical Methods for Recovery of Wastes from Extraction Processing of Birch Bark. Chemistry for Sustainable Development. 2005; 13: 439-447.

8. S. Kim , B. E. Dale. Global Potential Bioethanol Production from Wasted Crops and Crop Residues. Biomass and Bioenergy. 2004; 26 (4): 361-375.

9. J. A. Capunitan, S. C. Capareda. Assessing the Potential for Biofuel Production of Corn Stover Pyrolysis using a Pressurized Batch Reactor. Fuel. 2012; 95: 653-572.

10.L. V. Gaojin, W. Shubin. Analytical Pyrolysis Studies of Corn Stalk and its three Main Components by TG-MS and py-GC/MS. J. of Anal. and Appl. Pyrolysis. 2012; 97: 11-18.

11. O. Ioannidou, A. Zabaniotou, E. V. Antonakou, K. M. Papazisi, A. A. Lappas, C. Athanassiou. Investigating the Potential for Energy, Fuel, Materials and Chemical Production from Corn Residues (Cobs and Stalks) by Non-Catalytic and Catalytic Pyrolysis in two Reactor Configurations. Renewable and Sustainable Energy Reviews. 2009; 13 (4): 750-762.

12. E. Apydin-Varol, A. E. Pütün. Preparation and Characterization of Pyrolytic Chars from Different Biomass Samples. J. of Anal. and Appl.Pyrolysis 2012; 98: 29-36.

13. C. A. Mullen, A. A. Boateng, N. M. Goldberg, I. M. Lima, D. A. Laird, K. B. Hicks. Bio-oil and Bio-char Production from Corn Cobs and Stover by Fast Pyrolysis. Biomass and Bioenergy. 2010; 34 (1): 67-74.

14. A. Zabaniotou, O. Ioannidou. Evaluation and Utilization of Corn Stalks for Energy and Carbon Material Production by using Rapid Pyrolysis at high Temperature. Fuel. 2008; 87 (6): 834-843.

15. A. Pandey, C. R. SoccoI, P. Nigam, D. Brand, R. Mohan, S. Roussos. Biotechnological Potential of Coffee Pulp and Coffee Husk for Bioprocesses. Biochemical Engineering Journal. 2000; 6 (2): 153-162.

16. S. Roussos, M. de los Angeles Aquiahualt, M. del Refugio Trejo-Hernandez, I. Gaime Perraud, E. Favela, M. Ramakrishna, M. Raimbault, G. Viniegra-Gonzalez. Biotechnological Management of Coffee Pulp and Isolation, Screening, Characterization, Selection of Caffeine Degrading Fungi and Natural Microflora Present in Coffee Pulp and Husk. Applied Microbiology and Biotechnology 1995; 42 (5): 756-762.

17. D. Shenoy, A. Pai, R. K. Vikas, H. S. Neeraja. A Study on Bioethanol Production from Cashew Apple Pulp and Coffee Pulp Waste. Biomass and Bioenergy. 2011; 35 (10): 4107 - 4111.

18. M. Khanna, B. Dhungana, J. Clifton-Brown. Cost of Producing Miscanthus and Switchgrass for Bioenergy in Illinois. Biomass and Bioenergy. 2008; 32 (6): 482-493.

19. S. B. McLaughlin, L. A. Kszos. Development of Switchgrass (Panicum Virgatum) as a Bioenergy Feedstockin the United States. Biomass and Bioenergy. 2005; 28 (6): 515-535.

20. S. R. Chandrasekaran, P. K. Hopke. Kicnetics of Switch Grass Pellet Thermal Decomposition under Inert and Oxidizing Atmospheres. Biomass and Bioenergy. 2005; 28 (6): 515-535.

21. T. Imam, S. Capareda. Characterization of Bio-oil, Syn-gas and Bio-char from Switchgrass Pyrolysis at Various Temperatures. J. of Anal. and Appl. Pyrolysis. 2012; 93: 170-177.

22. C. Briens, L. Ferrante, F. Berruti. A New Mechanical Fluidized Reactor (MFR) for Biomass Pyrolysis. TCS2010 Symposium on Thermal and Catalytic Sciences for Biofuels and Biobased Products, Iowa State University, Sept. 21-23. 2010.

23. P. S. Murthy, M. M. Naidu. Sustainable Management of Coffee Industry by- Products and Value Additions - A Review. Resources, Conservation and Recycling. 2012; 66: 45 - 58.

24. C. Pang, T. Xie, L. Lin, J. Zhuang, Y. Liu, Q. Yang. Changes of the Surface Structure of Corn Stalk in the Cooking Process with Active Oxygen and MgO-based Solid Alkali as a Pretreatment of its Biomass Conversion. Bioresource Technology. 2012; 103 (1): 432-439.

25. P. R. Patwardhan, J. A. Satrio, R. C. Brown, B. H. Shanks. Influences of Inorganic Salts on the Primary Pyrolysis Products of Cellulose. Bioresource Technology. 2010; 101 (12): 4646 - 4655.

26. M. R. Gray, W. H. Corcoran, G. R. Gavales. Pyrolysis of a Wood - Derived Material. Effect of Moisture and Ash Content. Industrial and Engineering Chemistry Process Design and Development. 1985; 24 (3): 646 - 651.

27. S. R. G. Oudenhoven, R. J. M. Westerhof, N. Aldenkamp, D. W. F. Brilman, S. R. A. Kersten. Demineralization of Wood using Wood - Derived Acid: Towards a Selective Pyrolysis Process for Fuel and Chemical Production. J. of Anal. and Appl. Pyrolysis. 2012 (In press).

28. A. J. Baker. In: Wood Fuel Properties and Fuel Products from Woods 1982.

29. A. Demirbas. Relationships between Lignin Contents and Heating Values of Biomass. Energy Conversion & Management. 2001; 42 (2): 183 - 188.

30. B. Patel, B. Gami, H. Bhimani. Improved Fuel Characteristics of Cotton Stalk, Prosopis and Sugarcane Bagasse Through Torrefaction, Energy for Sustainable Development. Energy for Sustainable Development. 2012; 15 (4): 372-375.

5. Chapter 5: Conclusions

Performance of bio-coals and activated carbons differ greatly depending on the biomass from which they are produced.

Maple wood and Birch bark biomass torrefaction at temperatures of 238 ºC and 286 ºC are found optimal for bio-coal production towards coal substitution application in power stations. These bio-coals among the analyzed, reduce respectively, the biomass hygroscopy by 60 % and 57 %, and increase the biomass calorific value by 36 % and 20 %. The energy contained in these bio-coals was 84 % and 89 % of the energy in the biomass feedstock.

Corn stover, Switch grass and Coffee pulp are not recommended for bio-coal production because of poor bio-coal properties: poor hygroscopy reduction and small gain in calorific value.

Bio-chars from Birch bark were the most improved by CO_2 activation. More specifically bio-chars of birch bark reached surface areas of 226 m^2/g through pyrolysis and 418 m^2/g with subsequent CO_2 activation. Bio-chars produced using maple wood reached surface areas of 412 m^2/g, that were not enhanced by CO_2 activation

Coffee pulp, corn stover and switch grass bio-chars reported low surface areas and are not suitable feedstocks for activated carbon production.

5.1 Recommendations for Future Work

- Test bio-coals with suitable characteristics for their combustion performance, pelletization and hygroscopy after pelletization.
- Improve the MFR reactor design to perform activation experiments at higher temperatures. This starting by using a temperature resistant welding on the union between the gas inlet ports and the reactor chamber, or changing gas injection system in the reactor.

- Perform activation with different techniques (chemical activation techniques or steam activation) of bio-chars derived from various feedstocks. The aim should be to identify the most effective activation agent and activation process.
- Measure the micro-pore distribution and surface chemistry of activated carbons.. Implement the adsorption experiments that are best suited for some typical potential applications.
- Integrate the production of liquid and char to develop process that maximizes returns, i.e. for birch bark consider the optimal conditions for the integrated production of char and betulin-rich liquid.

6. Appendix

Appendix 1 : Nozzle Calibration

The following diagram shows how the nitrogen and carbon dioxide volumetric flow are controlled by using a sonic nozzle. The nozzle is located after the pressure regulator (Regulator 2 within a range of 0-120 psi) and flow is calibrated using regulator pressures. The nitrogen supply for the unit comes from a common line available at the ICFAR laboratory. The carbon dioxide line supply is a compressed gas cylinder.

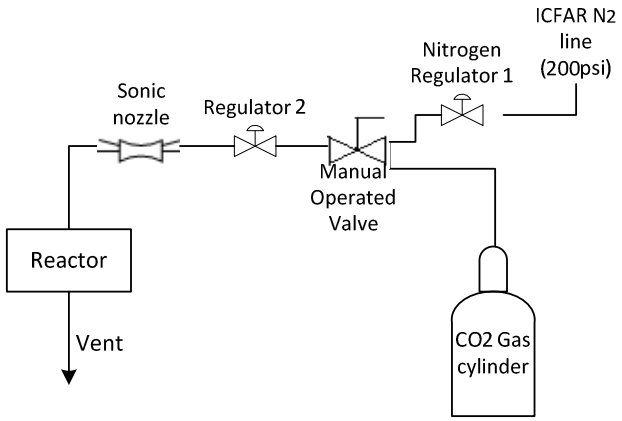

Figure 6-1. Gas Flow Diagram

For practical purposes the nitrogen calibration is done under the range as shown in the following graph (between 0.7 to 2.7 L/min).

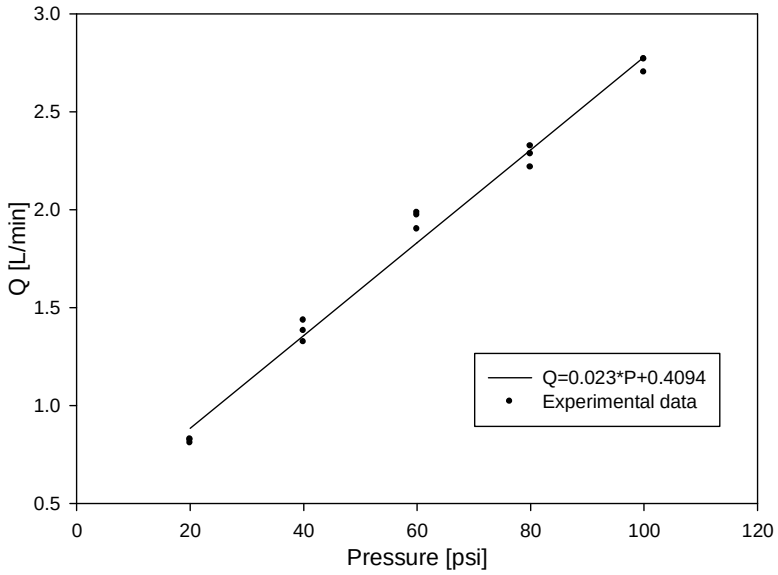

Figure 6-2. Nitrogen flow calibration through pressure regulator

Calibration of the same sonic nozzle for CO_2 was done between range of 0.6-2.2 L/min shown in the following graph.

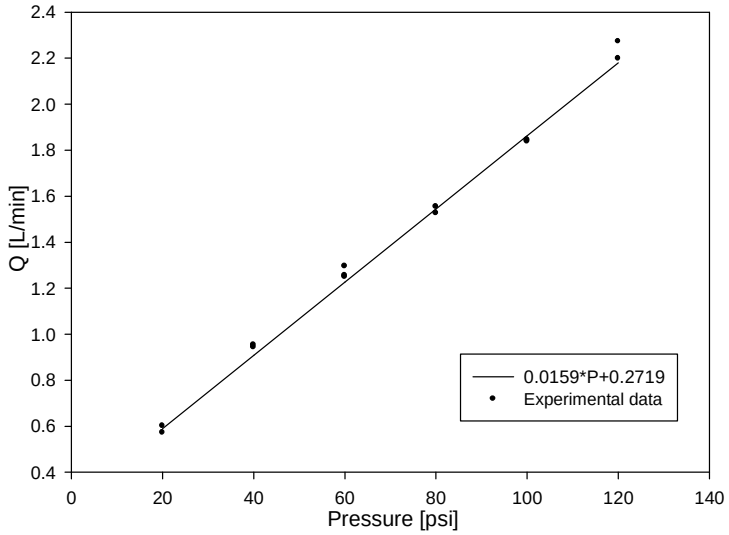

Figure 6-3 Carbon Dioxide Calibration through pressure regulator

Calibration Nozzle set up:

An Erlenmeyer of 1 L volume was filled with water and placed upside-down in a water tank supported with a clamp on a stand. The pressure regulator was connected to the sonic nozzle and the sonic nozzle was connected to a plastic tube which is placed inside the Erlenmeyer. The time of water displacement by the flow (either N_2 or CO_2) was recorded for different regulator pressures, and the data was plotted. A linear regression of the data with a R^2 value near to 1 check is enough to corroborate the mathematic relation between pressures in the regulator with the flow downstream. This linearity certifies constant flow through the sonic nozzle and validity of the calibration method.

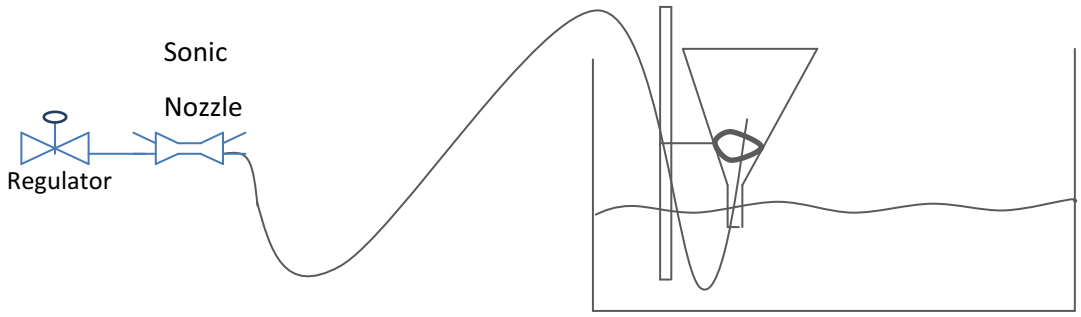

Figure 6-4 Calibration Experimental set up

Curriculum Vitae

Name:	Diana C. Cruz-Ceballos
Post-secondary Education and Degrees:	M.E.Sc 2010-2012 The University of Western Ontario London, Ontario, Canada B.E.Sc 2003 -2009 Universidad Industrial de Santander (UIS) Bucaramanga, Santander, Colombia
Related Work Experience	Teaching Assistant 2011 The University of Western Ontario